# CURRICULUM VITAE

Erin Harberts, PhD
Department of Microbiology and Immunology
University of Maryland School of Medicine

**April 23, 2014**

## Contact Information

Email: erin.harberts@gmail.com

## Education

| | | |
|---|---|---|
| 2004 – 2008 | BA | Colgate University, Hamilton, NY<br>Molecular Biology, Education |
| 2010 – 2014 | PhD | Univ. of Maryland School of Medicine, Baltimore, MD<br>Molecular Microbiology and Immunology |

## Certification

| | |
|---|---|
| 2008 | New York State Elementary Teaching Provisional Certificate |

## Laboratory Experience

| | |
|---|---|
| 2007 | Summer Student, Viral Immunology Section (VIS)/National Institute of Neurological Disease and Stroke (NINDS)/ National Institutes of Health (NIH), Bethesda, MD |
| 2008 – 2010 | Post-Baccalaureate Fellow, VIS/NINDS/NIH, Bethesda, MD |
| 2010 – 2014 | Graduate Student, University of Maryland School of Medicine, Baltimore, MD |

## Professional Society Memberships

| | |
|---|---|
| 2009 | International Society for Neurovirology |
| 2012 | American Association of Immunologists |
| 2012 | Society for Investigative Dermatology |

## Honors and Awards

| | |
|---|---|
| 2007 | Outstanding Summer Student Award, NINDS/NIH |
| 2012 | Graduate Student Travel Award, Biolegend |
| 2013 | Trainee Abstract Award, American Association of Immunologists |
| 2013 | Albert M. Kligman Travel Fellowship Award, Society for Investigative Dermatology |
| 2013 | National Graduate Student Research Conference, NIH |

## Funding

| | |
|---|---|
| 2013-2014 | Signaling Pathways in Innate Immunity Training Grant, T32AI095190-02 |

## Teaching Experience

| | |
|---|---|
| 2002 – 2008 | Captain/Senior Instructor, Annapolis Sailing School, Annapolis, MD |
| 2004 – 2006 | Mentor, Odyssey of the Mind Afterschool Program, Hamilton Middle School, Hamilton, NY |
| 2005 – 2006 | Tutor, High School Chemistry, Hamilton, NY |
| 2006 – 2007 | Teacher/Organizer, 4-H Literacy Club, Brookfield, NY |
| 2008 | Student Teacher, Fourth Grade, Hamilton Elementary, Hamilton, NY |
| 2011 – 2012 | Leader, Cutaneous Immunology Journal Club for Dermatology Residents, Dermatology Department, University of Maryland, Baltimore, MD |
| 2012 – 2013 | Leader, Small Group Discussions, Medical School Immunology, University of Maryland Medical School, Baltimore, MD |
| 2012 – 2013 | Teaching Assistant, Bioinformatics, University of Maryland Medical School, Baltimore, MD |

## University Service

University of Maryland Medical School

| | |
|---|---|
| 2010 – 2013 | Student Editor and Contributor, Quarterly Newsletter: 'The Microscoop', MMIC Department |
| 2010 – 2013 | Host, Prospective Student Interviews, MMIC Department |
| 2011 | Organizer, Career Symposium, Graduate Program in Life Sciences |
| 2012 – 2013 | Lead Organizer, Student Seminar Series, MMIC Department |
| 2012 – 2013 | Student Committee Chair, Qualifying Exam Practice Sessions, MMIC Department |

## Peer Reviewed Publications

1. Unsong Oh, Masahiro Fujita, Vasiliki Ikonomidou, Iordanis Evangelou, Eiji Matsuura, **Erin Harberts**, Joan Ohayon, Victor Pike, Yoshi Zhang, Sammi Zoghbi, Robert Innis, and Steven Jacobson. *Translocator protein PET imaging for glial activation in multiple sclerosis.* J of Neuroimmune Pharmacology. 2011. 6(3): 354-61. PMID: 20872081.
2. **Erin Harberts**, Karen Yao, Jillian Wohler, Dragin Maric, Joan Ohayon, Robert Henkin, and Steven Jacobson. *Human herpesvirus-6 entry into the central nervous system through the olfactory pathway.* Proc Natl Acad Sci USA. 2011. 108(33): 13734-9. PMID: 21825120.
3. Brian Astry, **Erin Harberts**, and Kamal D. Moudgil. *A cytokine-centric view of the pathogenesis and treatment of autoimmune arthritis.* J of Interferon and Cytokine Research. 2011. 31(12): 927-40. PMID: 22149412.
4. **Erin Harberts**, Anthony A. Gaspari. *TLR signaling and DNA repair: Are they associated?* J of Investigative Dermatology. 2013. 133(2): 296-302. PMID: 22931928.

5. **Erin Harberts**, Dibyadeep Datta, Jillian Wohler, Selby Chen, Unsong Oh, and Steven Jacobson. *Translocator protein 18 kDa (TSPO) expression in Multiple Sclerosis patients.* J of Neuroimmune Pharmacology. 2013. 8(1): 57-57. PMID: 22956240.
6. Anna Balato, Yuming Zhao, **Erin Harberts**, Patricia Groleau, Juan Liu, Rita Fishelevich, and Anthony A. Gaspari. *CD1d-dependent, NKT cell cytotoxicity against keratinocytes in allergic contact dermatitis.* Experimental Dermatology. 2012. 21(12): 915-920. PMID: 23171451.
7. Emily Leibovitch, Jillian Wohler, Sheila Macri, Kelsey Montanic, **Erin Harberts**, Gaitan Mines, Margret Pietro, Mary Ellis, Susan Westmoreland, Anthony Silva, Daniel Reich, and Steven Jacobson. *Novel marmoset (Callithrix jaccus) model of Human Herpesvirus 6A and 6B infections: Immunologic, virologic, and radiologic characterization.* PLOS Pathogens. 2013. 9(1): e1003138. PMID: 23382677.
8. Melissa A. McDiarmid, Joanna M. Gaitens, Stella Hines, Richard Breyer, Jade J. Wong-You-Cheong, Susan M. Engelhardt, Marc Oliver, Patricia Gucer, Robert Kane, Alison Cernich, B Kaup, Dennis Hoover, Anthony A. Gaspari, Juan Liu, **Erin Harberts**, Lawrence Brown, Jose A. Centeno, Patrick J. Gray, Hannah Xu, and Katherine S. Squibb. *The Gulf War depleted uranium cohort at 20: Bioassay results and novel approaches to fragment surveillance.* Health Physics. 2013. 104(4): 347-361. PMID: 23439138.
9. Jessica Shiu, **Erin Harberts**, Anthony A. Gaspari, and Brian J. Nickoloff. *Skin: Immunological Defence Mechanisms.* In: eLS 2013, John Wiley & Sons Ltd: Chichester http://www.els.net/ [DOI: 10.1002/9780470015902.a0001215.pub3]
10. **Erin Harberts**, Rita Fishelevich, Juan Liu, Sergei P. Atamas, and Anthony A. Gaspari. *MyD88 mediates the decision to die by apoptosis or necroptosis after UV irradiation.* Innate Immunity. 2013. Epub ahead of print on Sept. 18, [DOI: 10.1177/1753425913501706]. PMID: 24048771.
11. Juan Liu, **Erin Harberts**, Antonella Tammaro, Nicholas Girardi, Renata B. Filler, Rita Fishelevich, Angela Temann, Paula Lincona-Limon, Michael Girardi, Richard A. Flavell, and Anthony A. Gaspari. *Allergen-specific Th9 regulate responses in allergic contact dermatitis.* J of Investigative Dermatology. 2014. Epub ahead of print on Jan. 31, [DOI: 10.1038/jid.2014.61]. PMID: 24487305.
12. Laurie Shallcross, Simon Ritchie, **Erin Harberts**, Antonella Tammaro, Joanna Gaitens, and Anthony A. Gaspari. *Manganese oxidation state as a cause of irritant patch test reactions.* Dermatitis. 2014. 25(2):66-71. PMID: 24603521.
13. Hannah Liu, Papapit Tuchinda, Rita Fishelevich, **Erin Harberts**, and Anthony A. Gaspari. *Human in vitro skin organ culture as a model system for evaluating DNA repair.* J of Dermatological Science. 2014. Epub ahead of print on Feb 16, [DOI: 10.1016/j.jdermsci.2014.02.003]. PMID: 24636351.
14. **Erin Harberts**, Rita Fishelevich, Juan Liu, and Anthony A. Gaspari. *MyD88 deficiency allows for immune maintenance after UV-irradiation due to increased PARP-dependent DNA repair.* Under review at J of Biological Chemistry.

**Meetings, Posters, and Oral Presentations**

June 2008 6th International Conference on HHV-6 and 7 (Baltimore, MD).

June 2009 — 9th International Symposium on Neurovirology (Miami, FL). Abstract for poster presentation: *Human herpesvirus infection of olfactory ensheathing cells (OEC), nasal cavity as a reservoir for human herpesvirus 6 (HHV-6).* Karen Yao, **Erin O'Keefe**, Dragin Maric, Joan Ohayon, Robert Henkin, and Steven Jacobson.

May 2012 — 99th Annual Meeting of AAI (Boston, MA). Abstract for poster presentation: *TLR Agonist Treatment Elicits an Increase in DNA Repair Machinery.* **Erin Harberts**, Rita Fishelevich, and Anthony A. Gaspari.

May 2013 — 100th Annual Meeting of AAI (Honolulu, HI). Abstract selected for oral and poster presentation: *MyD88 plays a role in deciding between apoptotic and necroptotic cell death after UV irradiation.* **Erin Harberts**, Rita Fishelevich, Juan Liu, Sergei P. Atamas, and Anthony A. Gaspari.

May 2013 — International Investigative Dermatology (Edinburgh, Scotland). Abstract selected for oral and poster presentation: *MyD88 plays a role in deciding between apoptotic and necroptotic cell death after UV irradiation.* **Erin Harberts**, Rita Fishelevich, Juan Liu, Sergei P. Atamas, and Anthony A. Gaspari.

*October 2013 (cancelled)* — National Graduate Student Research Conference (Bethesda, MD). Abstract for poster presentation: *MyD88 Dependent TLR4 Signaling Controls Cell Fate and Constrains DNA Repair After UV-Irradiation.* **Erin Harberts**, Rita Fishelevich, Juan Liu, and Anthony A. Gaspari.

**Presentations at the University of Maryland, Baltimore**

June 2011 — MMIC Graduate Student Conference. Abstract for oral presentation: *Effects of corticosteroid treatment in a S. aureus murine biofilm model.* **Erin Harberts,** Janette Harro, Megan Harris, and Mark Shirtliff.

April 2012 — Immunology Journal Club. Paper presentation.

April 2012 — Graduate Research Conference. Abstract for poster presentation: *TLR Agonist Treatment Elicits an Increase in DNA Repair Machinery.* **Erin Harberts**, Rita Fishelevich, and Anthony A. Gaspari.

May 2012 — MMIC Student Seminar. Oral presentation entitled: *TLR signaling mediates UV induced apoptosis.* **Erin Harberts**, Rita Fishelevich, Juan Liu, and Anthony A. Gaspari.

June 2012 — MMIC Graduate Student Conference. Abstract for oral presentation: *TLR signaling mediates UV induced apoptosis.* **Erin Harberts**, Rita Fishelevich, Juan Liu, and Anthony A. Gaspari.

June 2012 — Cancer Biology Research Retreat. Abstract for poster presentation: *TLR Agonist Treatment Elicits an Increase in DNA Repair Machinery.* **Erin Harberts**, Rita Fishelevich, and Anthony A. Gaspari.

January 2013 — Immunology Journal Club. Paper presentation.

March 2013 — MMIC Student Seminar. Oral presentation entitled: *MyD88-dependent TLR4 signaling mediates cell fate after UV-irradiation.* **Erin Harberts**, Rita Fishelevich, Juan Liu, Sergei P. Atamas, and Anthony A. Gaspari.

April 2013 Graduate Research Conference. Abstract for oral presentation: *MyD88 plays a role in deciding between apoptotic and necroptotic cell death after UV irradiation.* **Erin Harberts**, Rita Fishelevich, Juan Liu, Sergei P. Atamas, and Anthony A. Gaspari.

Nov 2013 MMIC Student Seminar. Oral presentation entitled: *A Role for MyD88-dependent TLR 4 Signaling in UV Irradiation.* **Erin Harberts**, Rita Fishelevich, Juan Liu, Sergei P. Atamas, and Anthony A. Gaspari.

February 2014 Immunology Journal Club. Paper presentation.

## ABSTRACT

**Title of Dissertation:** TLR4/MyD88 Signaling Activates Ultraviolet Irradiation-Induced Apoptosis: Outcomes and Consequences

**Erin Marie Harberts, Doctor of Philosophy, 2014**

**Dissertation Directed By:** Anthony A. Gaspari, M.D.
Professor
Department of Dermatology,
Program of Molecular Microbiology and Immunology

Ultraviolet (UV) irradiation induces DNA damage leading to the accumulation of mutations in epidermal keratinocytes (KC), and immunosuppression, which contribute to development of non-melanoma skin cancers. How the decision to undergo apoptosis is made following UV exposure is not fully understood. We hypothesize that a central mediator of TLR signaling, MyD88, determines cell fate after UV exposure. Survival after UV of immortalized bone marrow-derived macrophages (BMM) and *ex vivo* peritoneal macrophages (PM) from MyD88 germline-deficient mice ($MyD88^{-/-}$) was significantly higher *vs*. wild-type (WT) PM. UV-induced apoptosis in PM and epidermis of $MyD88^{-/-}$ animals was decreased *vs*. WT. In $MyD88^{-/-}$ PM, decreased cleavage of caspase 3, PARP, and pro-necroptotic protein, RIP1, and a significant increase in pro-inflammatory TNF-α, suggest that necroptosis, rather than apoptosis, was initiated. *In vivo* studies confirm this hypothesis, showing low apoptosis by TUNEL and enhanced histologic inflammation in $MyD88^{-/-}$ skin sections after UV. Considering that MyD88 participates in most TLR signaling pathways, BMM from $TLR2^{-/-}$, $TLR4^{-/-}$, $TRAM/TRIF^{-/-}$, and WT mice were compared for evidence of UV-induced apoptosis.

Only TLR4$^{-/-}$ BMM and PM had a similar phenotype to MyD88$^{-/-}$, suggesting that the TLR4-MyD88 axis importantly contributes to cell fate decision. We then sought to determine how alteration of this pathway affects the UV-induced damage to critical epidermal cells. In the DNFB hypersensitization model, UV-irradiated, MyD88$^{-/-}$ mice had intact ear swelling, normal IFN-γ production by T lymphocytes, and higher levels of DNFB-specific IgG2a compared to WT, which were suppressed by UV. The UV-induced emigration of antigen presenting cells from the epidermis was maintained in MyD88$^{-/-}$ mice, yet UV-induced DNA damage in the local lymph nodes was less pronounced. We then hypothesized that the aforemention preservation of PARP promotes more efficient DNA damage recognition and repair. In support of this hypothesis, human primary KC treated with MyD88 siRNA and epidermal DNA from MyD88$^{-/-}$ and TLR4$^{-/-}$ mice that were UV-irradiated had an increased resolution rate of cyclobutane pyrimidine dimers (CBPD), which can be attenuated by treatment with a PARP-inhibitor. This work provides a strong rationale for future development of topical TLR4 modulating therapies to reduce the risk of UV-induced carcinogenesis.

# TLR4/MyD88 Signaling Activates Ultraviolet Irradiation-Induced Apoptosis: Outcomes and Consequences

by
Erin Marie Harberts

Dissertation submitted to the Faculty of the Graduate School of the
University of Maryland, Baltimore in partial fulfillment
of the requirements for the degree of
Doctor of Philosophy
2014

## DEDICATION

This thesis is dedicated to my grandfather, George Burns O'Brien, who taught me how to always find the fun in life, no matter what.

## ACKNOWLEDGEMENTS

First and foremost I would like to thank Dr. Anthony Gaspari and Rita Fishelevich for all of their help and guidance during my thesis research. I could not have asked for a more supportive environment in which to learn and grow as a scientist during my time in graduate school. I would also like to thank all of the former members of the Gaspari lab including, Juan Liu, Hannah Liu, Pappapit Tuchinda, Antonella Tammaro, and Nick Girardi; who made research fun and provided me with the friendship that made my day to day lab challenges manageable and fun. Also, thank you to all of my classmates and friends who were always there to get a cup of coffee and help put a smile on my face, even on my most frustrating days. I thank my thesis committee members, Dr. Sergei Atamas, Dr. John Basile, Dr. Kamal Moudgil, and Dr. Stefanie Vogel, who were always there to read drafts, brainstorm experiments, and without whose help this thesis would not be what it is today. Thank you to my readers, Drs. Atamas and Vogel, who took their time to carefully edit and provide extremely thoughtful comments for my thesis. A special thank you goes out to June Green, without who I'm not sure I could have navigated the graduate school waters.

This work was supported by the VA Merit Award 1 I01 BX000405-01A2 (A. A. Gaspari) and the NIH Signaling Pathways in Innate Immunity Training Grant T32AI095190-02 (S. N. Vogel).

## TABLE OF CONTENTS

List of Tables ..... vi

List of Figures ..... vii

List of Abbreviations ..... ix

**1. Introduction ..... 1**

1.1 Biological Effects of Ultraviolet (UV)-irradiation ..... 1

1.2 Diverse Modes of Cell Death ..... 5

1.3 Toll-like Receptor (TLR) Signaling Pathways ..... 9

1.4 DNA Repair Mechanisms ..... 16

1.5 Scope of My Dissertation ..... 21

**2. Materials and Methods ..... 23**

**3. UV-irradiation Activates a TLR4/MyD88-Dependent Apoptotic Signaling Cascade ..... 31**

3.1 Apoptosis Is Not Initiated in UV-irradiated MyD88$^{-/-}$ Mouse Models ..... 32

3.2 UV-induced Apoptotic Signaling Cascade is TLR4/MyD88-Dependent ..... 35

3.3 TLR4/MyD88 Pathway is also Activated in Human Cells ..... 40

**4. Death is Skewed Towards Necroptosis in TLR4/MyD88$^{-/-}$ Cells ..... 42**

4.1 Necrotic Morphology Observed in TLR4/MyD88$^{-/-}$ Models ..... 43

4.2 Initiation of Rip-dependent Necroptosis ..... 43

4.3 Proteins Classically Cleaved/inactivated during Apoptosis Persist Intact ..... 47

**5. MyD88$^{-/-}$ Mice are Resistant to UV-Induced Systemic Immunosuppression ..... 51**

5.1 Mouse Contact Hypersensitivity Model ..... 51

5.2 Antigen Presenting Cell Migration After UV-irradiation ..... 54

**6. Increased DNA Repair in UV-irradiated TLR4/MyD88$^{-/-}$ Models ..... 56**

6.1 Cyclobutane-pyrimidine Dimer (CBPD) Resolution After UV-irradiation ..... 57

6.2 Increased CBPD Resolution is Dependent on PARP-1 ..... 60

6.3 Nucleotide Excision Repair Proteins Are Necessary ..... 63

**7. Discussion ..... 65**

**8. References ..... 75**

## LIST OF TABLES

Table 1. *Summary of canonical cell death pathways* ..... 6

Table 2. *Selected DAMPs associated with DNA damage and DNA-damaging conditions* ..... 15

Table 3. *Summary of several mechanisms, outcomes, and types of DNA damage* ..... 17

## LIST OF FIGURES

Figure 1. *Biological effects of ultraviolet irradiation (UV)* 2

Figure 2. *TNF-induced formation of apoptotic and necroptotic signaling complexes* 8

Figure 3. *Mammalian TLR signaling pathways* 11

Figure 4. *Nucleotide excision repair* 19

Figure 5. *UV-irradiated MyD88$^{-/-}$ cell line exhibits increased survival and decreased apoptotic morphology*. 33

Figure 6. *Epidermal DNA from in vivo UV-irradiated MyD88$^{-/-}$ mice and ex vivo UV-irradiated PM have decreased DNA laddering when compared to WT.* 34

Figure 7. *TLR4$^{-/-}$ macrophages exhibit increased survival and decreased apoptosis following UV irradiation.* 36

Figure 8. *UV-induced apoptosis is not dependent on the TLR4/TRIF-TRAM pathway*. 38

Figure 9. *UV-induced apoptosis is not observed in macrophages with a catalytically inactive IRAK4 molecule*. 39

Figure 10. *Increased survival after UV-irradiation is observed in human primary keratinocytes with MyD88 knocked down.* 41

Figure 11. *Skin sections from UV-irradiated MyD88$^{-/-}$ mice have decreased epidermal apoptosis and increased evidence of epidermal necrosis.* 44

Figure 12. *Necroptotic pathway is activated by UV irradiation in MyD88$^{-/-}$ macrophages* 46

Figure 13. *UV-induced caspase-3 cleavage is dependent on the TLR4-MyD88 signaling pathway.* 48

Figure 14. *Decreased cleavage of DNA damage recognition molecule, PARP, after UV-irradiation in MyD88$^{-/-}$ and TLR4$^{-/-}$ PM* 49

Figure 15. *MyD88$^{-/-}$ mice are resistant to UV induced immunosuppression.* 53

Figure 16. *UV-induced emigration of APC from epidermis in maintained, and DNA damage is decreased in local lymph node of MyD88$^{-/-}$ mice.* 55

Figure 17. *Increased DNA repair is observed in MyD88$^{-/-}$ and TLR4$^{-/-}$ epidermal DNA.* 58

Figure 18. *Increased DNA repair is observed in human primary keratinocytes with MyD88 knocked down.* 59

Figure 19. *Increased resolution of CBPD is dependent on PARP.* 61

Figure 20. *Inhibition of PARP in vivo diminishes the increased DNA repair observed in MyD88$^{-/-}$ mice.* 62

Figure 21. *Knockdown of MyD88 in cells from a xeroderma pigmentosum group A (XPA) patient fails to resolve CBPD.* 64

Figure 22. *UV-activated TLR4 signaling may use FADD to initiate a non-canonical extrinsic apoptosis* 69

Figure 23. *Proposed non-canonical TLR4 extrinsic apoptotic signaling pathway and downstream biological consequences* 74

## LIST OF ABBREVIATIONS

| | |
|---|---|
| APC | Antigen presenting cell |
| Ab | Antibody |
| BMM | Bone marrow derived macrophages |
| BSA | Bovine serum albumin |
| CAD | Caspase activated DNase |
| CBPD | Cyclobutane pyrimidine dimers |
| CD | Cluster of differentiation |
| cDNA | Complementary deoxyribonucleic acid |
| CHS | Contact hyper-sensitivity |
| $CO_2$ | Carbon dioxide |
| DAMP | Danger associated molecular pattern |
| DAPI | 4’,6-diamidino-2-phenylindole |
| DDB | DNA-damage binding protein |
| DISC | Death inducing signaling complex |
| DMEM | Dulbecco’s modified Eagle’s medium |
| DMSO | Dimethyl sulfoxide |
| DNA | Deoxyribonucleic acid |
| DNFB | 1-fluoro-2,4-dinitrobenzene |
| DSB | Double strand break |
| ELISA | Enzyme linked immunosorbent assay |
| FADD | Fas-associated protein with a death domain |
| Fas | TNF receptor superfamily, member 6 |
| FCS | Fetal calf serum |
| FITC | Fluorescein isothiocyanate |
| GGR | Global genome repair |
| H&E | Hematoxylin and eosin |
| HMGB-1 | High-mobility group protein B1 |
| IACUC | Institutional animal care and use committees |
| i.d. | Intradermal |
| IFN | Interferon |
| Ig | Immunoglobulin |
| i.p. | Intraperitoneal |
| IRAK4 | Interleukin-1 receptor-associated kinase 4 |
| KC | Keratinocyte |
| KO | Knockout |
| LRR | Leucine rich repeat |
| MAPK | Mitogen-activated protein kinase |
| MHC | Major histocompatibility complex |

| | |
|---|---|
| mRNA | Messenger ribonucleic acid |
| MTT | 3-(4,5-dimethylthiazol-2-yl)-2,5-diphenyltetrazolium bromide |
| MyD88 | Myeloid differentiation primary response 88 |
| NER | Nucleotide excision repair |
| NF-κB | Nuclear factor kappa-light-chain-enhancer of activated B cells |
| OD | Optical density |
| PAMP | Pathogen associated molecular pattern |
| PARP | Poly ADP ribose polymerase |
| PBS | Phosphate buffered saline |
| PCR | Polymerase chain reaction |
| PHA | Phytohaemagglutinin |
| PM | Peritoneal macrophages |
| qPCR | Quantitative polymerase chain reaction |
| RA | Rheumatoid arthritis |
| RIP | Receptor-interacting serine-threonine kinase |
| RNA | Ribonucleic acid |
| ROS | Reactive oxygen species |
| RPMI | Roswell park memorial institute medium-1640 |
| RT-PCR | Real time polymerase chain reaction |
| siRNA | Small interfering ribonucleic acid |
| SLE | Systemic lupus erythematosus |
| SSB | Single strand break |
| Th1 | T-helper 1 cell |
| TIR | Toll/interleukin-1 receptor domain |
| TLR | Toll-like receptor |
| TNF | Tumor necrosis factor |
| TRADD | Tumor necrosis factor type 1-associated death domain protein |
| TRAM | TRIF-related adaptor molecule |
| Treg | T-regulatory cell |
| TRIF | TIR-domain-containing adaptor-inducing interferon-β |
| TUNEL | Terminal deoxynucleotidyl transferase |
| UV | Ultraviolet |
| WT | Wild-type |
| XP | Xeroderma pigmentosum |

# Chapter 1

## Introduction

### *1.1 Biological Effects of Ultraviolet (UV)-irradiation*

Non-melanoma skin cancer (NMSC), caused by UV-irradiation, is the most commonly observed neoplasm in the world. In 2006 in the United States alone there were about 25 million cases of NMSC reported, which cause significant morbidity and potentially mortality, while using significant health care resources [1]. Exposure to the harmful rays of UV represents a threat to humans from every walk of life and has resulted in the skin cancer epidemic that we are observing today.

Occupying the wavelengths between the visible light and x-ray spectrums, the UV light spectrum ranges from 400-10 nm. The UV spectrum is further broken down into UVA (400-315 nm), UVB (315-280 nm), UVC (280-100 nm), and EUV (100-10 nm) [2]. EUV, extreme UV, is not biologically relevant because it is absorbed strongly by air and can exist only in a vacuum [3]. Similarly, UVC is filtered out by the atmosphere and never reaches the earth's surface; therefore it does not have routine biological relevance, except where there are 'holes in the ozone layer' [4]. However, the UVA and UVB wavelengths filter down through the atmosphere to reach our skin and cause many varied consequences, both positive and negative, on our everyday health (Figure 1) [5, 6].

Human skin is ubiquitously exposed to UVA and UVB irradiation. The longer wavelengths of UVA are able to penetrate down through the epidermis to the dermis and associated connective tissue, while the shorter UVB wavelengths are absorbed by epidermal cells, mostly keratinocytes (KC) [7]. Genomic DNA in epidermal cells acts as a direct chromophore for UV by absorbing the UVA and UVB wavelengths causing

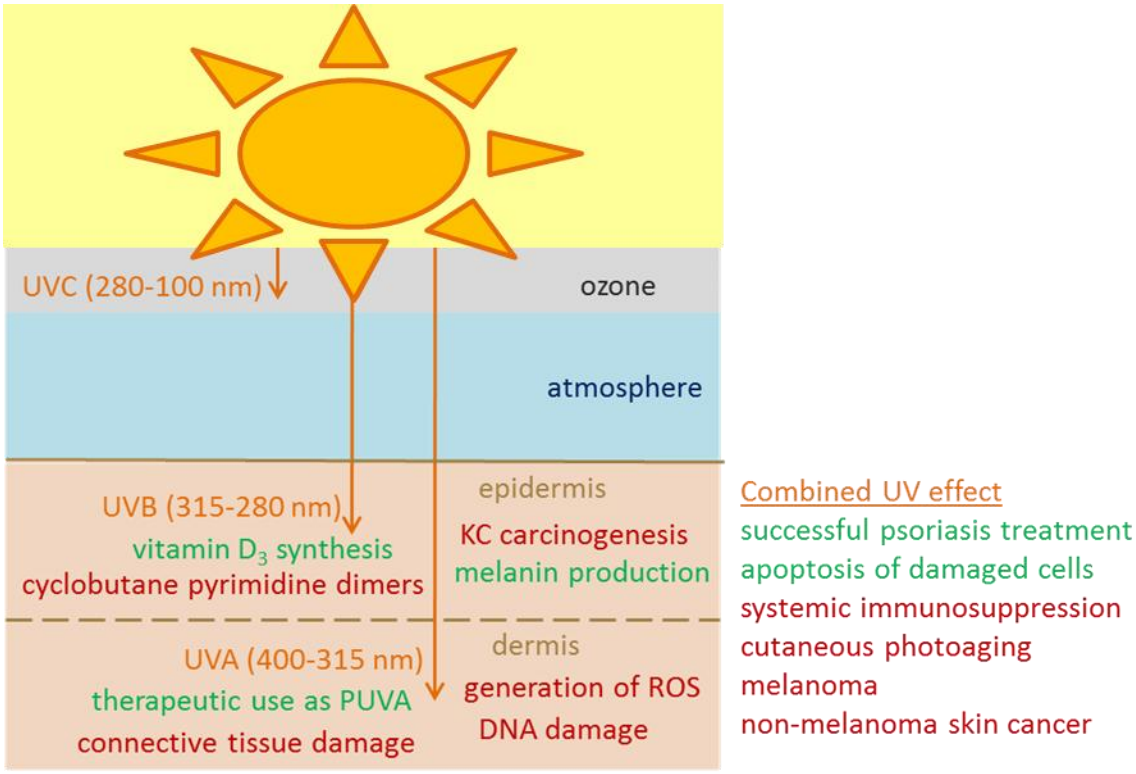


**Figure 1. Biological effects of ultraviolet-irradiation.** UVA and UVB have many varied biological effects on human health. UVA penetrates the skin through the epidermis and is absorbed mostly by dermal cells, while UVB is absorbed by epidermal cells and does not penetrate through the skin to the dermis. These wavelengths have many positive (shown in green) and negative (shown in red) specific and combined effects.

damage to the nucleic acid chains [8]. UVB is also responsible for the biosynthesis of vitamin $D_3$. When exposed to UVB, cholesterol in the skin, in the form of 7-dehydrocholesterol, is photolysed into previtamin $D_3$ which spontaneously isomerizes into the biologically active vitamin $D_3$ [9]. While vitamin $D_3$ can be obtained through diet, UVB photosynthesis is the primary source of this essential vitamin [10]. Other positive UV-effects include UVB-induced delayed tanning which stimulates the production of melanin and thereby reduces the rate of carcinogenesis, as well as reduction of blood pressure by the production of nitric oxide [11, 12]. UVB is also administered therapeutically to treat skin diseases such as psoriasis, vitiligo, localized scleroderma, and atopic dermatitis [13-16]. This treatment can cause local and systemic immune suppression which may be a reason it is of benefit to some immune-mediated inflammatory diseases. Although all of the mechanisms that cause this treatment to be effective have not yet been elucidated, effectiveness of UVB therapy is probably due to the activation of classical survival and death signaling pathways in diseased and the local immune cells [17, 18].

Along with the positive effects of UV-irradiation come many negative consequences. It has long been observed that exposure to UV causes alterations in connective tissue [19], depletion of epidermal-resident APC, Langerhans cells [20], and increased photocarcinogenesis [12, 21, 22]. UV-irradiation is now further identified as a potent immunosuppressant [23, 24], a major focus of this dissertation, and UV-induced carcinogenesis is now attributed to DNA damage which also directly activates apoptosis in epidermal KC [25]. Apoptotic cell death is widely viewed as a protective mechanism that the skin uses to eliminate KC with extensive genomic damage. The accumulation of

these negative effects over a lifetime leads to cutaneous photoageing, which manifests as wrinkled, discolored, less resilient skin [26, 27].

UVA is considered an oxidizing agent that is absorbed by dermal cells and creates free oxygen radicals, or intracellular reactive oxygen species (ROS) [28]. ROS can cause many different types of DNA damage including, single and double strand breaks that are not site-specific [29]. The predominant form of DNA damage inflicted on KC by UVB is cyclobutane pyrimidine dimers (CBPD). When active, the nucleotide excision repair (NER) machinery can easily excise and repair CBPD without propagating a mutation [30]. However, if DNA damage detected by cellular genome monitoring systems exceeds the amount that is able to be repaired, the DNA repair machinery is overcome by the apoptotic process [31]. Apoptotic KC that have been irreversibly damaged, termed "sunburn cells," are sloughed off and replaced [32]. This replacement of epidermal cells by apoptosis allows an intact skin barrier to be maintained without the inflammation associated with other forms of cell death. Fas-associated protein with a death domain (FADD) is a signaling molecule necessary for activation of extrinsic apoptosis by most extracellular death receptors, and the consequences of not being able to undergo homeostatic apoptosis are highlighted by the recent finding that $FADD^{-/-}$ mice show spontaneous epidermal KC necroptosis and subsequent pathogenic inflammation [33].

The apoptotic and immunosuppressive effect of UV irradiation on skin suggests that immunomodulatory molecules are either induced or released from epidermal cells upon UV [34]. However these specific molecules and signaling pathways have yet to be elucidated. It has been found that TLR4 plays a role in promoting cutaneous immunosuppression, as TLR4 deficient (C3HeJ) mice have no decrease in contact

hypersensitivity reactions after UV exposure [35]. Expression of TLRs 2 and 4 have also been shown to be increased in epidermal cells following UV, and an observed increase in immune signaling molecules, such as MAPK and NF-κB, is dependent on this TLR expression [36]. The importance of TLR signaling in the cutaneous immunomodulatory effect of UV, and advances in the understanding of the interconnectedness of cell fate pathways, led us to investigate how TLR signaling and the pathway scaffolding adapter molecule MyD88 may affect cell fate after UV-irradiation.

*1.2 Diverse Modes of Cell Death*

The process by which a cell dies has become recognized as a critical factor in determining the type of immune response that it stimulates locally and systemically [37-40]. Some modes of cell death are considered pro-inflammatory, *e.g.*, pyroptosis and necrosis, and are mostly associated with microbial infections and pathogenic conditions that lead to significant tissue damage [41]. Other modes of cell death are considered to be immunologically silent, such as apoptosis and autophagy, and are usually associated with homeostatic cell death and maintenance of healthy, mutation-free tissue [42]. All of the aforementioned cell death pathways have been, and continue to be, extensively studied and have specific characteristics, molecular markers, and signaling molecules associated with them (Table 1) [20, 21, 43-49]. In this dissertation, I have focused on the consequences of altering cell fate from an immunologically silent apoptotic cell death, to a pro-inflammatory necroptotic cell death, in response to UV irradiation.

There are two classical pathways that, upon activation, lead to an immunologically silent apoptotic cell death, the extrinsic pathway and the intrinsic

**Table 1.** Summary of canonical cell death pathways

| Type of Death | Characteristics | Molecular Markers | Critical Signaling Molecules |
|---|---|---|---|
| Apoptosis | -Can be induced extracellular (TNF-α, FasL, TLRs…) or intracellular (ROS, cytochrome-c) stimuli<br>-initiated by formation of the apoptosome<br>-considered 'anti-inflammatory' | Ladder; Blebbing; TUNEL positive; extracellular Annexin-V; Cleavage of: caspase-3, Rip1, iCAD, PARP; Cytoplasmic cytochrome-c; Membrane integrity maintained | TNFR, Fas, TRAIL, TLR4, TLR2, Bax, Bak, others…?<br>↓<br>FADD, TRADD, MyD88, APAF, other DD containing molecules<br>↓<br>Caspase-8, -9, -6, -7, -3 |
| Necrosis/Necroptosis | -Classical inflammatory cell death<br>-Originally thought to be 'unordered', but now specific signaling pathways have been identified | Release of PAMPS/DAMPS; Increased TNF-α; Cell swelling; Upregulation of Rip3; Phosphorylation of MLKL | Any apoptotic initiator in presence of caspase inhibitor, DNA damage<br>↓<br>Rip1, Rip3<br>↓<br>MLKL, others…? |
| Autophagy | -Homeostatic process<br>-Can lead to cell death by destruction of cellular components<br>-Involves formation of autophagosome which fuses with lysosome<br>-Is regulated by status of other cell death pathways | Covalent bonding of Atg5 with Atg12; Formation of LC3-II | Beclin, PI3K<br>↓<br>LC3-1, Atg family proteins<br>↓<br>Lysosomal fusion |
| Pyroptosis | -Initiated by activation of the caspase-1 inflammasome<br>-Dependent on intracellular PRR, many of which require a 'first hit' to be upregulated<br>-Leads to inflammatory cell death | Release of PAMPs/DAMPs; Increased IL-1β and IL-18; Cell swelling; Cleavage of caspase-1; TUNEL positive | NLRP1, NLRC4, Aim2, other intracellular PRR<br>↓<br>ASC, CARD domain containing adaptors<br>↓<br>Caspase-1 |

pathway [50]. The extrinsic pathway is initiated by engagement of cell surface death receptors, most notably TNFR and Fas, that associate with the scaffolding proteins, TRADD and FADD, respectively, to create a death-inducing signaling complex (DISC) [51]. The intrinsic pathway is initiated by release of cytochrome c from the mitochondria, followed by formation of the apoptosome [52]. Both pathways, either through a DISC or the apoptosome, result in cleavage of caspase-3 that, in turn, cleaves and activates caspase-activated DNase (CAD). Once activated, CAD translocates into the nucleus where it starts digesting genomic DNA, among other cellular components, which is released from the cell in apoptotic vesicles. This digestion process results in the "DNA laddering" that is a hallmark of apoptotic cells [53]. DNA laddering is the result of DNA cleavage by CAD between nucleosomes, which results in DNA fragments increasing in size consistently by about 180 base pairs, which is the amount of DNA wrapped around a histone. In addition to active cleavage of DNA, apoptotic cells undergo a loss of survival signals and homeostatic processes. Experiments using caspase inhibitors show that without the ability to activate the apoptotic pathway, cell death can be skewed to an inflammatory, caspase-independent cell death that is dependent on the formation of specific signaling complexes and is termed necroptosis [54].

Necroptosis is initiated by the Rip1-Rip3 protein complex and leads to inflammatory cell death [55]. The many consequences of and cellular mechanisms leading to the Rip1-Rip3 protein complex, and subsequently necroptosis, is still a widespread active area of investigation. However, to date, the necroptotic pathway has been most completely described downstream of extracellular death receptors, such as TNFR1 (Figure 2). In this scenario, TNF-α engages TNFR1 and inhibition of caspase 8

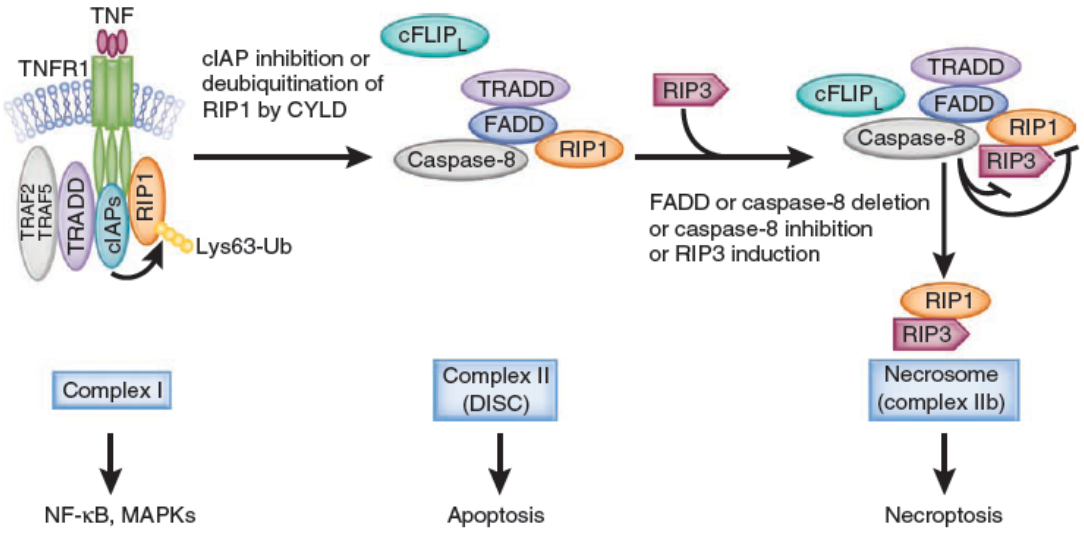


**Figure 2. TNF-induced formation of apoptotic and necroptotic signaling complexes.** After ligand binds to the receptor, the intracellular domains of TNFR1 recruit multiple proteins to form the membrane-proximal supramolecular structure complex I. Lys63-linked polyubiquitination (Lys63-Ub) of RIP1 in complex I, mediated by cIAP ligases, is crucial for the activation of NF-κB and mitogen-activated protein kinases (MAPKs). Deubiquitination of RIP1 by cylindromatosis (CYLD) or inhibition of cIAP proteins promote the conversion of complex I to complex II and inhibits NF-κB activation. Complex II contains RIP1, FADD, caspase-8 and TRADD. Caspase-8 becomes activated in complex II and initiates apoptosis, whereas cFLIP$_L$ can prevent activation of caspase-8. In cells with high expression of RIP3, RIP3 enters complex II via interaction with RIP1 after stimulation. The RIP3-containing complex is called complex IIb or the necrosome. In the presence of cFLIP$_L$, caspase-8 is unable to initiate apoptosis, but can cleave RIP1 and RIP3 and thus inhibits necroptosis. Depletion of FADD or caspase-8, inhibition of caspase-8 or induction of RIP3, can free RIP1-RIP3 from inhibition and initiate necroptosis of TNF-α-treated cells. Reprinted by permission from Macmillan Publishers Ltd: *Nature Immunology* [55], copyright 2011.

activation by zVAD has been shown to activate the necrosome which leads to a necroptotic cell death. A limited number of markers of necroptosis have been identified, among them an increase in Rip3, and maintenance of intact Rip1. This is in contrast to Rip1 cleavage which is associated with caspase-8 activation and apoptosis [56, 57]. The recently reported ability of Rip1 to mediate production of TNF-α during necroptosis helps to describe the inflammatory nature of necroptotic cell death and may prove to also be a hallmark of necroptosis [58]. Many inflammatory and necrotic phenotypes are reported as a result of inhibiting the apoptosis pathway components. For example, mice in which caspase 8 is conditionally knocked-out in hepatic cells die of necrosis of the liver [59]. Also, FADD conditional knockout (KO) in intestinal epithelial cells leads to a spontaneous colitis phenotype that is rescued when Rip3 is also knocked out [60]. Previously described inflammatory phenotypes may now be better explained as a consequence of using necroptosis as a default death pathway when apoptosis is inhibited.

*1.3 Toll-like Receptor (TLR) Signaling Pathways*

Toll-like receptors (TLR) are a main component of the innate immune system, which serves as a first line of defense against a wide range of injurious substances. TLR activation not only initiates an inflammatory response that works to combat pathogens, but also potentially results in tissue damage that must be repaired after the infection is neutralized. Among humans and mice, there are currently thirteen known TLRs, some of which localize at the cell membrane and are presumed to defend against extracellular pathogens, while others are located in the endosome and detect intracellular pathogens. These receptors function by recognizing pathogen-associated molecular patterns

(PAMPs). Each TLR responds to very specific PAMPs and initiates the appropriate cellular response to defend against the pathogen recognized. The elegant and complex TLR signaling pathways are the subject of many well written and comprehensive reviews and, as such, we will only give a brief overview [61-63]. Teleologically, it is tempting to speculate that it may be of survival value to the host to have a mechanism by which damage created by TLR activating agonists is repaired. This idea is a main theme of my dissertation.

All TLRs contain two main signaling domains. The first is an extracellular or endosomal pathogen sensing domain that consists of leucine rich repeats (LRR) in the conformation of a shepherd's crook, and the second is an intracellular TIR domain that interacts with signaling and adapter molecules to relay the message that a pathogen has been sensed. These trans-membrane proteins function by either homo- or hetero-dimerization to create functional sensing and signaling complexes. TLRs 2/1, 2/6, 4/4, and 5/5 are known to be extracellular sensors in that reside in the plasma membrane of the cell, while TLRs 3/3, 7/7, 8/8, and 9/9 are considered intracellular sensors that reside in the membrane of the endosome. There are also reports of TLRs 2 and 4 localizing to and functioning from the endosome [64, 65], as well as some unusual associations, including TLR2/2 homodimerization [66], and TLR4/6 dimerization in the brain [67]. MyD88 is the adapter molecule that interacts with the TIR domain of all TLRs except for TLR3 that utilizes TRIF as its sole adapter molecule to lead to downstream signaling. TLR4 can use either MyD88 or TRIF to relay its signal, which is thought to depend on whether it is localized at the cell surface (MyD88-dependent) or endosomally (TRIF-dependent) signaling (Figure 3) [68]. The varied location of and large number of

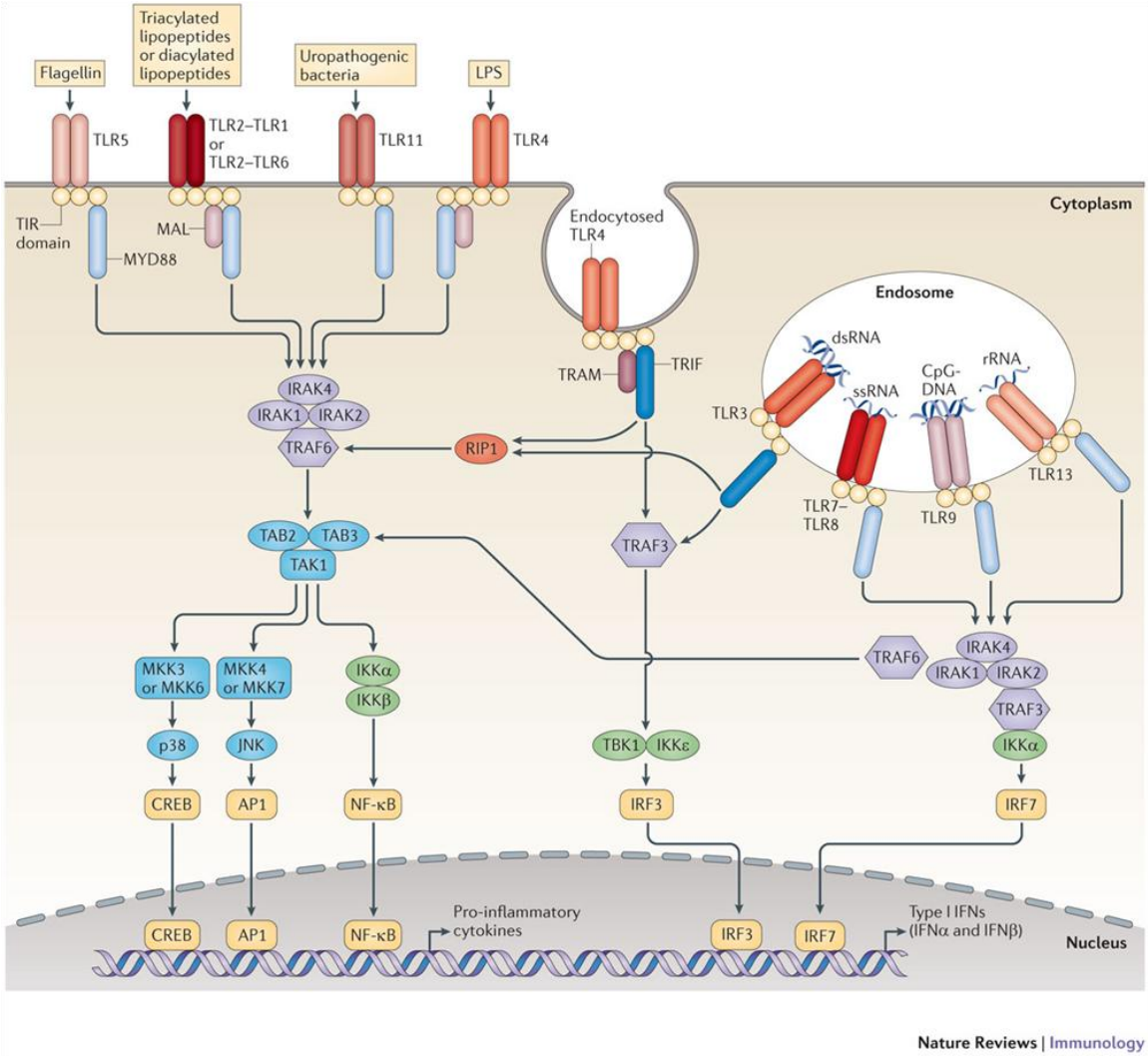


**Figure 3. Mammalian TLR signaling pathways.** A detailed knowledge of how mammalian Toll-like receptors (TLRs) signal has developed over the past 15 years. TLR5, TLR11, TLR4, and the heterodimers of TLR2–TLR1 or TLR2–TLR6, bind to their respective ligands at the cell surface, whereas TLR3, TLR7, TLR8, TLR9, and TLR13 localize to the endosomes, where they sense microbial and host-derived nucleic acids. TLR4 localizes at both the plasma membrane and the endosomes. TLR signaling is initiated by ligand-induced dimerization of receptors. Following this, the Toll–IL-1-resistence (TIR) domains of TLRs engage TIR domain-containing adaptor proteins (either myeloid differentiation primary-response protein 88 (MyD88) and MyD88-adaptor-like protein (MAL), or TIR domain-containing adaptor protein inducing IFN-β (TRIF) and TRIF-related adaptor molecule (TRAM)). TLR4 moves from the plasma membrane to endosomes enabling the switch in signaling from MyD88- to TRIF-dependent. Engagement of the signaling adaptor molecules stimulates downstream signaling pathways that involve interactions between IL-1R-associated kinases (IRAKs) and the adaptor molecules TNF receptor-associated factors (TRAFs), and that lead to the

activation of the mitogen-activated protein kinases (MAPKs) JUN N-terminal kinase (JNK) and p38, and to the activation of transcription factors. Two important families of transcription factors that are activated downstream of TLR signaling are nuclear factor-κB (NF-κB) and the interferon-regulatory factors (IRFs), but other transcription factors, such as cyclic AMP-responsive element-binding protein (CREB) and activator protein 1 (AP1), are also important. A major consequence of TLR signaling is the induction of pro-inflammatory cytokines, and in the case of the endosomal TLRs, the induction of type I interferon (IFN). dsRNA, double-stranded RNA; IKK, inhibitor of NF-κB kinase; LPS, lipopolysaccharide; MKK, MAP kinase kinase; RIP1, receptor-interacting protein 1; rRNA, ribosomal RNA; ssRNA, single-stranded RNA; TAB, TAK1-binding protein; TAK, TGFβ-activated kinase; TBK1, TANK-binding kinase 1. Reprinted by permission from Macmillan Publishers Ltd: *Nature Reviews: Immunology* [69], copyright 2013.

possible signals deriving from TLR4 activation makes it the most functionally diverse and widely studied TLR. Using distinct combinations of adapter and signaling molecules, each TLR elicits a tailored response to the pathogen that it senses. For an extensive overview of TLR ligands, both synthetic and naturally occurring, please refer to the review by Kawai et al. [63]. The pathogen-specific response of TLRs involves the release of cytokines tailored for neutralization of the activating pathogen, recruitment of necessary immune components by release of specific chemokines, up-regulation of co-stimulatory molecules, regulation of cell cycle, and, when appropriate, mediation of inflammation [70-72].

TLRs are not only able to sense PAMPs, but also respond to danger-associated molecular patterns (DAMPs), endogenous signaling molecules released by cells upon acute damage and/or infection. DAMPs are also sensed by TLRs present on surrounding cells. The notion that TLRs are able to recognize and respond to these DAMPs has become widely recognized and the number of known DAMPs has grown rapidly over the past few years [73]. These DAMPs are most notably created under conditions of oxidative stress, DNA damage, viral infection, and ischemia/reperfusion [74-77]. Comprised of many categories of molecules, the list of TLR-activating DAMPs contains proteins/peptides, fatty acids/lipoproteins, proteoglycans/glycosaminoglycans, and nucleic acids/nucleic acid-protein complexes. Endogenous DAMPs have now been identified for all of the TLRs and are the subject of many previous reviews that compile lists of known DAMPs associated with many different environmental and disease conditions [78-82].

Among the currently identified DAMPs that are known to signal through TLRs there are a few that are particularly relevant to this review because they are associated with DNA damage and DNA damaging conditions (Table 2). In a mouse model of hepatic ischemia/reperfusion. endogenous histone proteins, which are released during DNA damaging conditions, are shown to activate TLR9 [76]. Another DNA related DAMP is high-mobility group protein B1 (HMGB-1), a chromatin binding protein, that is a well-recognized marker of necrotic cell death capable of signaling through TLRs 2, 4, and 9. This DNA-associated molecule has been implicated in the pathogenesis of a wide range of diseases including skin cancer, epilepsy, and sepsis [83-85]. Chromatin and other self-DNA complexed with proteins/peptides, when released from the cell, are involved in the pathogenesis of autoimmune disorders, such as systemic lupus erythematosus (SLE) and Sjogren's syndrome, by serving as antigen for autoantibody production, antibodies complexed with self-nucleic acid can then signal through TLRs 7 and 9 to exacerbate pathogenic inflammation [86, 87]. The antimicrobial peptide LL37 has also been shown to complex with free self nucleic acids and serve as a TLR 7 and 8 agonist [88, 89]. This aberrant TLR activation has been implicated in the pathogenesis of psoriasis. Interestingly, a recent publication shows that UVB-irradiated keratinocytes release damaged self non-coding RNAs that serve as potent TLR3 agonists [90]. As UVB can cause extreme DNA damage, depending on the dose, that must be repaired, further experiments should be performed to determine if possibly the described TLR3 activation leads to increased DNA repair. Simple mislocalization and/or aberrant release of these ubiquitously present DAMP molecules can stimulate potentially harmful

**Table 2.** Selected DAMPs associated with DNA damage and DNA damaging conditions.*

| DAMP | TLR(s) Antagonized | Conditions When Released | Associated Organ/Disease | Reference(s) |
|---|---|---|---|---|
| damaged self non-coding RNAs | TLR3 | UVB irradiation | skin | Bernard *et al.*, 2012 |
| histone proteins | TLR9 | ischemic injury | hepatic ischemia/reperfusion | Huang *et al.*, 2011 |
| HMGB-1 | TLR2, TLR4 | oxidative stress, physical injury, ischemic injury, inflammation | skin cancer, epilepsy, sepsis | Maroso et al., 2010; Mittal *et al.*, 2010; Yu *et al.*, 2006 |
| chromatin-protein complexes | TLR7, TLR9 | unknown | SLE, Sjogren's syndrome | Celhar *et al.*, 2012; Rubin *et al.*, 1986 |
| antimicrobial peptide-nucleic acid complex | TLR7, TLR8 | cell death | psoriasis | Ganguly *et al.*, 2009; Lande *et al.*, 2007 |

*for a more extensive list of DAMPs and their receptor molecules please refer to the following reviews: [73, 78-82]

inflammation through recognition by TLRs and other pattern recognition receptors. The ability of the cell to differentiate a genuine danger signal from a normally functioning molecule speaks to how tightly regulated the TLR signaling process is. This dissertation focuses on how activation of TLR pathways might stimulate increased DNA repair, the aforementioned DAMPs serve as intriguing venues to investigate if DAMPs arising from DNA damaging conditions may be helping to initiate repair by signaling through TLRs.

With all of the opportunity present for these TLR signaling pathways to go awry, it is not surprising that they are implicated in the pathogenesis of many diseases and are a target for therapeutics seeking to control the immune response stimulated by TLR agonists. TLR antagonist therapies are routinely used and continue to be under development for treatment of a wide range of diseases including sepsis, viral infection, lymphoma, NMSC, melanoma, SLE, and rheumatoid arthritis (RA) [91-94]. These drugs target many different parts of the signaling pathway including controlling TLR signaling by competitive inhibition of the ligand binding site, and suppression of homodimerization of the receptors [95, 96]. Understanding the many complicated and varied mechanisms of regulation and outcomes from the TLR signaling pathways will allow for more specific and appropriate immune modulation therapy in diseased tissue.

### *1.4 DNA Repair Mechanisms*

DNA damage can occur by many mechanisms, including UV radiation, ionizing radiation, chemical agents, oxidative stress, and defective receptor editing [97-100]. These injurious circumstances result in several types of damage that lead to varied phenotypic outcomes in the cell (Table 3). UV and ionizing radiation (γ-irradiation) most

**Table 3.** Summary of several mechanisms, outcomes, and types of DNA damage.

| | Classical Phenotype | Hallmark Types of Damage Induced |
|---|---|---|
| UV Radiation | impaired antigen presentation, immune suppression, loss of contact hypersensitization (CHS), gradual formation of mutations | SSB, CBPD |
| Ionizing Radiation | depletion of cells by apoptosis, immune suppression, heritable gene mutations | DSB, chromosome abnormalities, mutagenesis |
| Chemical Agents | intercalate with or alter DNA resulting in cytotoxicity | SSB, DSB |
| Oxidative Stress | tissue and organ damage related to inflammation | SSB, histone instability |
| Receptor Editing | defects cause: clonal deletion during maturation, decreased Ab repertoire limited adaptive immune response | abasic site, DSB |

classically result in single strand breaks (SSB) and double strand breaks (DSB), respectively [4, 26]. CBPD are another main type of damage associated mainly with UVB irradiation. These dimers require the NER complex to be excised and corrected, and once this process occurs, the integrity of the affected DNA is maintained [3]. Because γ-irradiation results in DSB that cannot be repaired using a complementary template, it is associated with mutagenesis and chromosome abnormalities that often lead to cell death. Repair of both UV- and γ-irradiation are altered in the presence of endosomal TLR agonists [101, 102], implying that both the NER and DSB repair complexes may be affected by TLR activation status. In my dissertation, I focused on DNA damage caused by UV-irradiation in the form of CBPD that requires NER machinery to excise and repair the damaged segment of DNA.

Not only is the NER pathway responsible for excising and repairing CBPD after UV-irradiation, but it is a necessary mechanism used to repair a wide range of DNA lesions [103]. NER can be categorized into two sub-pathways, global genome repair (GGR) and transcription coupled repair [104, 105]. The removal of UV-induced CBPD falls into the category of GGR, while transcription coupled repair ensures that an intact and accurate genome is maintained and passed on during cell division [2]. GGR begins when a DNA damage-sensing molecule, such as PARP or DDB, recognizes a DNA lesion. XP family proteins are then recruited to the damaged base pairs, these XP proteins then begin to repair the lesion by unwinding the surrounding DNA, stabilizing the now single stranded DNA, and excising the mutated base pairs. A DNA polymerase and DNA ligase are then recruited to fill in the necessary base pairs that are complementary to the intact template strand (Figure 4) [7].

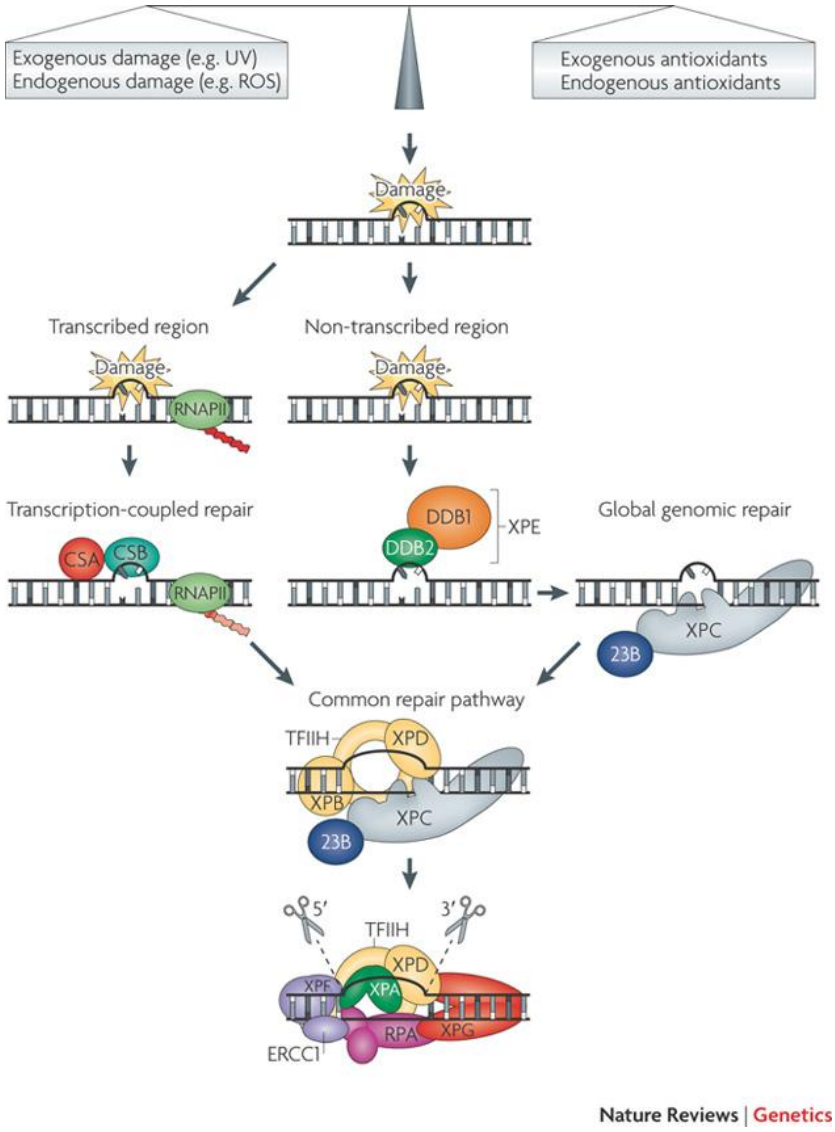


**Figure 4. Nucleotide excision repair.** The nucleotide excision repair (NER) system consists of a series of reactions by which DNA damage caused by, for example, ultraviolet radiation-induced photoproducts or similar chemically induced products is recognized and repaired [106, 107]. Damage can occur from external and endogenous sources (shown as a balance in the figure). Photoproducts include cyclobutane pyrimidine dimers (CBPDs) and 6–4 photoproducts, which can both involve T and C pyrimidines. When repair of these photo- or chemical products is faulty owing to mutations in the NER system, replication errors lead to characteristic C to T mutations, especially CC to TT mutations, which are found in P53, PTCH1 and other oncogenes in sunlight-induced skin cancers of patients with xeroderma pigmentosum (XP) and others [108-111]. The

damage is endogenous in other systemic disorders and is thought to be caused mainly by reactive oxygen species (ROS) [112-114].

Depending on whether the damage occurs in a transcriptionally active or inactive domain, repair can occur by two pathways: global genomic repair (GGR) or transcription-coupled repair (TCR) (shown in the figure). Damage in transcriptionally active regions is detected through the arrest of transcription by RNA polymerase I (RNAPI; not shown) and RNAPII. Transcription arrest is enhanced by mutations in the Cockayne syndrome A (CSA) and CSB proteins, and both are required for ubiquitylation of the carboxy-terminal domain of RNAPII [115, 116]. Cells with mutations in CSA (also known as ERCC8) and CSB (also known as ERCC6) do not show the increased rate of photoproduct repair in transcriptionally active regions that occurs in normal cells, and carry out GGR at normal rates. Arrested polyubiquitylated RNAPII is removed and degraded, leaving the active genes accessible for repair and the resumption of transcription [117]. CSA is a WD40 protein that is part of the ubiquitin E3 ligase that acts on XPC and DNA damage-binding 2 (DDB2) [115]. Damage in transcriptionally inactive regions is detected by the DNA damage-binding protein XPC and complex XPE. Mutation of either of these can cause XP [118]. The individual DNA damage-binding proteins have weak affinities for their substrate, so the binding process can be viewed either as a sequential process in which one protein facilitates binding by another [119, 120] or as a grouping of weakly interacting partners that form transient pre-incision complexes that are locked in place by the XPB (also known as ERCC3) ATPase [107]. The CPDs and 6–4 photoproducts make substantially different structural changes in DNA: CPDs are much less distorting and require more active participation of XPE.

Damage recognition is followed by binding of the ten-component basal transcription factor TFIIH through interaction with either XPC or the arrested transcription apparatus. XPD (also known as ERCC2) is a component of TFIIH and is a DNA helicase that is involved in 5' to 3' unwinding of the DNA in the vicinity of a damaged base. ATP hydrolysis by the XPB component of TFIIH facilitates binding of the NER complex to the damaged site [107, 121]. The amino terminus of XPB interacts with XPD and XPG (also known as ERCC5), whereas the carboxyl terminus is required for 5' cleavage [122]. XPD carries out a further damage recognition step when its migration along the helix is blocked by a photoproduct [107, 121, 123-126].

The DNA around the damaged site is then cleaved by the XPG 3' nuclease and the XPF–ERCC1 5' nuclease. Recent evidence suggests that 5' cleavage occurs first [127]. XPG is bound through interaction with XPC and TFIIH. The nucleases are anchored by XPA–replication protein A (RPA), which defines the cleavage sites and strand specificity. Once the damaged oligonucleotide is removed, a patch is resynthesized by proliferating cell nuclear antigen, polymerases δ, ε, or κ, and a ligase [106, 128]. In quiescent cells, ligation involves X-ray repair cross-complementing protein 1 (XRCC1) and ligase III. In proliferating cells, ligation involves ligase I [129]. Reprinted by permission from Macmillan Publishers Ltd: *Nature Reviews: Genetics* [130], copyright 2009.

Without a functional NER pathway, an organism will be plagued with genomic instability and frequent cancers throughout its life [1]. This phenotype can be observed in xeroderma pigmentosum (XP) patients, who are categorized into subgroups depending on which XP family protein deficiency they express [67]. These patients present with multiple basal cell carcinomas and other skin malignancies at an extremely young age [34, 66]. To avoid skin cancers, XP patients often must be completely guarded from the sunlight and other sources of radiation.

*1.5 Scope of my dissertation*

When I began my dissertation research, it was known that TLR4 signaling was involved in the cellular response to UV-irradiation, but a mechanism(s) for this observation had not been delineated. Our first observation was that MyD88$^{-/-}$ cells survive at a significantly higher rate than WT cells after being exposed to UV-irradiation. This observation led us to formulate the hypothesis that TLR signaling is indeed playing a role in determining cell fate after UV-irradiation. After multiple experiments, it became clear that not only were TLR playing a role in the cellular UV-response, but that TLR4 was necessary for UV-induced apoptosis. These conclusions were extended by investigating our second main hypothesis, that cell fate after UV-irradiation has systemic immune consequences. This dissertation reports the results of experiments performed to investigate these hypotheses. My work has revealed four major findings: (1) UV-irradiation activates a TLR4/MyD88-dependent, apoptotic signaling cascade, (2) TLR4/MyD88-deficient cells die by necroptosis after UV-irradiation, (3) MyD88$^{-/-}$ mice are resistant to UV-induced systemic immunosuppression, and (4) TLR4/MyD88-deficient cells resolve UV-induced CBPD more quickly than WT cells. These findings

provide evidence for the existence of a biologically relevant, non-classical, extrinsic apoptotic pathway that is dependent upon TLR4/MyD88 signaling and activated by UV-irradiation, and provides a strong rationale for future development of topical TLR4 modulating therapies to reduce the risk of UV-induced carcinogenesis.

## Chapter 2

## Materials and Methods

*Cell Culture*

Immortalized BMM cell lines, utilized in experiments from Figure 1, were derived from MyD88$^{-/-}$ and WT C57BL/6 mice and are a generous contribution of Dr. Douglas Golenbock (Univ. of Massachusetts Medical School) and were cultured as previously described [131]. Immortalized BMM from WT, TLR2$^{-/-}$, TLR4$^{-/-}$, and TRAM/TRIF$^{-/-}$ mice on a C57BL/6 background, utilized in experiments from Figures 7 and 8, were obtained from BEI resources (repository numbers NR-9456, NR-9457, NR-9458, and NR-9459 respectively), and were cultured in DMEM supplemented with 10% FCS, 100 µg/mL Pen-Strep, Sodium Pyruvate, and 200mM L-glutamine. Peritoneal macrophages (PM) obtained by thioglycollate administration in mouse abdomen were purified by short plastic adherence in culture media, DMEM supplemented with 20% FCS, and 100 µg/mL Pen-Strep, then washed three times and cultured as described for experimental use. Primary human KC were derived as previously described from neonatal foreskins [132]. Use of human samples has been approved by the University of Maryland Medical School Institutional Review Board. KC were cultured in Epi-Life growth medium supplemented with epidermal growth factor and pituitary extracts (Cascade Biologics, Portland, OR). Lymph node single cell suspensions were made by passing lymph node tissue through a 70µm nylon cell strainer, cells were then washed twice with PBS and plated at a concentration of 1 million cells/ mL of RPMI supplemented with 10% FCS, and 100 µg/mL Pen-Strep. For some experiments PJ-34

(Sigma cat# P4365) or Dynabeads Mouse T-Activator CD3/CD28 (Gibco ref# 11456D) were added to cell culture medium at indicated concentration.

*Ultraviolet Light Source*

Groups of four mice at a time or cell culture plates with the media removed were irradiated with a panel of 48 inch Q-Sun light bank (Q-Panel Laboratory products, Cleveland, OH) (equipped with a UVC WG320 filter) at a distance of 12 inches from the light source to their shaved abdominal skin. The spectral emission profile of this light source closely mimics that of natural sunlight, emitting predominantly UVA. A UVB radiometer (National Biologic Corporation, Twinsburg, OH) was used to determine UVB output, and calculate the time necessary to deliver the desired doses of UVB.

*DNA Extraction and Ladder Assay*

Whole genomic DNA was extracted using DNeasy Blood and Tissue Kit (Qiagen) following manufacturer's protocol. To assay for DNA laddering, 500 ng of DNA was loaded next to a 1kb DNA ladder (Fermentas cat# SM0313) into a 1.2% agarose gel and electrophoresed at 100 V for 10 min followed by 70V for 60 min. The gels were then stained with ethidium bromide and visualized using ChemiDoc XRS (BioRad).

*RNA Extraction and qPCR*

Expression of MyD88 is knocked down in a pool of primary KC from three different donors using siRNA (Qiagen cat# SI00300909) transfected into the cells using the Amaxa Human KC Nucleofector Kit following manufacturer's instructions. Scrambled siRNA is used as a control (Qiagen cat# 1022076). RNA extraction, cDNA synthesis kit, and RT-PCR were carried out according to previously published methods [133, 134]. Relative levels of MyD88 mRNA were normalized to 18s mRNA. Primers used in the reactions were purchased from Qiagen: MyD88: NM_002468.4 (reference position: 979), TNF: NM_013693.2 (reference position: 857-879), 18s: X03205.1 (reference position: 1447).

*MTT Assay*

BMM cell lines or primary KC cells were cultured in a 96 well plate in 6 replicates, then UV-irradiated as indicated. Twenty-four hours after UV irradiation, MTT assay was completed as previously published.[102] Briefly, MTT was added to the cell culture at a final concentration of 500 µg/mL and culture dishes placed back in 37$^{o}$C, 5% $CO_2$ incubator for 4 h. Media was then removed from cells and cells were dissolved in DMSO. The OD @ 540nm was then read in a flat bottom 96 well plate, and the percent survival, as compared to un-irradiated control, was calculated.

*In Vivo Experiments*

Mouse experiments were approved by University of Maryland, Baltimore IACUC. Hair was removed from the abdomen of 14-16 week old female WT C57BL/6 mice (The Jackson Laboratory, Strain Name: C57BL/6J, Stock Number: 000664) or MyD88$^{-/-}$ mice on a C57BL/6 background (The Jackson Laboratory, Strain Name: B6.129P2(SJL)-*Myd88*$^{tm1.1Defr}$/J, Stock Number: 009088), the abdomen was then exposed to 70 mJ/cm$^2$ UVB. For CHS experiments mice were UV-irradiated for 4 consecutive days before sensitization, for other experiments only a single dose of 70 mJ/cm$^2$ UVB was given. Numbers of mice irradiated and samples collected are described in the figure legend associated with each experiment. For skin section staining and epidermal DNA laddering experiments, skin biopsy specimens are taken immediately preceding, and 24 hours after UV exposure. Samples for sectioning and staining were placed in formalin, while sections for epidermal DNA extraction were incubated at 37$^o$ C for 2 hours in Dispase (BD Biosciences cat# 354235). The epidermal layer was removed from the dermis then used for genomic DNA extraction. When ears were exposed to UV-irradiation mice were anesthetized by intraperitoneal injection of a ketamine (80 mg/kg)/xylazine (10 mg/kg) mixture, and ears were taped down to a surface so only the distal side was exposed to UV. To obtain *ex vivo* peritoneal macrophages, 2 mL of thioglycollate medium (Remel cat# R064712) was injected i.p. into 6-8 week old mice and the peritoneal exudates collected 4 days later. For TLR4$^{-/-}$ PM, 6-8 week old mice were purchased (The Jackson Laboratory, Strain Name: B6.B10ScN-*Tlr4*$^{lps-del}$/JthJ, Stock Number: 007227). IRAK4$^{KDKI}$ mice were derived on a C57BL/6J background by Dr. Kirk A. Staschke and Dr. Raymond Gilmour (Lilly Research Laboratories, Indianapolis,

IN), and were bred homozygously in the laboratory of Dr. Stefanie N. Vogel at the University of Maryland, School of Medicine.

*Protein Extraction, and Western Blots*

Protein concentration from cell lysates made using RIPA buffer was measured using *DC* protein assay (BioRad). For Western blots, 10 μg of protein per lane was loaded into NuPAGE 10% Bis-Tris gel (Life Technologies cat# NP0301), then electrophoresed and transferred to nitrocellulose membranes using the Novex mini-gel system (Invitrogen). Membranes were then probed with one of the following primary antibodies: anti-β-actin polyclonal antibody (Cell Signaling cat# 4967), anti-RIP1 monoclonal antibody (Cell Signaling cat# 3493), anti-RIP3 polyclonal antibody (Santa Cruz cat# sc-47364), anti-Caspase3 (Cell Signaling cat# 9665), anti-MyD88 monoclonal antibody (Cell Signaling cat# D80F5), anti-PARP monoclonal antibody (Cell Signaling cat# 46D11). Then developed using the Western Breeze kit (Invitrogen cat# WB7104 or WB7106) according to manufacturer's protocol.

*ELISA*

TNF-α quantification was carried out by the Cytokine Core Laboratory (Univ. of Maryland, Baltimore) using the Luminex$^{TM}$ Multianalyte Assay. DNFB-specific IgG1 and IgG2a serum ELISA were performed as previously described [135]. Briefly, serum was collected from CHS mice 21 days after initial sensitization. ELISA plates (Corning

Glass Works) were coated with 10 μg trinitrophenyl-ovalbumin or dinitrophenyl-ovalbumin (Sigma Chemical, St Louis, Mo), and the plates were blocked with 0.25% BSA in Tween/PBS. Sera were diluted 1:100,000 then plated in triplicate to allow for antibody binding. Unbound antibody was washed off, and biotinylated antimouse IgG1, or IgG2a (BD Pharmingen, San Diego, Calif) were added at 2 μg/mL. The level of trinitrophenyl-specific or DNP-specific IgE was then analyzed by adding streptavidin-horseradish peroxidase at a dilution of 1:2000. *o*-Phenylenediamine dihydrochloride (Sigma Chemical Co) was added according to Sigma instructions for color development. Plates were read on a BioRad benchmark microplate reader (BioRad Laboratories, Hercules, Calif), at an optical density of 570 nm.

*Contact Hypersensitivity Model*

DNFB contact hypersensitivity model was carried out as previously described [37]. Briefly, hair was removed from the abdomen of WT or MyD88$^{-/-}$ mice, which was then exposed to an immunosuppressive dose of UV, 70 mJ/cm$^2$, for four consecutive days, days -3 through 0. On the last day of UV, day 0, and day 1 mice were sensitized with 20 μL of 0.5% DNFB on the abdomen. On day 5, baseline ear thickness measurements were taken then and immune reaction was elicited by painting 20 μL of 0.2% DNFB onto the ear. Twenty-four hours after elicitation, day 6, ear thickness was measured and amount of swelling was determined by subtracting the baseline thickness.

*DNA Dot Blot*

Whole genomic DNA was extracted using DNeasy Blood and Tissue Kit (Qiagen) following manufacturer's protocol. For DNA dot blots, 500 ng of heat-denatured DNA was spotted onto a nitrocellulose membrane allowed to dry at room temperature for 1 hour, then baked at $80^{o}$ C for 20 minutes. The membrane is then probed with an anti-CBPD antibody (Cosmo Bio cat# NMDND001) and developed using secondary Ab and reagents from the WesternBreeze kit (Invitrogen cat# WB7104) according to manufacturer's protocol. Image density quantification was performed using Image-Pro Plus software version 4.5.1.29 (Media Cybernetics).

*Immunohistochemistry*

Formalin-fixed WT and $MyD88^{-/-}$ mouse skin sections were paraffin-embedded, sectioned, and stained using TUNEL In Situ Death Detection kit (Roche cat# 11684809910) or hematoxylin and eosin (H&E). *Ex vivo* PM were cultured and irradiated with 25 $mJ/cm^2$ UV in chamber slides, then fixed in paraformaldehyde and stained with $1^{o}$ Ab for cleaved caspase-3 (Cell Signaling cat# 9664), slides were then stained with FITC-conjugated $2^{o}$Ab (Pierce cat# 31583) for fluorescent visualization. To harvest mouse epidermal sheets, ears were obtained 24 hours after irradiation of one side of the ear with 100 $mJ/cm^2$ UV. The irradiated side was split from the control side and then incubated with Dispase (BD Biosciences cat# 354235) at $4^{o}$ C for 2 hours. The epidermis was then separated off, and fixed in ice cold methanol for 20 min. The epidermal sheets were then stained with FITC-conjugated anti-mouse I-A/I-E clone

M5/114.15.2 (BioLegend cat# 107605) and mounted onto slides with DAPI-containing mounting medium for fluorescent visualization. Slides were visualized using a Nikon Eclipse E600 microscope and the images documented using SpotTM imaging system (Diagnostic Instruments, Sterling Heights, MI). This microscope was also used to visualize cultured macrophage cell lines for morphology after UV.

*Statistical Analysis*

Quantitative data was analyzed for statistically significant differences, between groups of n replicates as described in associated figure legend, using the GraphPad Instat Software Program (GraphPad Software, San Diego, CA). An unpaired students t-test was applied to the quantitative data with a value of $p < 0.05$ considered significant. Significance is indicated on graphs by a *.

## Chapter 3

## UV-Irradiation Activates a TLR4/MyD88-dependent Apoptotic Signaling Cascade

There are many known mechanisms of UV-induced apoptosis including activation of the classical intrinsic apoptotic pathway by the generation of reactive oxygen species [136], initiation of the apoptosis by DNA damage recognition molecules [137], and autocrine signaling through extracellular death receptors by inflammatory cytokines induced by UV [50]. More recently, a role for TLR signaling in apoptotic signaling has become recognized. It has been found that under circumstances not yet fully elucidated that TLR2 signaling is capable of initiating a non-canonical extrinsic apoptotic cell death that is mediated by the activation of caspase-3 [138-141]. It has also been observed that TLR4-deficient mice are resistant to UV-induced immunosuppression which has, so far, been attributed to attenuated Treg formation [35]. As the literature evolves, it is becoming clear that TLRs are frequently implicated in signaling cascades leading to outcomes not previously associated with TLR signaling, including apoptosis.

In this chapter, we investigated the role of TLR4/MyD88 signaling after UV-irradiation. The central hypothesis is that UV activates a non-canonical extrinsic apoptotic pathway that is dependent on a functional TLR4/MyD88. Most of the data presented in chapters three and four have been published by *Innate Immunity* in September 2013 online, ahead of print. Content from that publication has been included in this dissertation with permission of the publisher.

*3.1 Apoptosis is Not Initiated in UV-irradiated MyD88$^{-/-}$ Mouse Models*

To investigate if MyD88 is involved in the cell fate decision after UV-irradiation, immortalized BMM from WT C57BL/6 and MyD88$^{-/-}$ mice were cultured and irradiated with increasing doses of UV. After irradiation, the MyD88$^{-/-}$ cells exhibited significantly increased survival ($p < 0.0001$; Figure 5A). To characterize this phenotype further, morphology of the cell lines was visualized 24 hours after UV irradiation. The WT BMM showed characteristic apoptotic morphology with condensed chromatin and blebbing of cellular material. However, MyD88$^{-/-}$ cells appeared swollen and rounded, and without nuclear chromatin condensation (Figure 5B). The morphologic changes seen in the WT macrophages are characteristic of the non-inflammatory apoptotic cell death associated with UV irradiation, while MyD88$^{-/-}$ cell morphology is consistent with that of a cell undergoing necrosis.

To confirm that these observations hold true *in vivo*, the abdomens of WT and MyD88$^{-/-}$ mice were irradiated with an immunosuppressive dose of UV, and the exposed skin evaluated for signs of apoptosis or necrosis. At 24 hours after UV exposure, there were no gross differences (*i.e.*, erythema, scale or eschar) between the appearance of the skin of MyD88$^{-/-}$ mice and that of WT mice. Epidermal genomic DNA extracted from the irradiated skin of WT mice shows evidence of apoptosis in the form of prominent DNA laddering 24 hours after irradiation, when UV-induced apoptosis is known to peak. Epidermal DNA from MyD88$^{-/-}$ mice does not show this prominent laddering (Figure 6B). An apoptotic DNA ladder is also present in WT, but absent in MyD88$^{-/-}$ peritoneal macrophages (PM) examined *ex vivo* 24 h after 25 mJ/cm$^2$ UV irradiation (Figure 6C). These *ex vivo* MyD88$^{-/-}$ PM also exhibited increased survival after UV when compared to

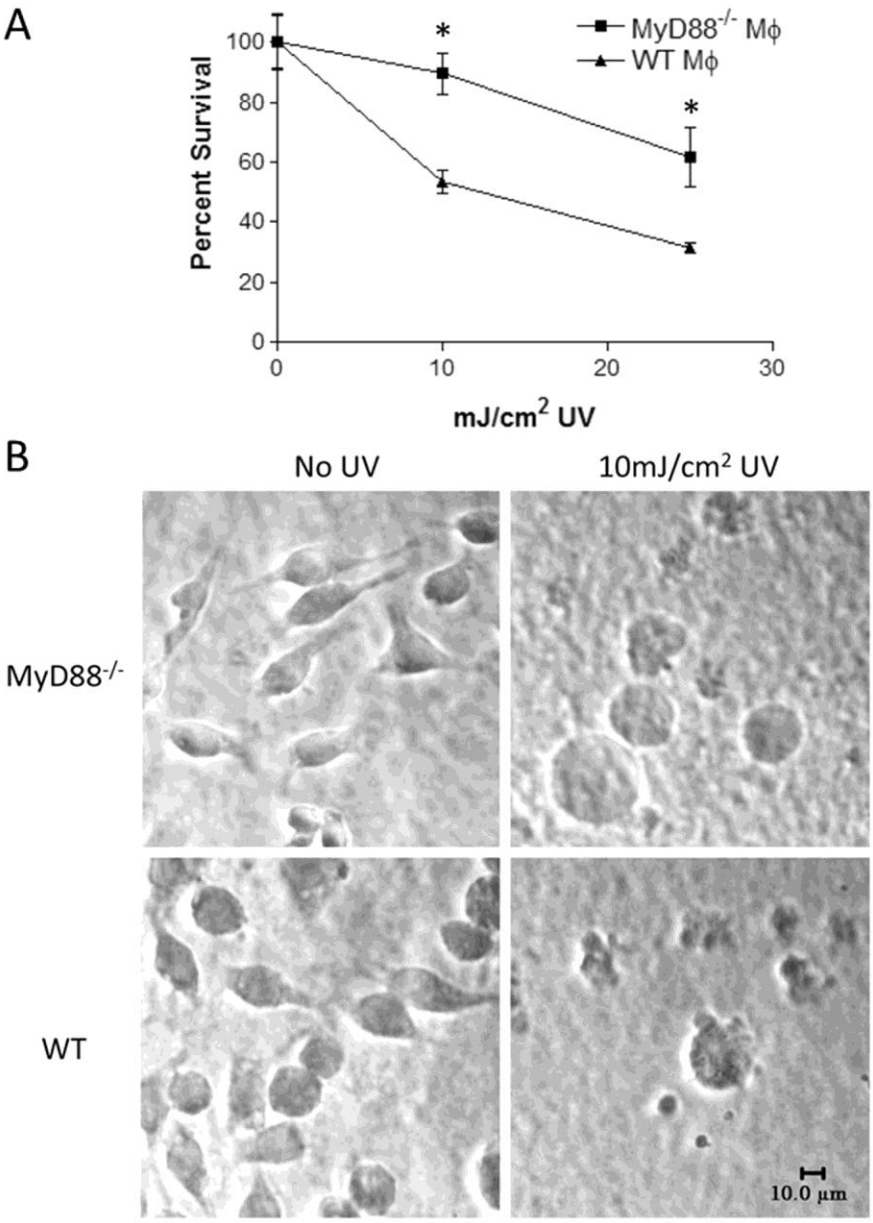


**Figure 5. UV irradiated MyD88$^{-/-}$ cell line exhibits increased survival and decreased apoptotic morphology.** A. Percent survival of immortalized BMM from WT C57BL/6 and MyD88$^{-/-}$ mice is measured 24 hours after UV using an MTT assay, mean of 6 replicates ± SD is shown. Percent survival is normalized to unirradiated control. A significant difference (*, $p<0.0001$) in survival is seen at both UV doses, 10 mJ/cm$^2$ and 25 mJ/cm$^2$. B. The WT and MyD88$^{-/-}$ cell lines were unirradiated or irradiated with 10 mJ/cm$^2$of UV and visualized 24 hours after irradiation for signs of apoptotic morphology. WT cells show condensed nuclei and blebbing off of cellular material, MyD88$^{-/-}$ cells appear swollen and show decreased apoptotic morphology. Results are representative of three separate experiments.

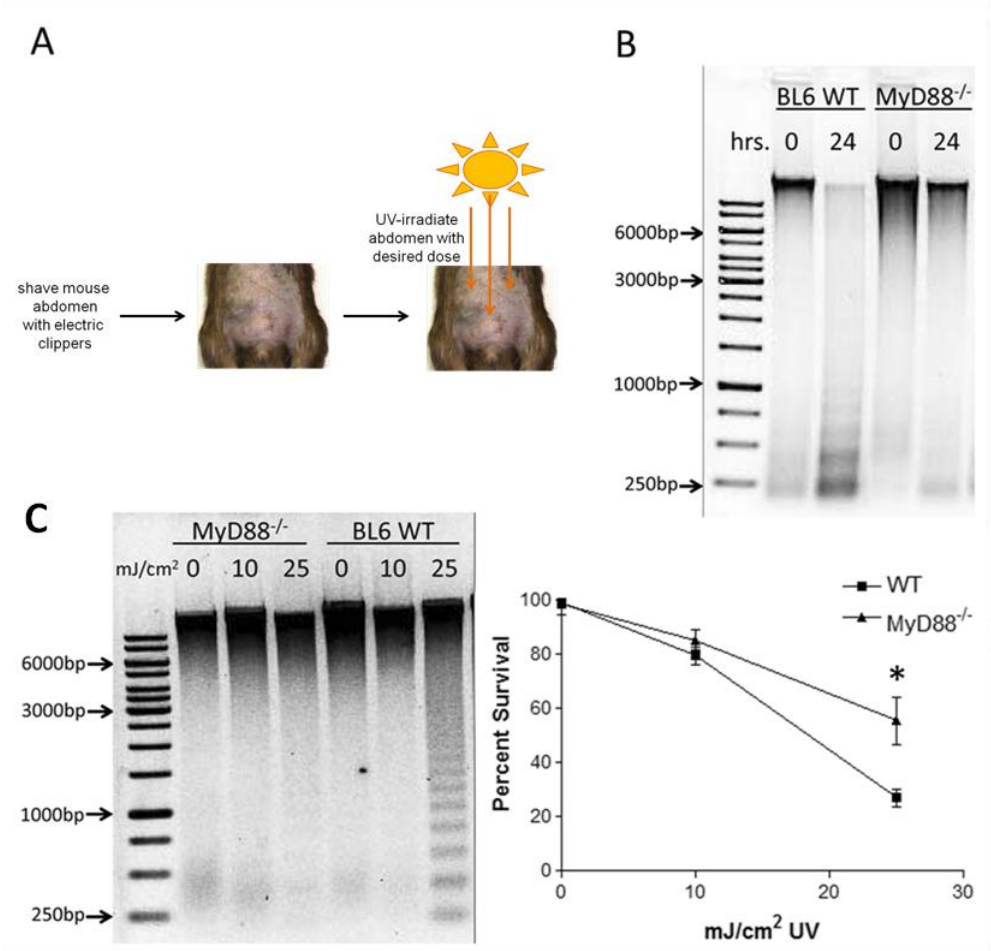


**Figure 6. Epidermal DNA from *in vivo* UV-irradiated MyD88$^{-/-}$ mice and *ex vivo* UV-irradiated PM have decreased DNA laddering when compared to WT.** A. Schematic of methods used for UV-irradiation of mouse abdomens. B. Epidermal DNA was extracted from C57BL/6 WT and MyD88$^{-/-}$ abdomen skin biopsies immediately after, and 24 hours after 70 mJ/cm$^2$ UV irradiation. To assay for apoptotic laddering, 500 ng of epidermal genomic DNA is electrophoresed on an agarose gel. A gel with DNA from one representative mouse from each group of 3 is shown. B. DNA extracted from cultured MyD88$^{-/-}$ and WT PM 24 hours after either no UV, 10, or 25 mJ/cm$^2$ UV. A prominent ladder is seen in the WT cells that received 25 mJ/cm$^2$ UV, but not in cells from MyD88$^{-/-}$ mice. Inverted images of ethidium bromide stained agarose gels are shown in both panels. Survival of WT and MyD88$^{-/-}$ PM 24 h after UV was measured using an MTT assay. At the 25 mJ/cm$^2$ dose of UV, the MyD88$^{-/-}$ PM have significantly increased survival (*, $p<0.0001$) when compared to WT, mean of 6 replicates ± SD is shown.

WT PM, with a significant difference observed 24 h after 25 mJ/cm$^2$ of UV irradiation (Figure 6C). MyD88$^{-/-}$ cells show increased survival and decreased apoptosis after UV irradiation.

*3.2 UV-induced Apoptotic Signaling Cascade is TLR4/MyD88 Dependent*

To elucidate if this cell death phenotype is a result of activation of the TLR signaling pathways for which MyD88 is a necessary scaffolding protein, immortalized BMM from WT, TLR2$^{-/-}$, and TLR4$^{-/-}$ mice on a C57BL/6 background were used in cell death assays. In an MTT assay, the TLR4$^{-/-}$ macrophages were found to have significantly increased survival ($p<0.001$) 24 hours after exposure to increasing doses of UV irradiation when compared to both WT and TLR2$^{-/-}$ cells (Figure 7A). This is the same survival phenotype observed in MyD88$^{-/-}$ cells, suggesting that the TLR4 signaling pathway and its components, including MyD88, are mediating cell fate after UV irradiation. This observation is supported by the lack of DNA laddering seen 24 hours after UV irradiation in TLR4$^{-/-}$ cells (Figure 7B). While a typical apoptotic DNA ladder is seen at both doses of UV in the WT and TLR2$^{-/-}$ cells, it is not visible in TLR4$^{-/-}$ cells even though high doses of UV were used to induce laddering. This evidence supports the hypothesis that the MyD88-dependent TLR4 signaling pathway is contributing to the cell fate decision after UV irradiation.

TRAM and TRIF are also adaptor molecules that can be activated downstream of TLR4 dimerization and represent the second classically recognized arm of the TLR4 signaling pathway. To determine whether these proteins are involved in the UV-induced apoptotic cascade, a BMM cell line immortalized from TRAM/TRIF$^{-/-}$ mice was used in a

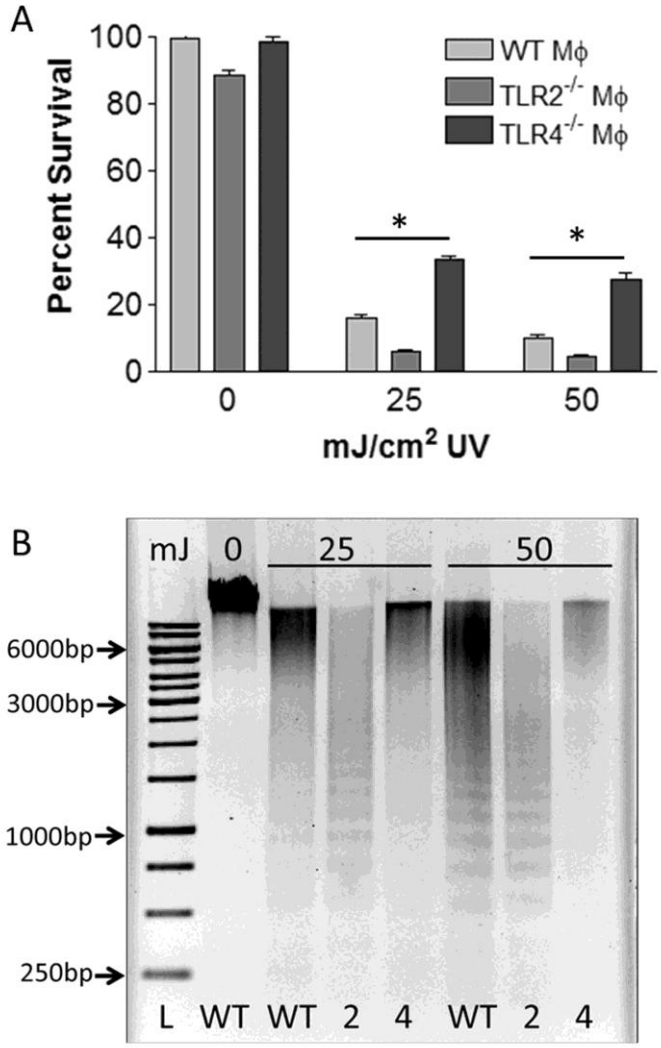


**Figure 7. TLR4$^{-/-}$ macrophages exhibit increased survival and decreased apoptosis following UV irradiation.** A. Percent survival of immortalized BMM from C57BL/6 WT, TLR2$^{-/-}$, and TLR4$^{-/-}$ mice was measured 24 hours after 0, 25, or 50 mJ/cm$^2$ UV using an MTT assay. Mean of 6 replicates from 2 independent experiments ± SD is shown. Percent survival is normalized to unirradiated control. When compared to WT and TLR2$^{-/-}$ BMM, the TLR4$^{-/-}$ BMM have a significant increase in survival, as measured by MTT assay, at both doses of UV (*, $p<0.001$). B. Five hundred ng of genomic DNA extracted from C57BL/6 WT (WT), TLR2$^{-/-}$ (2), and TLR4$^{-/-}$ (4) immortalized BMM cell lines 24 hours after 0, 25, or 50 mJ/cm$^2$ UV-irradiation were electrophoresed on an agarose gel, a 1 kb DNA ladder (L) was included. TLR4$^{-/-}$ DNA does not show a UV-inducible ladder and so is considered not to be apoptotic. Inverted image of ethidium bromide-stained agarose gel is shown, and is a representative of 3 independent experiments.

MTT assay. When compared to WT, TRAM/TRIF$^{-/-}$ cells have similar levels of death 24 h after UV-irradiation (Figure 8). In contrast to MyD88$^{-/-}$ and TLR4$^{-/-}$ macrophages, no increase in survival is seen, suggesting that the TRAM/TRIF-dependent TLR4 signaling pathway is not involved in UV-induced apoptosis.

The canonical TLR4 signaling pathway shows MyD88 interacting with IRAK4 downstream of the dimerization of intracellular TIR domains of TLR4 (Figure 3). To determine if IRAK4 is necessary for the observed TLR4-dependent UV-induced apoptosis, we utilized mice that homogeneously express a catalytically inactive mutant of IRAK4 (IRAK4$^{KDKI}$). Previous publications show that the IRAK4$^{KDKI}$ mice exhibit impaired responses to TLR4 agonists and impaired responses to gram-negative bacteria. While presence of a catalytically inactive protein may allow for some of the scaffolding activity to be retained, which permits some signaling, the majority of TLR4 signaling is ablated in these mice. Twenty-four hours after UV-irradiation, PM from IRAK4$^{KDKI}$ mice show the same dose-dependent genomic DNA ladder as PM from WT mice (Figure 9A), indicating that they are capable of efficiently initiating apoptotic cell death. This finding is supported by data showing that WT and IRAK4$^{KDKI}$ PM have similar survival rates 24 h after being exposed to UV-irradiation (Figure 9B). The ability of IRAK4$^{KDKI}$ cells to undergo apoptosis suggests that the TLR4/MyD88 pathway that is being activated by UV-irradiation diverges from the canonical TLR4 pathway after MyD88, and that MyD88 is most likely cascading with a different molecule, other than IRAK4, to initiate apoptosis.

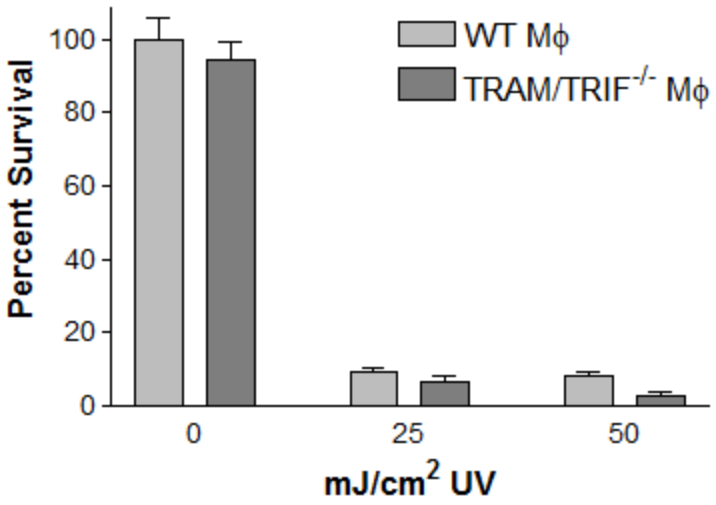


**Figure 8. UV-induced apoptosis is not dependent on the TLR4/TRIF-TRAM pathway.** Percent survival of immortalized BMM from C57BL/6 WT, and TRAM/TRIF$^{-/-}$ mice was measured 24 hours after 0, 25, or 50 mJ/cm$^2$ UV using an MTT assay. Mean of 6 replicates from 2 independent experiments ± SD is shown. Percent survival is normalized to unirradiated control. No significant differences were observed in survival when comparing WT to TRAM/TRIF$^{-/-}$ macrophages.

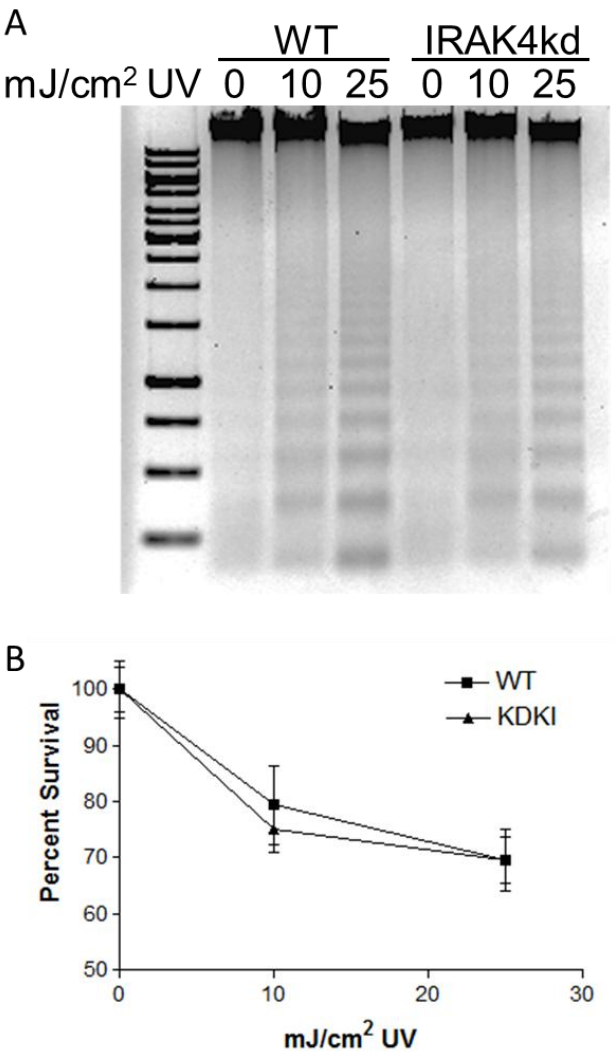


**Figure 9. UV-induced apoptosis is not observed in macrophages with a catalytically inactive IRAK4 molecule.** A. Five hundred ng genomic DNA was extracted from C57BL/6 WT (WT) and IRAK4-kinase-dead mice (KDKI) PM 24 hours after 0, 10, or 25 mJ/cm$^2$ UV-irradiation were electrophoresed on an agarose gel, a 1kb DNA ladder (L) was included. Both WT and KDKI PM show a UV-inducible ladder and are considered apoptotic. Inverted image of ethidium bromide stained agarose gel is shown, and is a representative of two independent experiments. B. Percent survival of PM from WT and KDKI macrophages was measured 24 hours after 0, 10, or 25 mJ/cm$^2$ UV using an MTT assay. Mean of 6 replicates from 2 mice ± SD is shown. Percent survival is normalized to un-irradiated control. There are no significant differences observed in survival when comparing WT to KDKI.

*3.3 TLR4/MyD88 Pathway is also Activated in Human Cells*

To confirm that this phenotype can also be observed in human skin cells, a siRNA knock-down of MyD88 in pools of human primary KC derived from surgical specimens from 3 different healthy donors was performed. A greater than 80% knock down of MyD88 was achieved at both the mRNA and protein level as measured by RT-PCR 24 hours after transfection and Western blot 48 h after transfection, respectively (Figures 10A and 10B). The KC were UV-irradiated 48 h after transfection, then 24 h after UV-irradiation, survival was measured. Similar to the phenotype observed in $MyD88^{-/-}$ and $TLR4^{-/-}$ cell lines, we see that the human primary KC with MyD88 knocked down exhibit increased survival compared to control transfected KC (Figure 10C). These data provide evidence that a functional TLR4/MyD88 signaling pathway is not only necessary for efficient UV-induced apoptosis in mice, but also in human skin cells that are routinely exposed to UV-irradiation.

Here we show that in both mouse and human models MyD88 is necessary for efficient apoptosis after UV-irradiation. Evidence is provided that TLR4 is also necessary for UV-induced apoptosis, but TLR2, TRAM/TRIF, and IRAK4 are not. Data presented in this chapter describes a specific TLR4- and MyD88-dependent signaling pathway that initiates apoptosis after UV-irradiation.

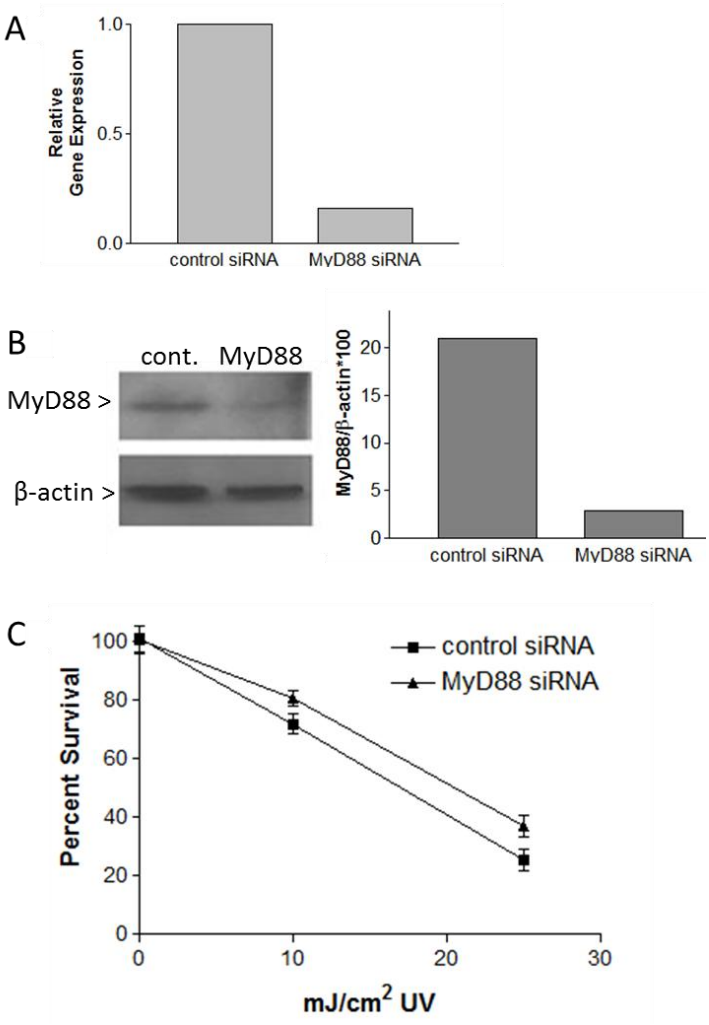


**Figure 10. Increased survival after UV-irradiation is observed in human primary keratinocytes with MyD88 knocked down.** A pool of human primary keratinocytes (KC) from 3 patient samples were transfected with either a MyD88-specific siRNA or a scrambled control siRNA. A. RT-PCR for MyD88 was performed on cDNA made from the transfected KC 24 h after transfection. A >80% knockdown of MyD88 mRNA was achieved. MyD88 transcript levels were normalized to 18S RNA. B. The knockdown was confirmed at the protein level by Western blot with lysates made 48 h after transfection. A >80% knockdown of MyD88 protein was repeatedly achieved. C. Forty-eight h after transfection, the KC were irradiated with either 0, 10, or 25 mJ/cm$^2$ UV, and 24 h after irradiation, an MTT assay was performed to determine cell survival. Samples in which MyD88 has been knocked down exhibited increased survival 24 h after UV-irradiation as compared to control transfected KC. Mean ± SD of triplicate wells are graphed. A representative experiment of 4 replicates with similar results is shown.

## Chapter 4

## Death is Skewed Towards Necroptosis in TLR4/MyD88$^{-/-}$ Cells

The swollen morphology observed in UV-irradiated MyD88$^{-/-}$ BMM indicates that instead of undergoing classical apoptotic death, the cells might be necrotic. Necrosis has long been recognized as a default cell death that occurs when apoptosis cannot be initiated [142]. It is classically thought that necrosis is an unordered and non-specific mechanism of cell death that involves the simple explosion of cellular material into surrounding tissue [143]. However, it has more recently been recognized that activation of specific signaling molecules can lead to the necrosis of a dying cell [144]. Death by these necrotic cell death signaling pathways have been termed necroptosis [145], and is dependent on the formation of a RIP1/RIP3 signaling complex (Figure 2). While a necroptotic signature has not yet been fully identified, this type of cell death causes production and release of a combination of cytokines and DAMPs that distinguish it from other inflammatory cell deaths, such as pyroptosis.

In chapter 3, the data presented indicate that TLR4/MyD88-deficient cells are not able to undergo efficient apoptosis after UV-irradiation. In this chapter, the mechanism by which MyD88- and TLR4-deficient cells are dying is explored. We hypothesize that, in the absence of an active apoptotic pathway, TLR4/MyD88-deficient cells are undergoing Rip1-dependent necroptosis.

*4.1 Necrotic Morphology Is Observed in TLR4/MyD88$^{-/-}$ Models*

To look for further evidence of apoptosis or necrosis, skin biopsy specimens from UV-irradiated and unirradiated mouse abdomens were sectioned and stained with H&E or TUNEL (Figure 11). Unirradiated skin from both WT and MyD88$^{-/-}$ mice exhibited normal histologic features, and, as expected, no TUNEL-positive cells were observed (Figure 11, top two panels). UV-irradiated skin from WT mice maintain an intact epidermis with multiple shrunken, pyknotic KCs scattered throughout the epidermis; TUNEL staining confirmed these were apoptotic KC (Figure 11, third panels). In contrast, the epidermis of UV-irradiated MyD88$^{-/-}$ mice revealed histologic signs of epidermal necrosis. A sheet of eosinophilic staining of the upper epidermis with abnormal retained nuclei indicating necrotic cell death is observed, while having sparse TUNEL positivity (Figure 11, fourth panels). There was no grossly different exaggerated sunburn response in MyD88$^{-/-}$ mice compared to WT mice. These histologic features are consistent with the lack of DNA laddering seen in the epidermal DNA of these MyD88$^{-/-}$ mice, and further contribute to the microscopic and biochemical evidence that MyD88$^{-/-}$ cells are not able to efficiently undergo UV-induced apoptosis.

*4.2 Initiation of Rip-dependent Necroptosis*

The proteins RIP1 and RIP3 are thought to be main components of the recently described “necroptisome” that results in an ordered necrotic cell death (Figure 2) [55]. To investigate if MyD88$^{-/-}$ cells might exhibit necroptotic cell death, PM from WT and MyD88$^{-/-}$ mice were cultured and UV-irradiated *in vitro*, then 0, 10, 60, and 120 minutes

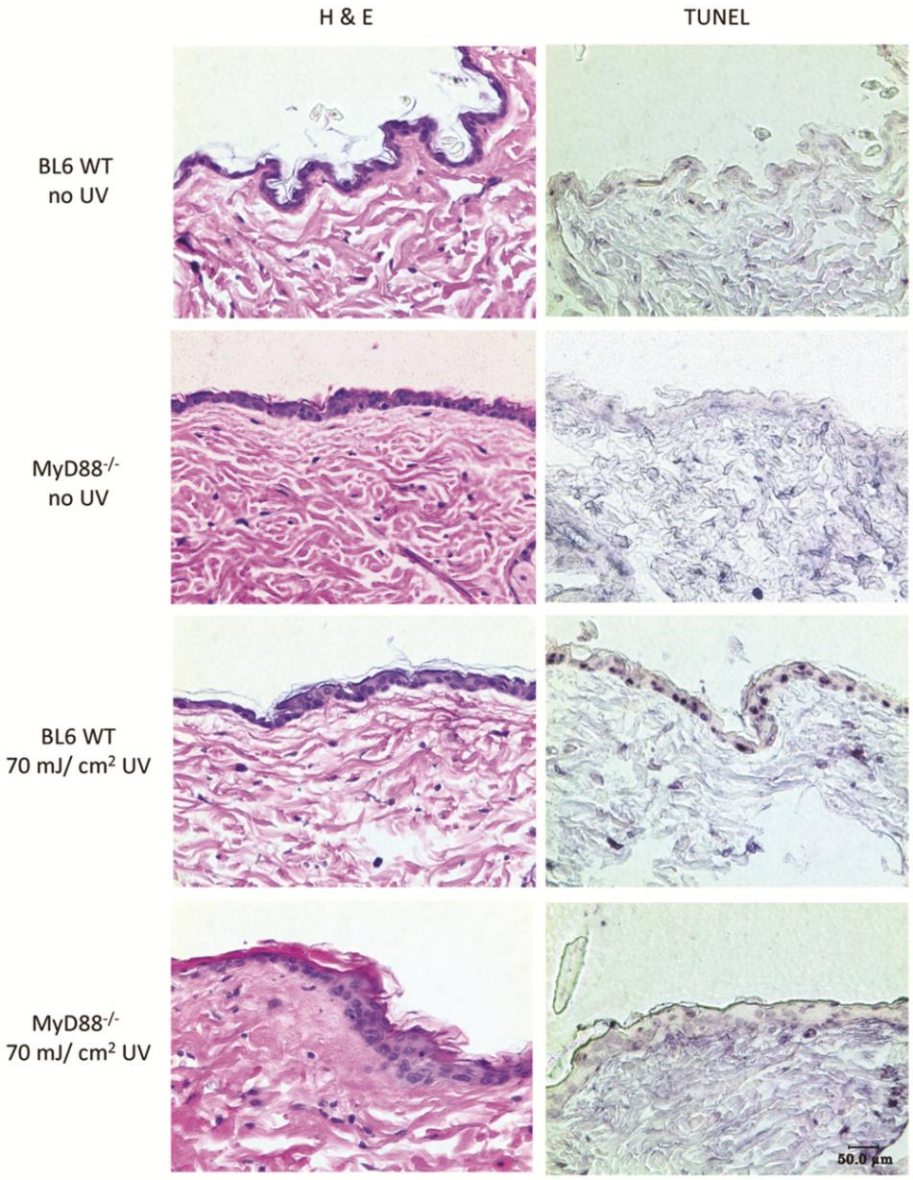


**Figure 11. Skin sections from UV-irradiated MyD88$^{-/-}$ mice have decreased epidermal apoptosis and increased evidence of epidermal necrosis.** Skin biopsy specimens taken 24 h after UV exposure and unirradiated biopsies from each group were formalin-fixed and stained with H&E or TUNEL. A representative image from each group of 6 mice is shown. Only sections from irradiated MyD88$^{-/-}$ mice show markedly decreased epidermal cell apoptosis (very rare TUNEL positive cells), and histologic signs of intense inflammation and possibly, beginning stages of necrosis (*i.e.*, epidermal membrane disappearing, with enlarged undistinguished epidermal cells showing enlarged clear nuclei and DNA, and associated edema and inflammation), while sections from irradiated WT mice show an intact epidermal architecture and highly TUNEL positive (dark blue) epidermal cells (indicative of nicked dsDNA labeled by TUNEL, suggesting that these cells are undergoing early apoptosis), as compared to non-UV epidermal layer and cells (TUNEL negative).

after UV irradiation, levels of RIP1 and RIP3 proteins were investigated by Western analysis. In WT cells, there was observed a time-dependent cleavage of RIP1 that is characteristic of apoptosis [146, 147], and this cleavage was absent in the MyD88$^{-/-}$ cells (Figure 12A). In WT cells, full-length RIP1 decreases 10 minutes after UV, consistent with the appearance of cleaved RIP1, and is restored and then augmented 60 and 120 minutes after UV. MyD88$^{-/-}$ cells showed little variation in full-length RIP1 protein levels; however, they show induction of the necroptotic protein RIP3 120 minutes after UV (Figure 12A), in contrast to WT cells where RIP3 protein levels were consistent throughout time course.

Necroptosis results in an inflammatory cell death that leads to the release of pro-inflammatory cytokines, and specifically, TNF-α. Supernatants from primary PMs were collected 24 h after *in vitro* UV exposure and assayed by ELISA for TNF-α release. A significant increase in TNF-α release was observed in the MyD88$^{-/-}$ cells, but not in WT cells ($p = 0.0139$; Figure 12B). In support this finding, RNA was extracted from UV-irradiated PM and levels of TNF-α mRNA were measured by qRT-PCR. Consistent with the ELISA data, we find that TNF-α mRNA was up-regulated to a significantly higher level in MyD88$^{-/-}$ PM when compared to WT ($p < 0.05$, Figure 12C). The lack of RIP1 cleavage, induction of RIP3, and the enhanced release of TNF-α support the hypothesis that the necroptotic pathway, rather than an apoptotic pathway, is activated by UV irradiation in the absence of MyD88.

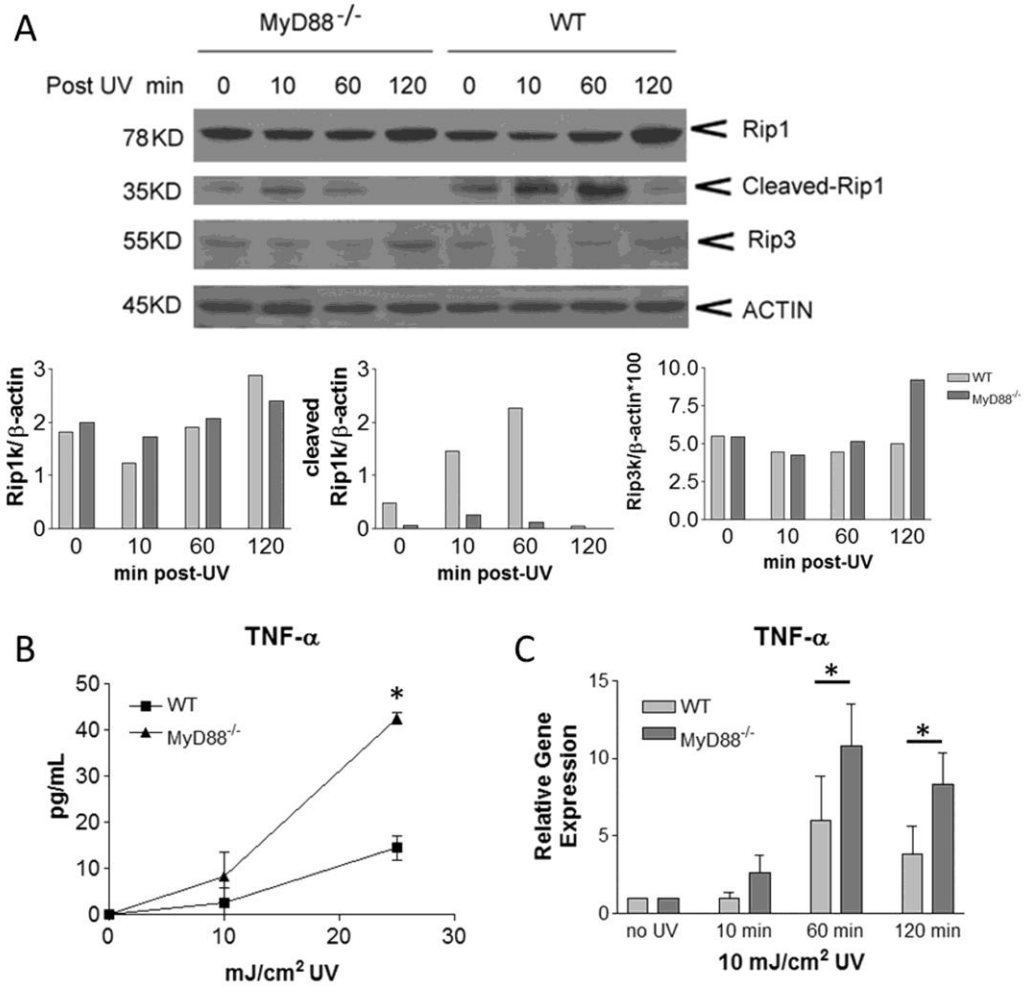


**Figure 12. Necroptotic pathway is activated by UV irradiation in MyD88$^{-/-}$ macrophages.** A. A western blot of UV-irradiated peritoneal macrophages (PM) from MyD88$^{-/-}$ or WT mice shows the kinetics of expression of RIP1, its activation by cleavage, and RIP3 expression. The amount of full-length RIP1, cleaved RIP1, and RIP3 were measured by Western-blot in WT and MyD88$^{-/-}$ PM. Protein is measured 0, 10, 60, and 120 min after 25 mJ/cm$^2$ UV. Densitometry was used to quantify relative protein levels normalized to β-actin, from a single representative experiments (n = 2). This data suggests the possible activation of the necroptosis pathway by UV in MyD88$^{-/-}$ PM. B. Supernatants from PM cultures were collected 24 h after 0, 10, or 25 mJ/cm$^2$ UV irradiation and assayed by ELISA for TNF-α release. The mean ± SD of two independent experiments is shown (*, p = 0.0139). C. TNF-α mRNA expression was measured in MyD88$^{-/-}$ and WT PM 0, 10, 60, and 120 min after 10 mJ/cm$^2$ UV. Significantly greater TNF-α mRNA expression in response to UV irradiation was observed in the MyD88$^{-/-}$ PM as compared to WT. The mean ± SD of 2 independent experiments is shown (*, p < 0.05).

*4.3 Proteins Classically Cleaved/inactivated during Apoptosis Persist Intact*

To define and characterize the observed UV-induced apoptotic pathway further, cleavage/activation of caspase-3 was investigated in PM from WT, MyD88$^{-/-}$, and TLR4$^{-/-}$ mice. Western analysis was carried out with protein lysates collected from cultured WT and MyD88$^{-/-}$ PM at 0, 4, and 8 h after 25 mJ/cm$^2$ UV. There was a time-dependent cleavage of full-length 35 kD caspase-3 into its active 17 kD form in WT cells; however, this cleavage was absent in MyD88$^{-/-}$ cells (Figure 13A). Absence of caspase-3 cleavage in MyD88-deficient cells supports our conclusion that these cells that lack an intact TLR4 signaling pathway cannot undergo apoptosis after UV irradiation. We also performed immunohistochemistry to stain for cleaved caspase-3 8 h after 25 mJ/cm$^2$ UV in PM from WT, MyD88$^{-/-}$, and TLR4$^{-/-}$ cells irradiated *in vitro*. Cleaved caspase-3 was visible in the WT culture, but was absent in the MyD88$^{-/-}$ and TLR4$^{-/-}$ cultures (Figure 13B). Instead, only intact caspase 3 was observed, providing further evidence that the MyD88-dependent TLR4 signaling pathway is necessary for initiation of apoptosis after UV irradiation.

Poly ADP ribose polymerase (PARP) is a DNA damage recognition protein that is cleaved by caspases during apoptosis [148]. Consistent with the previous finding that MyD88$^{-/-}$ and TLR4$^{-/-}$ mice, do not undergo efficient apoptosis after UV compared to WT [34], we found that PARP was cleaved in a time-dependent manner after UV-irradiation in WT PM; however, this cleavage was significantly decreased in MyD88$^{-/-}$ (Figure 14A) and TLR4$^{-/-}$ PM (Figure 14B). Proteins that are classically cleaved during apoptosis, *i.e.*, PARP and RIP1, are not cleaved after UV-irradiation in MyD88$^{-/-}$ and TLR4$^{-/-}$ cells. This lack of cleavage contributes to the evidence that these cells are not able to undergo

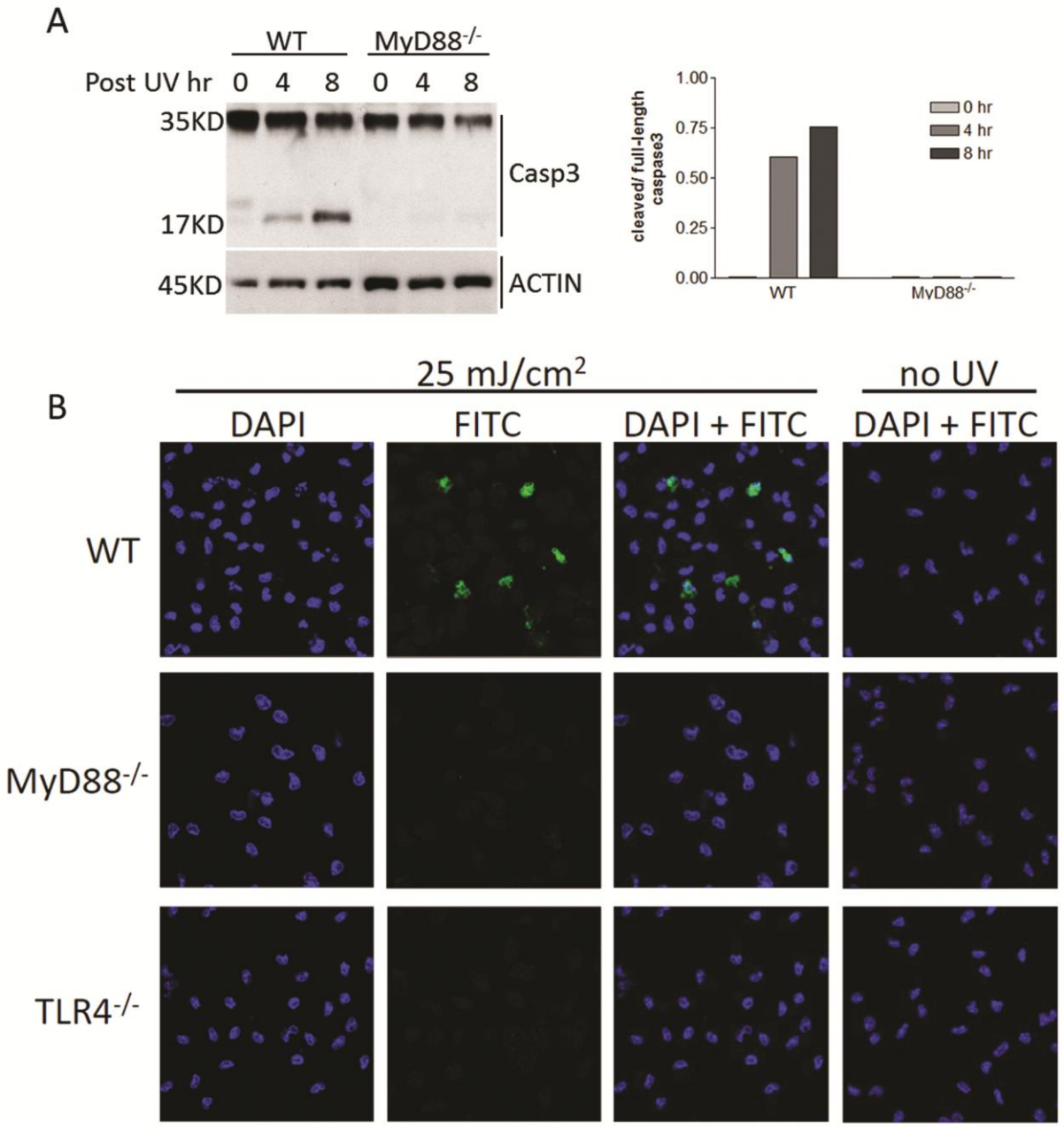


**Figure 13. UV-induced caspase-3 cleavage is dependent on the TLR4-MyD88 signaling pathway.** A. Western blot of PM lysates from WT and MyD88$^{-/-}$ mice taken 0, 4, or 8 h after 25 mJ/cm$^2$ UV irradiation. Blot was probed with an anti-caspase-3 Ab, which shows a 35 KD band that represents full-length caspase-3 and a 17 KD band that represents the cleaved/activated form of caspase-3, or with an anti-β-actin Ab as a loading control. Ratio of density of cleaved/full-length caspase-3 is graphed next to image of blot. B. Cultured PM from WT, MyD88$^{-/-}$, and TLR4$^{-/-}$ mice were fixed 24 h after 25 mJ/cm$^2$ UV and stained for cleaved caspase-3 (FITC) or with a nuclear stain (DAPI).

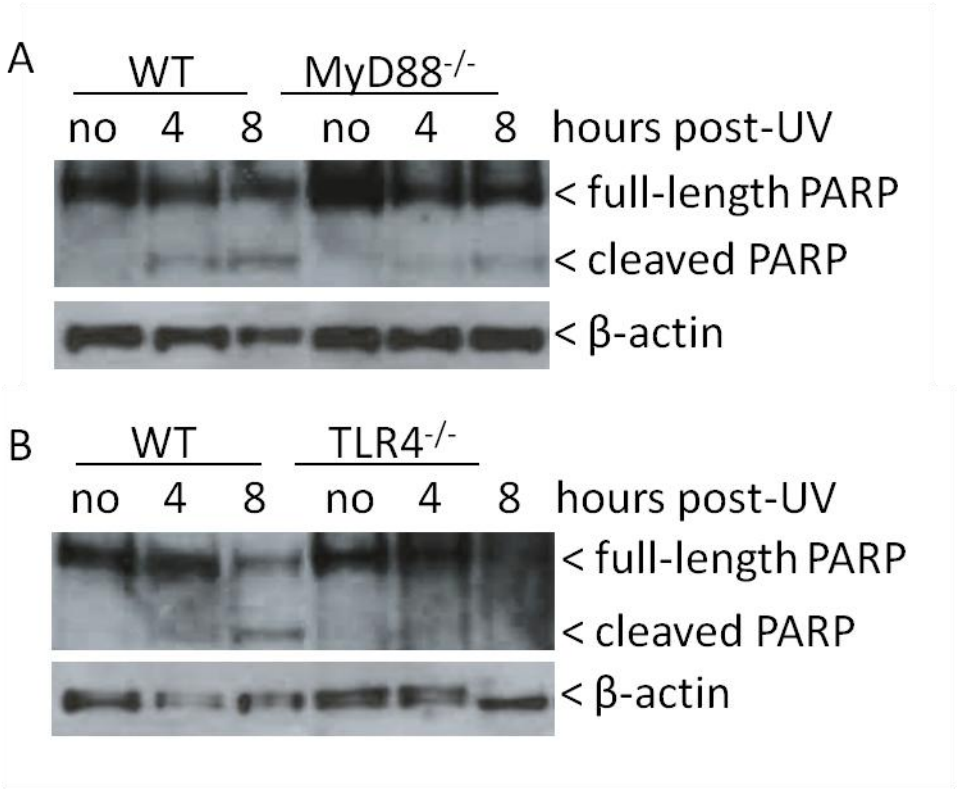


**Figure 14. Decreased cleavage of DNA damage recognition molecule, PARP, after UV-irradiation in MyD88$^{-/-}$ and TLR4$^{-/-}$ PM.** PARP cleavage was measured by Western blot in cultured PM before, 4 h, and 8 h after 25mJ/cm$^2$ UV. Cells from WT mice exhibited a time-dependent cleavage of PARP after UV-irradiation. This cleavage was greatly diminished in MyD88$^{-/-}$ (A) and TLR4$^{-/-}$ (B) macrophages. Representative blots are shown from 3 separate experiments.

apoptosis efficiently and, combined with evidence of necroptisome activation, suggests that without an intact TLR4/MyD88 signaling pathway UV-induced death is skewed from apoptosis to necroptosis.

Evidence presented in this chapter reveals that skin sections from MyD88$^{-/-}$ mice show histologic signs of necrosis, while sections from WT mice exhibit a classical apoptotic histology in response to UV irradiation. Furthermore, full-length (active) PARP and RIP1 persists in MyD88$^{-/-}$ mice, suggesting that such cells are capable of undergoing necroptosis after UV-irradiation. It is also found that there is an augmentation of TNF-α production in MyD88$^{-/-}$ cells, which has been identified as a marker of necroptotic cell death [58]. In addition to RIP1, other proteins, such as caspase-3 and PARP, that are cleaved during apoptosis persist in their full length form in MyD88$^{-/-}$ cells after UV-irradiation. These data allow us to conclude that UV-irradiation causes cells without functional MyD88 to die by necroptosis.

## Chapter 5

## MyD88$^{-/-}$ Mice are Resistant to UV-induced Systemic Immunosuppression

Systemic immunosuppression is a well-recognized consequence of UV-irradiation. In fact, this immunosuppression has been used therapeutically, *i.e.*, phototherapy is often prescribed for treating psoriasis [13]. However, it can also lead to propagation of infections [149] and malignant cancers, such as NMSC and melanoma [150], that would be routinely neutralized in a fully immune-competent individual. While extensive research has been done investigating the mechanisms of UV-immunosuppression, this phenomenon is not yet fully understood. Elucidating a more complete picture of how UV induces immunosuppression will allow this observed effect to be used more effectively as a therapeutic, and guarded against when immunosuppression is an unwanted consequence of UV exposure.

It has been previously shown that TLR4-deficient mice are resistant to UV-induced immunosuppression [35]. After taking into consideration our data presented in chapters three and four, I hypothesized that MyD88$^{-/-}$ mice would exhibit the same resistance to immunosuppression as TLR4$^{-/-}$ mice, and that this phenotype is due to the necroptotic rather than apoptotic mechanism of death in UV-irradiated cells.

### *5.1 Mouse Contact Hypersensitivity Model*

To determine how MyD88 deficiency affects UV-induced immunosuppression, the DNFB contact hypersensitivity (CHS) mouse model was used. Twenty-four hours after elicitation, restimulation with the same sensitizing antigen, both WT and MyD88$^{-/-}$

mice that were sensitized with DNFB exhibit robust ear swelling, while naïve mice have a low level of baseline ear swelling. The WT mice that were UV-treated before DNFB sensitization show a significant ($p<0.0001$) reduction in ear swelling as compared to the WT mice that were not exposed to UV. However, ear swelling in the MyD88$^{-/-}$ mice that were exposed to the same UV-immunosuppressive regimen was not significantly diminished and is significantly ($p = 0.0096$) greater than the paired WT group of mice (Figure 15B). These data support the hypothesis that MyD88$^{-/-}$ are resistant to UV-induced immunosuppression.

In further support of this conclusion, serum was obtained from each mouse on day 21 after sensitization and DNFB-specific IgG2a, an antibody response that is dependent on Th1 lymphocyte-derived IFN-γ [151], was measured. There was significantly ($p = 0.0127$) less DNFB-specific IgG2a in the sera of UV-irradiated WT mice than in sera from UV-irradiated MyD88$^{-/-}$ animals (Figure 15C). It has been previously reported that DNFB elicits mainly a Th1 response that results in production of IgG2a, so as expected, a significant DNFB-specific IgG1 response was not observed (data not shown); however, there was a significant difference seen in DNFB-specific IgG2a in WT vs. MyD88$^{-/-}$ mice. Ear sections stained with H&E from unirradiated and UV-irradiated MyD88$^{-/-}$ mice show similar histologic morphology, with significant edema and cellular infiltrate. While the ear sections from unirradiated WT mice show similar histologic signs of an intact immune response, the ear sections from UV-irradiated WT mice show limited edema and decreased histologic signs of inflammation (Figure 15D).

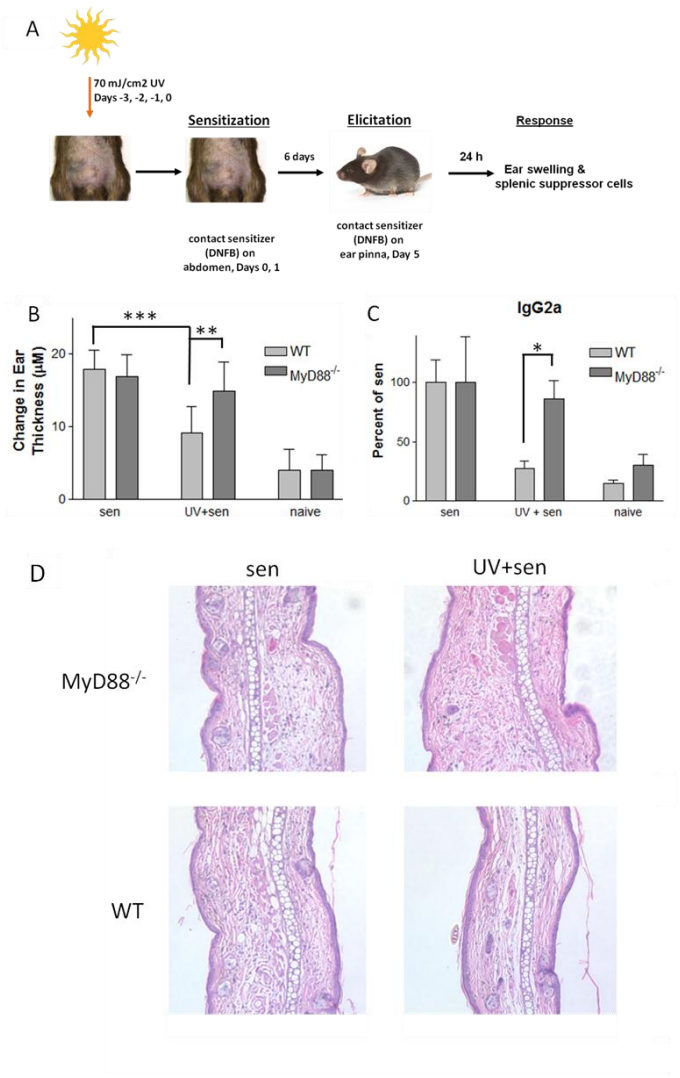


**Figure 15. MyD88$^{-/-}$ mice are resistant to UV induced immunosuppression.** A. WT and MyD88$^{-/-}$ mice are used in the DNFB CHS model. One group was sensitized on the abdomen and restimulated with DNFB on the ear (sen), the second was UV-treated with 70 mJ/cm$^2$ for 4 consecutive days before being sensitized and elicited with DNFB (UV+sen), the final group was naïve and only restimulated with DNFB (naïve). B. Ear thickness was measured before and 24 h after antigen challenge, the amount of swelling elicited by DNFB is graphed. C. Using the same mice from panel A, 21 days after sensitization with DNFB, serum levels of DNFB-specific IgG2a were measured. For each treatment group, n = 7 mice were tested and the mean ± SD is shown; *p = 0.0127; **p = 0.0096; ***p < 0.0001. D. Ear sections from WT and MyD88$^{-/-}$, sen and UV+sen groups were stained with H&E and examined for histologic evidence of inflammation. A representative ear section from each group (n=7) is shown.

*5.2 Antigen Presenting Cell Migration After UV-irradiation*

To address the possibility that UV-irradiation is causing emigration of antigen presenting cells (APC) to local lymph nodes at different rates in WT and MyD88$^{-/-}$ animals, epidermal sheets were stained for MHC II, which stains epidermal Langerhans cells [152]. Twenty-four hours after exposure of mouse ears *in vivo* to 100 mJ/cm$^2$ UV, similar levels of APC emigration from the epidermis was observed in WT and MyD88$^{-/-}$ mice (Figure 16A). Single cell suspensions made from the local lymph nodes of the same irradiated mice show that MyD88$^{-/-}$ mice are capable of producing significantly more ($p = 0.0094$) IFN-γ when stimulated with CD3/CD28-activating beads, as compared to cells from WT mice (Figure 16B). Although WT and MyD88$^{-/-}$ mice exhibit the same amount of APC emigration, the IFN-γ production capabilities of local lymph node cells from MyD88$^{-/-}$ mice was higher. In conjunction with this higher level of immune-competence after UV-irradiation, 24 h after irradiation a significantly lower ($p=0.0469$) amount of DNA damage was detected in the local lymph nodes of MyD88$^{-/-}$ mice as compared to WT mice (Figure 16C). In addition to TLR4$^{-/-}$ mice that were previously reported to be resistant to immune suppression [151], MyD88$^{-/-}$ mice exhibit the same phenotype that may be attributable to the more efficient repair of DNA-damaged APC from the irradiated epidermis.

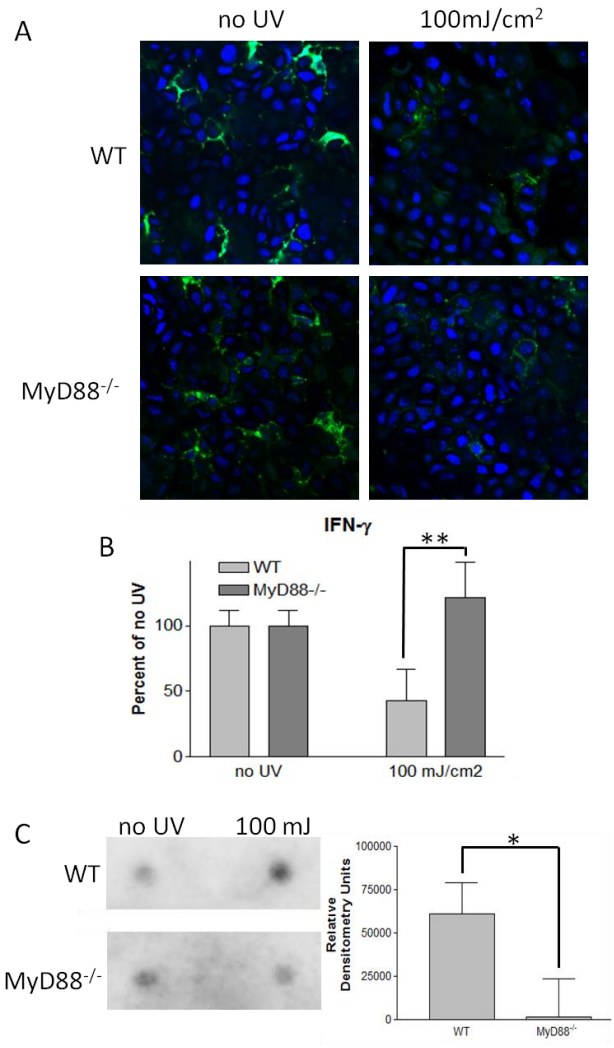


**Figure 16. UV-induced emigration of APC from epidermis is maintained, and DNA damage is decreased in local lymph nodes of MyD88$^{-/-}$ mice.** A. Epidermal sheets from ears irradiated with 100 mJ/cm$^2$ or paired skin from the unirradiated side of the same ear were stained with MHC-II antibody (clone M5/114.15.2). Similar levels of APC are observed to emigrate from the epidermis 24 h after UV in WT and MyD88$^{-/-}$ mice. Representative images are shown from each group. B. Single cell suspensions from inguinal lymph nodes harvested 24 h after ears were irradiated with 100 mJ/cm$^2$ UV, were stimulated with CD3/CD28-activating beads for 72 h, and cell-free supernatants were analyzed for release of IFN-γ. Numbers are graphed as a percentage of IFN-γ released by a paired no-UV control animal, n=3 for each group, **p = 0.0094. C. Whole genomic DNA was extracted from the inguinal lymph nodes 24 h after ears were irradiated with 100 mJ/cm$^2$ UV, CBPD amounts were measured by DNA dot blot. A representative blot is shown. The increase in CBPD over an unirradiated control animal is measured by densitometry and mean ± SD is graphed, n=4 for each group, *p = 0.0469.

## Chapter 6

## Increased DNA Repair in UV-irradiated TLR4/MyD88$^{-/-}$ Models

Cyclobutane pyrimidine dimers (CBPD) are the main form of DNA damage caused by exposure to the UVB spectrum [153]. In healthy cells, CBPD are readily recognized and repaired without mutagenic consequence [46]. However, if CBPD are not able to be excised, carcinogenic mutations are propagated, leading to the development of non-melanoma skin cancers [47]. This consequence is exemplified by xeroderma pigmentosum (XP) patients who are deficient in their nucleotide excision repair (NER) machinery [48]. XP patients have an extraordinary number of malignant skin carcinomas that begin to be visible immediately after birth. The only way to avoid these carcinomas is to completely shield themselves from DNA-damaging UV-irradiation early in life. Functional NER is necessary to maintain genomic stability and immune surveillance in the skin [49].

Previous chapters provide evidence that APC emigrate from the epidermis of MyD88$^{-/-}$ and WT mice at similar rates; however, less UV-induced DNA damage can be detected 24 h after irradiation in MyD88$^{-/-}$ mice. These observations led us to hypothesize that, after UV-irradiation, MyD88$^{-/-}$ mice are capable of more efficient DNA repair than WT mice.

*6.1 Cyclobutane-pyrimidine Dimer (CBPD) Resolution After UV-irradiation*

The reduction of DNA damage in the local lymph nodes of MyD88$^{-/-}$ mice led us to speculate if this phenotype would also be manifested as increased resolution of CBPD in the UV-irradiated skin. To test this hypothesis, serial biopsies were taken from the abdomen of UV-irradiated WT, MyD88$^{-/-}$, and TLR4$^{-/-}$ mice. Immediately after being exposed to 70 mJ/cm$^2$ UV, all three strains of mice showed similar levels of CBPD in epidermal DNA. However, 24 h after UV, levels of CBPD in epidermal DNA from MyD88$^{-/-}$ and TLR4$^{-/-}$ mice were significantly ($p < 0.05$) lower than CBPD detected in WT epidermal DNA (Figure 17). These data suggest that mice without the TLR4/MyD88 signaling pathway are able to be resolve UV-irradiation induced CBPD more efficiently, presumably by more active DNA repair.

To confirm that this phenotype can also be observed in human skin cells, a siRNA knock down of MyD88 in pools of human primary keratinocytes (KC) derived from surgical specimens from 3 different healthy donors was performed. A >80% knock down of MyD88 was achieved at both the mRNA and protein levels as measured by RT-PCR 24 hours after transfection and Western blot 48 h after transfection, respectively (Figures 10A and 10B). The KC were UV-irradiated 48 h after transfection, DNA was extracted 24 h after UV, and a DNA dot blot was carried out to evaluate CBPD resolution. KC with MyD88 knocked-down, as compared to control transfected, were able to resolve about twice as many of the CBPD 24 h after irradiation with 25 mJ/cm$^2$ (Figure 18). MyD88 siRNA-treated human keratinocytes, similar to MyD88$^{-/-}$ mice, are able to repair UV-induced DNA damage at a faster rate than paired control treated KC.

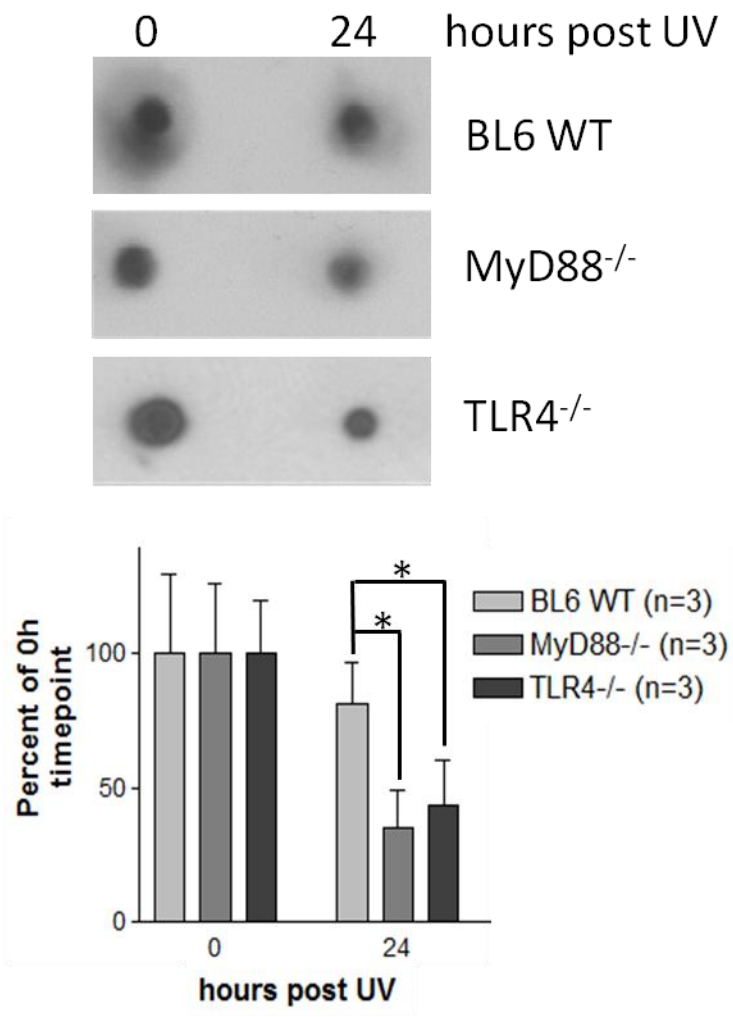


**Figure 17. Increased DNA repair is observed in MyD88$^{-/-}$ and TLR4$^{-/-}$ epidermal DNA.** Epidermal DNA was extracted from WT, MyD88$^{-/-}$, and TLR$^{-/-}$ abdominal skin biopsies from mice that have been irradiated with 70 mJ/cm$^2$ UV. A DNA dot blot was performed with 500 ng of epidermal DNA extracted immediately after (0 h) or 24 h after UV-irradiation. A representative dot blot image is shown, while the mean ± SD percent of densitometry from the 0 h time point is graphed, n=3 for each group, *$p < 0.05$.

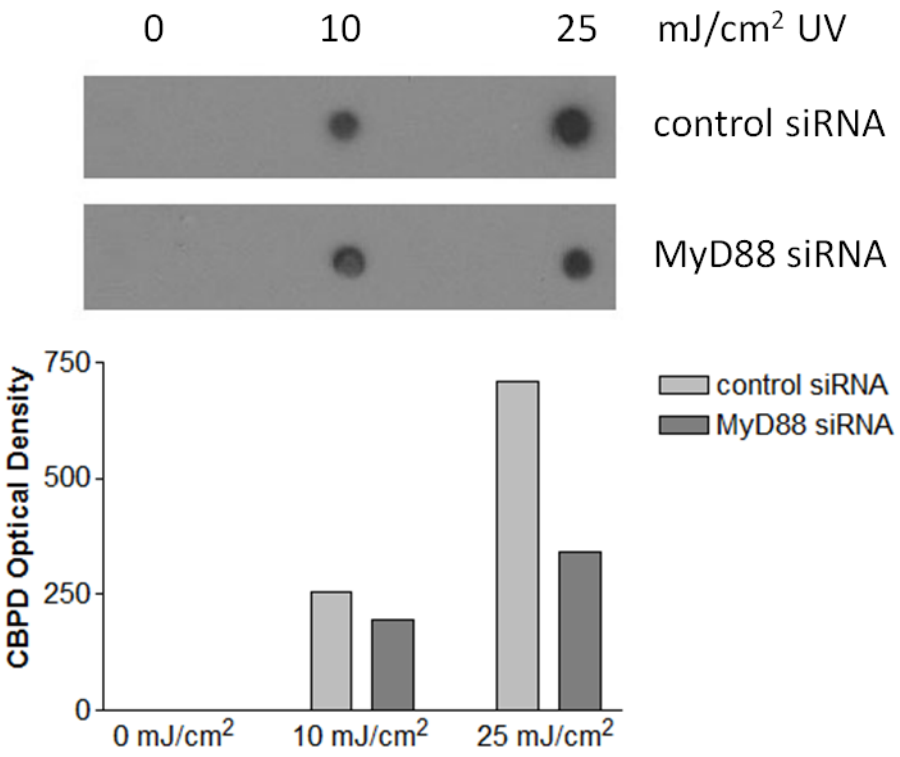


**Figure 18. Increased DNA repair is observed in human primary keratinocytes with MyD88 knocked down.** A greater than 80% knock down of MyD88 mRNA and protein is achieved in human primary KC (Figure 6A and 6B). Forty-eight h after transfection, the KC were irradiated with either 0, 10, or 25 mJ/cm$^2$ UV, and 24 h after irradiation, CBPD levels were measured in extracted genomic DNA using a DNA dot blot. Samples in which MyD88 has been knocked down show a reduction in CBPD 24 h after UV-irradiation as compared to control transfected KC. A representative experiment of 4 replicates with similar results is shown.

*6.2 Increased CBPD Resolution is Dependent on PARP-1*

DNA damage recognition is crucial for effective repair and resolution of lesions. Damage recognition molecules, such as PARP, are cleaved by caspases during apoptosis, a condition when DNA repair is no longer necessary because the cell is dying [148]. Consistent with the previous finding that MyD88$^{-/-}$ and TLR4$^{-/-}$ mice, compared to WT, do not undergo efficient apoptosis after UV [34], we found that PARP is cleaved in a time-dependent manner after UV-irradiation in WT PM; however, this cleavage is significantly decreased in MyD88$^{-/-}$ (Figure 14A) and TLR4$^{-/-}$ PM (Figure 14B). To investigate if the DNA-damage recognition molecule PARP is necessary for the increased resolution of dimers observed in MyD88 and TLR4 deficient models, the water soluble PARP-inhibitor, PJ-34, was used in PM culture experiments. In the presence of PJ-34, MyD88$^{-/-}$ PM lose their ability to resolve CBPD at a higher rate, while PJ-34 treatment has no effect on the resolution of CBPD in WT PM (Figure 19).

Since these data showed that PARP is necessary for increased DNA repair *in vitro*, we next sought to determine if PJ-34 would also be effective in mouse skin cells in an *in vivo* model of DNA repair. WT and MyD88$^{-/-}$ mouse abdomens were injected intradermally with a previously described effective dose of PJ-34 [154] 2 h before irradiation with 70 mJ/cm$^2$ UV. Serial biopsies were then taken immediately after and 24 h after UV to measure the resolution of epidermal CBPD. Consistent with the *in vitro* data, we found that *in vivo* inhibition of PARP with PJ-34 resulted in MyD88$^{-/-}$ epidermal DNA having a WT level of CBPD resolution 24 h after irradiation (Figure 20). The increased DNA damage resolution observed in cells without a functional TLR4/MyD88

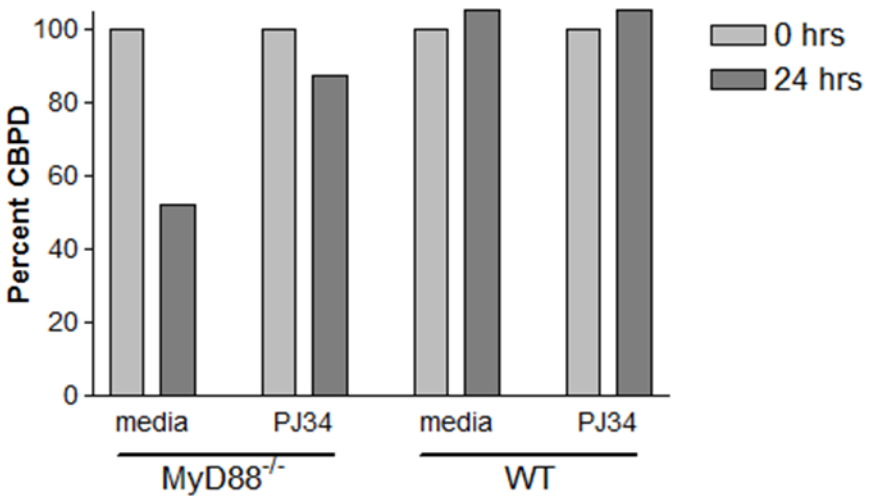


**Figure 19. Increased resolution of CBPD is dependent on PARP.** PM from WT and MyD88$^{-/-}$ mice were treated for 30 min with either media alone or media with 1 µg/mL PJ-34. Cells were then irradiated with 25 mJ/cm$^2$ UV, and DNA was extracted immediately after or 24 h after UV. DNA dot blots were run with 500 ng of genomic DNA. Densitometry of CBPD is graphed as a percentage of dimers detected immediately after UV. A representative experiment of 3 replicates with similar results is shown.

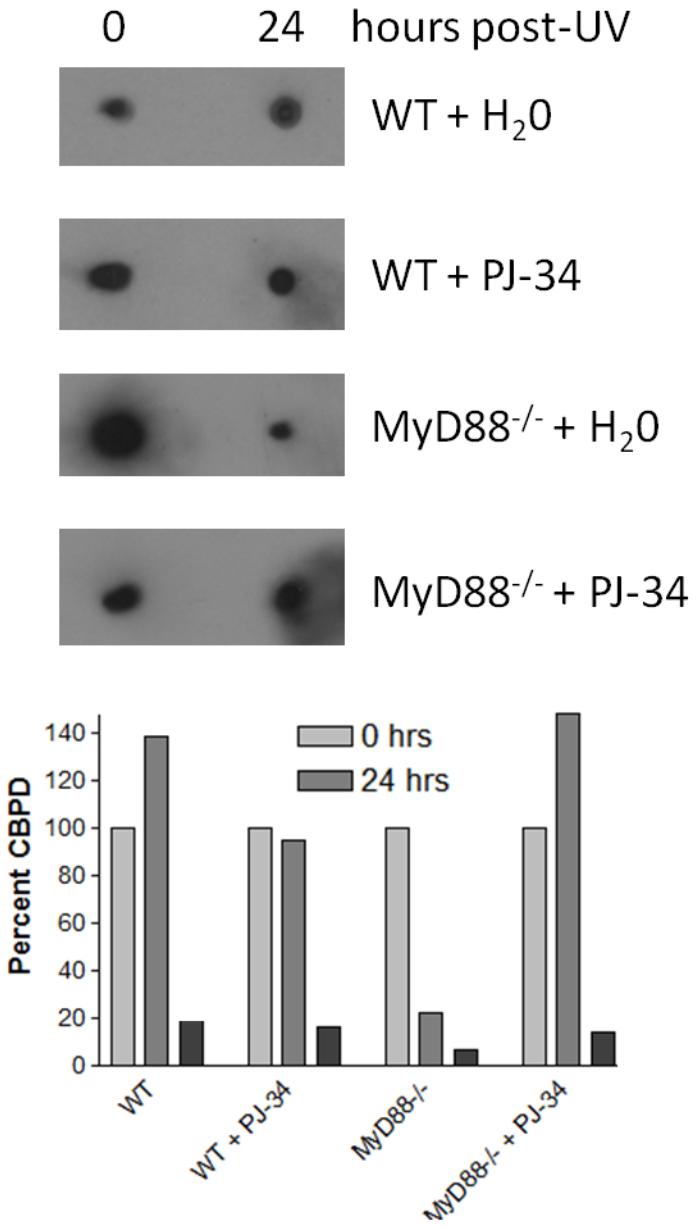


**Figure 20. Inhibition of PARP *in vivo* diminishes the increased DNA repair observed in MyD88$^{-/-}$ mice.** A. Hair was removed from the abdomens of WT and MyD88$^{-/-}$ mice, which were then injected intradermally with either 235 µg of PJ-34 or water, as a vehicle control. Two hours after injection, mouse abdomens were irradiated with 70 mJ/cm$^2$. Serial skin biopsies were taken immediately following and 24 h after irradiation. B. Epidermal DNA was extracted from the skin biopsies and 500 ng of each sample was used in a DNA dot blot. A representative blot is shown for each condition. The mean percent of 0 h densitometry is graphed, n = 4 for each group.

signaling pathway is dependent on the persistence of the DNA-damage recognition molecule PARP.

*6.3 Nucleotide Excision Repair Proteins are Necessary*

In addition to damage recognition by PARP, we investigated if the observed increase in damage resolution is dependent on NER machinery, the predominant repair pathway for CBPD [148]. I hypothesized that NER machinery is involved in the observed increase in repair because the XP family of genes work in collaboration with PARP to facilitate DNA repair in the NER pathway. It has previously been shown that bone marrow-derived macrophages responded similarly to UV-irradiation as skin cells that are routinely physiologically exposed [155]. Because bone marrow-derived macrophages responded similarly, we utilized a lymphoblast cell line from a XP patient who is deficient in XPA, one of the critical NER molecules. A >75% knock down of MyD88 was achieved by siRNA tansfection, at both the mRNA and protein levels in XP and WT lymphoblasts as compared to control transfected (data not shown). Forty-eight hours after transfection, the cells were irradiated with 50 mJ/cm$^2$ UV, then CBPD were detected by DNA dot blot immediately following and 24 h after irradiation. As predicted, the WT cells with MyD88 knocked down showed an increased resolution of CBPD 24 h post-UV, however the XPA-deficient cells did not exhibit this phenotype of increased repair (Figure 21). These data describe a pathway for DNA repair that is dependent on CBPD recognition by PARP and repair by NER machinery. This repair is activated by UV-irradiation in the absence of the apoptosis initiating TLR4/MyD88 signaling pathway.

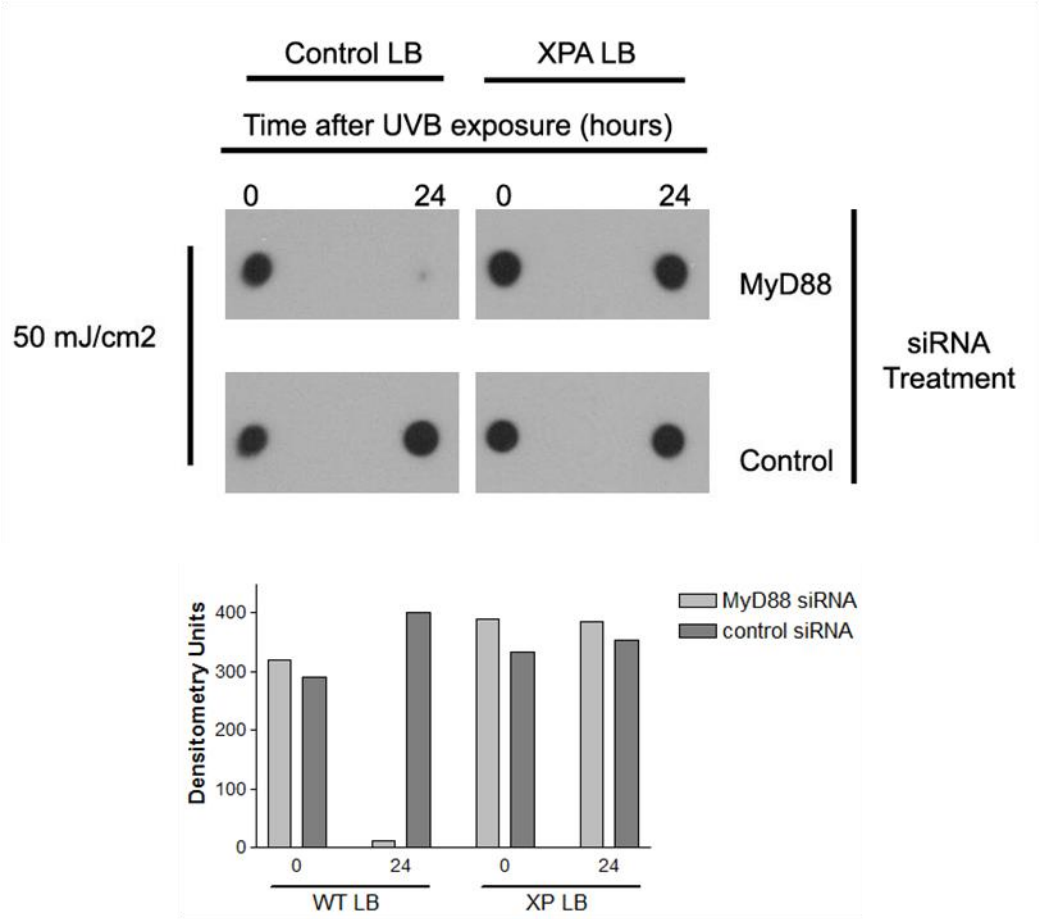


**Figure 21. Knockdown of MyD88 in cells from a xeroderma pigmentosum group A (XPA) patient fails to resolve CBPD.** Lymphoblasts from a healthy donor and XPA patient were transfected with either MyD88 or control siRNA. A >75% knockdown of MyD88 was achieved, by siRNA tansfection, at both the mRNA and protein level in XPA and WT lymphoblasts as compared to control transfected (data not shown). Forty-eight h after transfection, cells were irradiated with 50 mJ/cm$^2$ UV, then DNA was extracted immediately after or 24 h after irradiation. Densitometry from a representative experiment of 3 replicates is graphed. There was a decrease in CBPD detected 24 h after UV in the WT cells with MyD88 siRNA, as compared to control. This difference is not observed in the XPA cells.

## Chapter 7

## Discussion

Activation of extracellular death receptors, such as TNFR and Fas, leads to apoptotic cell death through the activation of caspases. Discussion about how this immunologically silent mode of cell death affects the outcome of damaged, inflamed, or infected tissue continues to be ongoing in many areas of research, including the arena of UV-induced tissue damage. UV-irradiation is well known to induce apoptotic cell death by several mechanisms: DNA damage activating intrinsic cell death, autocrine/paracrine cytokine signaling activating extracellular death receptors, and UV-irradiation directly trimerizing/activating extracellular death receptors. Dysfunctional TLR4 signaling has been associated with attenuated classical responses to UV, specifically systemic immunosuppression. This thesis describes a novel UV-activated extrinsic apoptotic signaling pathway downstream of TLR4/MyD88, which if disrupted skews UV-induced cell death to necroptosis.

Herein we first describe that MyD88-deficient mouse immortalized cell lines do not undergo apoptosis efficiently after UV irradiation and exhibit increased survival (Figure 5). Consistent with this finding, a characteristic apoptotic signature, DNA laddering, was also diminished in *ex vivo* UV irradiated MyD88$^{-/-}$ mouse epidermal and PM cells, but is present in WT cells (Figure 6). Staining of skin sections from these UV-irradiated MyD88$^{-/-}$ mice shows signs of epidermal necrosis and an absence of TUNEL staining, while WT skin sections show characteristic apoptotic KC after UV irradiation (Figure 11). Although MyD88 is not classically associated with UV-induced apoptosis,

because this protein contains a death domain, it may be capable of acting as a scaffold for caspase-activating proteins. There are other known mechanisms of UV-induced apoptosis, and so it is interesting, and perhaps surprising, that MyD88 plays such a critical role in the apoptotic phenotype. FADD is another death domain-containing protein, and has been demonstrated to control the axis between apoptosis and necrosis [156]. Collectively, the results presented herein suggest that MyD88, like FADD, may play an important role in deciding cell fate after UV irradiation.

Necroptosis is rapidly becoming recognized as an alternative to apoptotic cell death. In this study, we observed activation of necroptotic markers in MyD88$^{-/-}$ cells that are not able to undergo an efficient apoptosis after UV irradiation (Figure 12). Our data is consistent with evolving literature that describes necroptosis as a default cell death pathway in the absence of apoptosis [56, 60, 157, 158]. It has recently been shown that RIP1 controls and induces TNF-α production during necroptosis [58]. The data indicate that after UV irradiation, MyD88$^{-/-}$ cells up-regulate TNF-α mRNA, and release a significantly increased amount of TNF-α protein compared to WT cells, consistent with necroptotic cell death (Figure 12B, 12C). This TNF-α release may act as a secondary inducer of apoptosis, and thereby represent an elegant compensatory strategy that the cell has evolved to induce apoptosis in cells in which the apoptotic pathway has otherwise been inhibited. Increased production of TNF-α may also contribute to necroptotic cell death, as signaling through the TNF receptor has been shown to induced necroptosis in the presence of RIP3 [159]. During studies of glioblastomas, it has also been found that TNF-α signaling leads to increased expression of TLR4 [160]. Upregulation of both TNF-α and TLR4, and the positive feedback of one on the other [34, 161], may be

contributing to the exacerbated inflammatory phenotype we observed in our model. Further investigation will be required to further confirm if these MyD88$^{-/-}$ and TLR4$^{-/-}$ cells are dying by necroptosis, and to determine the role TNF-α is playing in the necroptotic phenotype observed in this study.

If MyD88 is involved in cell fate secondary to its role as an adapter protein in TLR signaling pathways, then we would expect TLR$^{-/-}$ cells to have a similar phenotype as MyD88$^{-/-}$ cells after UV irradiation. Our data suggest that TLR4, but not TLR2, is involved in the apoptotic response to UV irradiation (Figure 7). The MyD88-dependent TLR4 signaling pathway is specifically necessary for this apoptosis, as the TRAM/TRIF-dependent TLR4 signaling pathway remained intact in MyD88$^{-/-}$ mice and the necroptotic phenotype is observed. To support this conclusion, we find that cells from TRAM/TRIF$^{-/-}$ (Figure 8) and IRAK4$^{-/-}$ (Figure 9) mice also show a WT survival phenotype after UV-irradiation. MyD88 has been demonstrated to couple TLR signaling to the caspase-activating, extrinsic apoptotic pathway through its death domain, although specific conditions resulting in this have not yet been elucidated [162]. In this dissertation, a lack of caspase-3 activation after UV was observed in both MyD88$^{-/-}$ and TLR4$^{-/-}$ mice (Figure 13). It is possible that after UV irradiation, TLR4 is activated in a way that allows MyD88 to serve as a scaffold for apoptotic proteins as opposed to classical TLR signaling intermediates that form the Myddosome [163]. There is also a report that UV irradiation can directly induce ligand-independent trimerization of TNF-α receptor and lead to apoptosis [164]. It will be important in future studies to determine if TLR4 is activated directly by UV irradiation, similarly to other extrinsic death pathways such as TNFR1 and Fas [165], or by DAMPs released after UV irradiation. The observation that oxidized

phospholipids such as OxPAPC [166] and HMGB1 [167] are DAMPs known to activate TLR4 support the possibility of a role for TLR4 in this pathway.

Not only is the mode of TLR4 activation unknown, the TLR4 signaling pathway activated by UV that leads to apoptosis still needs to be identified and is the subject of ongoing investigation. Currently, I hypothesize that after UV-activation of the TLR4 signaling pathway, the death domain of MyD88 is able to cascade with the extracellular death receptor scaffolding molecule FADD and lead to a non-canonical extrinsic apoptosis (Figure 22). There is preliminary evidence that FADD migrates to the cell membrane after UV-irradiation (data not shown), and then possibly interacting with MyD88 to initiate apoptosis. Future studies will confirm that MyD88 and FADD are interacting after UV, compare UV-initiated TLR4 signaling with extracellular death receptor signaling, and use protein structure modeling software to identify possible domains on MyD88 and FADD that could be interacting.

Consistent with our findings, C3H/HeJ mice, which are TLR4-hyporesponsive due to a spontaneous point mutation in the TLR4 TIR domain that rendered it incapable of signaling in response to TLR4 agonists, exhibit a decreased susceptibility to UV-induced immunosuppression [158]. Given our findings, we would expect MyD88$^{-/-}$ mice to exhibit a similar phenotype, *i.e.*, resistance to UV immunosuppression. Perhaps, this decreased sensitivity to UV immunosuppression is a result of the lack of apoptotic cell death and subsequent initiation of proinflammatory mediators during necroptotic cell death. This hypothesis is supported by the increase in TNF-α mRNA expression and protein release by irradiated MyD88$^{-/-}$ cells (Figure 12B, 12C). Apoptosis initiated by UV irradiation has long been thought of as a positive consequence that enables the skin to

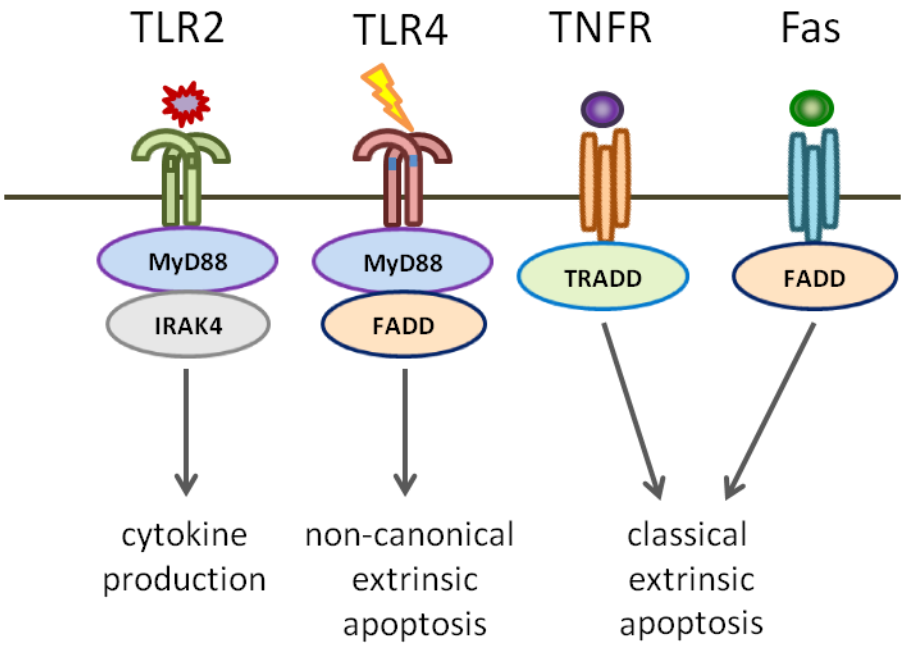


**Figure 22. UV-activated TLR4 signaling may use FADD to initiate a non-canonical extrinsic apoptosis.** Classical TLR signaling, in this diagram TLR2, leads to cytokine production and inflammation, while classical extracellular death receptor signaling, in this diagram TNFR and Fas, leads to apoptotic cell death. The observation that TLR4 signaling after UV-irradiation results in apoptotic cell death lead us to propose that after UV-activation of the TLR4 signaling pathway, the death domain of MyD88 is able to cascade with the extracellular death receptor scaffolding molecule FADD and lead to a non-canonical extrinsic apoptosis.

rid damaged cells in a way that does not cause undue inflammation. The immunosuppressive effects of UV irradiation have broad-reaching effects on the immune system, and by allowing cells to die without inflammation, apoptosis caused by signaling through MyD88 may substantially contribute to this impaired immune surveillance.

To substantiate this hypothesis, we carried out contact hypersensitivity experiments in WT and MyD88$^{-/-}$ mice and, as hypothesized, found that MyD88$^{-/-}$ mice were resistant to UV-induced immunosuppression (Figure 15). Work by Margret Kripke during the 1970's found that this UV-induced immunosuppression was a critical step that allowed for the growth of cancerous tumors on the skin [161, 163, 168]. Not only does UV cause the proliferation of tumor-specific T regulatory cells [166], but also, it damages skin resident APC and causes them to migrate out of the skin to the local lymph node (LLN) [169]. In our model, we find that skin resident APC migrated out of the epidermis at a similar rate in WT and MyD88$^{-/-}$ mice (Figure 16A). However, when stimulated with CD3/CD28-activating beads, LLN cells from MyD88$^{-/-}$ mice were capable of producing significantly more IFN-γ (Figure 16B). While IFN-γ production is suppressed in WT mice by UV, it is slightly augmented in MyD88$^{-/-}$ mice, perhaps as a consequence of the previously described inflammatory necroptotic cell death. Additionally, when probed for DNA damage, the LLN of the MyD88$^{-/-}$ mice presented with less CBPD than WT mice (Figure 16C). These data suggest that there is increased DNA repair in MyD88$^{-/-}$ cells that may be allowing for the observed resistance to UV-immunosuppression.

As previously discussed, TLR4$^{-/-}$ and MyD88$^{-/-}$ cells do not undergo a typical apoptotic cell death after UV-irradiation, they instead, die by necroptosis [167]. During UV-induced apoptosis, the DNA damage recognition molecule PARP is routinely

cleaved by caspase-3 [170]. In our experimental systems we find that PARP is not cleaved/inactivated after UV-irradiation in TLR4$^{-/-}$ and MyD88$^{-/-}$ cells (Figure 14). We also find that in both mouse and human cells that lack a functional TLR4/MyD88 pathway, increased resolution of CBPD is observed after UV-irradiation (Figures 17 and 18). PARP is able to recognize CBPD and function as a recruiter of the NER machinery, which can work to repair the DNA lesion [171]. In TLR4/MyD88-deficient cells that maintain full-length/functional PARP after UV-irradiation, it is not surprising that we observe increased resolution of CBPD and cell survival related to increased repair.

If this increased resolution of CBPD is dependent on full-length PARP, then when PARP is inhibited, more CBPD should be detected in UV-irradiated TLR4/MyD88-deficient cells. Using PJ-34, a water soluble PARP-inhibitor, we find both *in vitro* (Figure 19) and *in vivo* (Figure 20) that CBPD in MyD88$^{-/-}$ cells are restored to WT levels. Futher, using MyD88 knockdown approach in cells from an XP patient, we observed that increased repair in MyD88-deficient cells was also dependent on having functional NER machinery (Figure 21). These data provide a previously unappreciated, direct link between TLR signaling and DNA repair after UV-irradiation, and may begin to change the way we think about classical TLR signaling, along with the possible conditions that activate and consequences of activating them.

During my dissertation research, I discovered a novel MyD88-dependent TLR4 signaling pathway that directly activates apoptosis in response to UV. In addition, I observed that in the absence of a functional TLR4/MyD88 signaling pathway, cell death after UV-irradiation is skewed to a more inflammatory ordered necrotic cell death termed necroptosis. Because TLR4/MyD88-deficient cells are dying in a more inflammatory and

immunogenic way, MyD88$^{-/-}$ and TLR4$^{-/-}$ animals are resistant to systemic immune suppression caused by UV-irradiation, which plays a critical role in the development of UV-induced skin cancers. Lack of apoptosis in these deficient cells allows for more efficient repair of DNA damage caused by UV-irradiation. This increase in DNA repair is dependent on PARP and molecules of the nucleotide excision repair pathway. My research identified activation of a previously unrecognized non-classical extrinsic apoptotic signaling cascade that is activated by UV-irradiation. These studies provide a rationale for treatment of UV-induced damage by blockade of the TLR4 signaling pathway which would be predicted to aid in dampening immune suppression by increasing immune surveillance, allow for increased DNA repair in damaged cells, and lead to the development of fewer UV-induced skin cancers.

Eritoran is a TLR4 antagonist that has been successful in treating conditions ranging from hemorrhagic shock and ischemia-reperfusion injury, to chronic inflammation [170-172]. This drug represents a possible treatment that would convey our observed beneficial necroptotic cell death phenotype on skin cells after UV-irradiation. To test this hypothesis we could create a topical emulsion of Eritoran and apply it to the abdomen of mice in a prophylactic manner, similarly to sunscreen, before UV-irradiation. Treatment with Eritoran should cause UV-irradiated skin cells to die by necroptosis, and should convey all of the positive phenotypes observed to go along with this inflammatory cell death such as decreased immunosuppression and increased DNA repair. If these studies are then expanded to include a chronic UV-carcinogenesis model, Eritoran could represent a therapeutic active compound that could be added to sunscreen to prevent the propagation of UV-induced cancerous mutations.

Additional future research projects will use molecular biology techniques to (1) identify the molecules in the TLR4-apoptosis signaling cascade activated after UV irradiation; (2) develop more concrete signatures of necroptotic cell death, which has only recently been described and is currently poorly defined; and (3) screen for microbial activators of the apoptotic cascade through pattern recognition receptors (Figure 22). Identifying cell death pathways activated by microbial, environmental, and viral stimuli will allow for a greater understanding of the immunogenicity of a wide range of infections. Further research into the immunogenicity of cell death may lead to a shift in how we think about inflammation during infection. Activated apoptotic mechanisms previously thought to be a less damaging, less inflammatory, and therefore more desirable outcome during infection, may prove to facilitate the propagation of long-term consequences, such as carcinogenesis. If we can identify non-classical cell death pathways activated during tissue damaging circumstances, and determine the consequences of them, we may be able to skew to alternative cell deaths toward necroptosis that will allow for a more immunogenic environment and propagation of fewer potentially cancerous mutations.

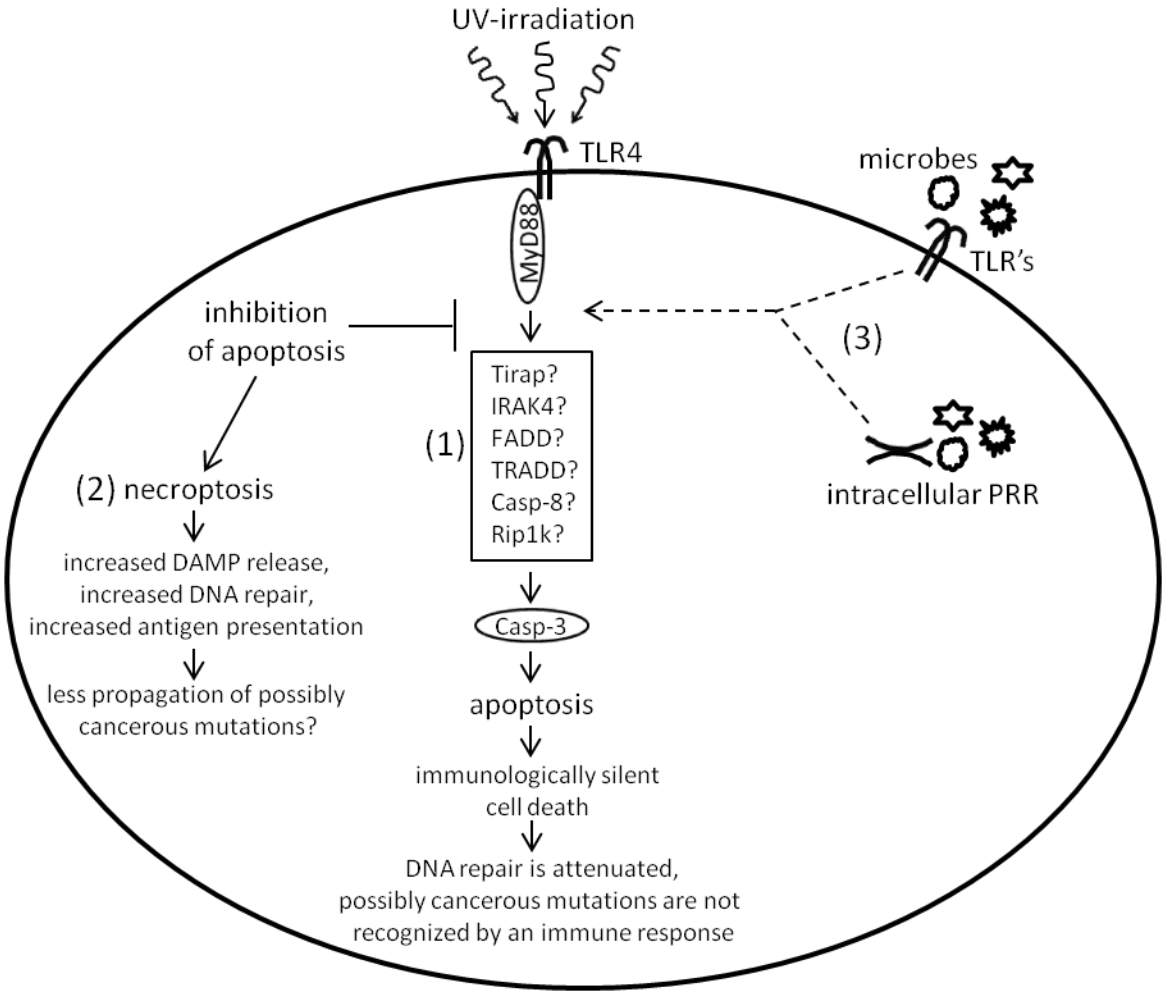


**Figure 23. Proposed non-canonical TLR4 extrinsic apoptotic signaling pathway and downstream biological consequences.** UV-irradiation activates a TLR4/MyD88 dependent non-canonical extrinsic apoptotic signaling cascade. While we know that this signaling pathway is dependent on the scaffolding protein MyD88, it is still unknown what the other scaffolding molecules might be. Due to their involvement in other extracellular death receptor signaling, some likely candidates are (1) Tirap, IRAK4, FADD, TRADD, Caspase-8 and RIP1k. Future studies will include investigation into how these molecules may interact to lead to the phenotype I have described in this thesis. (2) Additional studies will seek to provide a clearer signature of necroptotic cell death after UV-irradiation in our model. We will also employ a chronic UV-carcinogenesis mouse model to determine if our observations result in less cancerous mutations. (3) It is also possible that other TLR agonists may induce a similar apoptotic signaling cascade as UV-irradiation. A third arm of future investigations will screen for agonists that also induce apoptotic cell death.

## Chapter 8

## References


1. Emanuele, E., J.M. Spencer, and M. Braun, *From DNA repair to proteome protection: new molecular insights for preventing non-melanoma skin cancers and skin aging.* J Drugs Dermatol, 2014. 13(3): p. 274-81.

2. Meunier, L., *Ultraviolet light and dendritic cells.* Eur J Dermatol, 1999. 9(4): p. 269-75.

3. Martin, C., M. Hurwitz, and S. Bowyer, *Spectroscopic limits to an extragalactic far-ultraviolet background.* Astrophys J, 1991. 379: p. 549-63.

4. Pitts, D.G., *Sunlight as an ultraviolet source.* Optom Vis Sci, 1990. 67(6): p. 401-6.

5. Pfeifer, G.P. and A. Besaratinia, *UV wavelength-dependent DNA damage and human non-melanoma and melanoma skin cancer.* Photochem Photobiol Sci, 2012. 11(1): p. 90-7.

6. Anderson, R.R. and J.A. Parrish, *The optics of human skin.* J Invest Dermatol, 1981. 77(1): p. 13-9.

7. Tyrrell, R.M., *Biological dosimetry and action spectra.* J Photochem Photobiol B, 1995. 31(1-2): p. 35-41.

8. Horio, T., H. Miyauchi-Hashimoto, and H. Okamoto, *DNA damage initiates photobiologic reactions in the skin.* Photochem Photobiol Sci, 2005. 4(9): p. 709-14.

9. Pillai, S. and D.D. Bikle, *Epidermal vitamin D metabolism, function, and regulation.* Adv Lipid Res, 1991. 24: p. 321-41.

10. Zheng, Y., et al., *Meta-analysis of long-term vitamin d supplementation on overall mortality.* PLoS One, 2013. 8(12): p. e82109.

11. Juzeniene, A. and J. Moan, *Beneficial effects of UV radiation other than via vitamin D production.* Dermatoendocrinol, 2012. 4(2): p. 109-17.

12. Staberg, B., et al., *Carcinogenic effect of sequential artificial sunlight and UV-A irradiation in hairless mice. Consequences for solarium 'therapy'.* Arch Dermatol, 1983. 119(8): p. 641-3.

13. Almutawa, F., et al., *Efficacy of localized phototherapy and photodynamic therapy for psoriasis: a systematic review and meta-analysis.* Photodermatol Photoimmunol Photomed, 2013.

14. Bansal, S., B. Sahoo, and V. Garg, *Psoralen-narrowband UVB phototherapy in treatment of vitiligo in comparison to narrowband UVB phototherapy.* Photodermatol Photoimmunol Photomed, 2013.

15. Fett, N., *Scleroderma: nomenclature, etiology, pathogenesis, prognosis, and treatments: facts and controversies.* Clin Dermatol, 2013. 31(4): p. 432-7.

16. Silverberg, J.I., *Atopic Dermatitis: An Evidence-Based Treatment Update.* Am J Clin Dermatol, 2014.

17. Anderson, T.F., T.P. Waldinger, and J.J. Voorhees, *UV-B phototherapy. An overview.* Arch Dermatol, 1984. 120(11): p. 1502-7.

18. Lee, C.H., et al., *Molecular Mechanisms of UV-Induced Apoptosis and Its Effects on Skin Residential Cells: The Implication in UV-Based Phototherapy.* Int J Mol Sci, 2013. 14(3): p. 6414-35.

19. Kligman, L.H., F.J. Akin, and A.M. Kligman, *The contributions of UVA and UVB to connective tissue damage in hairless mice.* J Invest Dermatol, 1985. 84(4): p. 272-6.

20. Aberer, W., et al., *Ultraviolet light depletes surface markers of Langerhans cells.* J Invest Dermatol, 1981. 76(3): p. 202-10.

21. Staberg, B., et al., *The carcinogenic effect of UVA irradiation.* J Invest Dermatol, 1983. 81(6): p. 517-9.

22. Epstein, J.H., *Photocarcinogenesis: a review.* Natl Cancer Inst Monogr, 1978(50): p. 13-25.

23. Pamphilon, D.H., A.A. Alnaqdy, and T.B. Wallington, *Immunomodulation by ultraviolet light: clinical studies and biological effects.* Immunol Today, 1991. 12(4): p. 119-23.

24. Kripke, M.L., *Immunological effects of ultraviolet radiation.* J Dermatol, 1991. 18(8): p. 429-33.

25. Darzynkiewicz, Z., et al., *DNA damage signaling assessed in individual cells in relation to the cell cycle phase and induction of apoptosis.* Crit Rev Clin Lab Sci, 2012. 49(5-6): p. 199-217.

26. Dalziel, K.L., *Aspects of cutaneous ageing.* Clin Exp Dermatol, 1991. 16(5): p. 315-23.

27. Reardon, J.T., et al., *Efficient nucleotide excision repair of cisplatin, oxaliplatin, and Bis-aceto-ammine-dichloro-cyclohexylamine-platinum(IV) (JM216) platinum intrastrand DNA diadducts.* Cancer Res, 1999. 59(16): p. 3968-71.

28. Cadet, J., T. Douki, and J.L. Ravanat, *Oxidatively generated base damage to cellular DNA.* Free Radic Biol Med, 2010. 49(1): p. 9-21.

29. Scott, T.L., et al., *Repair of oxidative DNA damage and cancer: recent progress in DNA base excision repair.* Antioxid Redox Signal, 2014. 20(4): p. 708-26.

30. Petit, C. and A. Sancar, *Nucleotide excision repair: from E. coli to man.* Biochimie, 1999. 81(1-2): p. 15-25.

31. Vreeswijk, M.P., et al., *Impairment of nucleotide excision repair by apoptosis in UV-irradiated mouse cells.* Cancer Res, 1998. 58(9): p. 1978-85.

32. Bernerd, F., A. Sarasin, and T. Magnaldo, *Galectin-7 overexpression is associated with the apoptotic process in UVB-induced sunburn keratinocytes.* Proc Natl Acad Sci U S A, 1999. 96(20): p. 11329-34.

33. Bonnet, M.C., et al., *The adaptor protein FADD protects epidermal keratinocytes from necroptosis in vivo and prevents skin inflammation.* Immunity, 2011. 35(4): p. 572-82.

34. Harberts, E., et al., *MyD88 mediates the decision to die by apoptosis or necroptosis after UV irradiation.* Innate Immun, 2013.

35. Lewis, W., et al., *Regulation of ultraviolet radiation induced cutaneous photoimmunosuppression by toll-like receptor-4.* Arch Biochem Biophys, 2011. 508(2): p. 171-7.

36. Wang, X., et al., *Increased MAPK and NF-kappaB expression of Langerhans cells is dependent on TLR2 and TLR4, and increased IRF-3 expression is partially dependent on TLR4 following UV exposure.* Mol Med Report, 2011. 4(3): p. 541-6.

37. Gaspari, A.A. and S.I. Katz, *Contact hypersensitivity.* Curr Protoc Immunol, 2001. Chapter 4: p. Unit 4 2.

38. Ono, K., et al., *Distinct effects of cevimeline and pilocarpine on salivary mechanisms, cardiovascular response and thirst sensation in rats.* Arch Oral Biol, 2012. 57(4): p. 421-8.

39. Onoprienko, L.V., *[Molecular mechanisms regulating the activity of macrophages]*. Bioorg Khim, 2011. 37(4): p. 437-51.

40. Francis, H.L., et al., *Histamine stimulates the proliferation of small and large cholangiocytes by activation of both IP3/Ca2+ and cAMP-dependent signaling mechanisms.* Lab Invest, 2012. 92(2): p. 282-94.

41. Wamsley, E.J., et al., *Reduced sleep spindles and spindle coherence in schizophrenia: mechanisms of impaired memory consolidation?* Biol Psychiatry, 2012. 71(2): p. 154-61.

42. Mustari, M.J. and S. Ono, *Neural mechanisms for smooth pursuit in strabismus.* Ann N Y Acad Sci, 2011. 1233: p. 187-93.

43. Jundong, J., et al., *Poor school performance in offspring of patients with schizophrenia: what are the mechanisms?* Psychol Med, 2012. 42(1): p. 111-23.

44. Asami, R., et al., *Distinct mechanisms underlie the regulation of body fluid balance by neurokinin B and angiotensin II in the rat brain.* Brain Res, 2011. 1383: p. 179-86.

45. Machida, T., et al., *5-Hydroxytryptamine induces cyclooxygenase-2 in rat vascular smooth muscle cells: Mechanisms involving Src, PKC and MAPK activation [corrected]*. Eur J Pharmacol, 2011. 656(1-3): p. 19-26.

46. Budden, T. and N.A. Bowden, *The Role of Altered Nucleotide Excision Repair and UVB-Induced DNA Damage in Melanomagenesis.* Int J Mol Sci, 2013. 14(1): p. 1132-51.

47. Chen, A.C., G.M. Halliday, and D.L. Damian, *Non-melanoma skin cancer: carcinogenesis and chemoprevention.* Pathology, 2013. 45(3): p. 331-41.

48. DiGiovanna, J.J. and K.H. Kraemer, *Shining a light on xeroderma pigmentosum.* J Invest Dermatol, 2012. 132(3 Pt 2): p. 785-96.

49. Nakanishi, M., et al., *DNA damage responses in skin biology--implications in tumor prevention and aging acceleration.* J Dermatol Sci, 2009. 56(2): p. 76-81.

50. Pustisek, N. and M. Situm, *UV-radiation, apoptosis and skin.* Coll Antropol, 2011. 35 Suppl 2: p. 339-41.

51. Chen, M. and J. Wang, *Initiator caspases in apoptosis signaling pathways.* Apoptosis, 2002. 7(4): p. 313-9.

52. Riedl, S.J. and G.S. Salvesen, *The apoptosome: signalling platform of cell death.* Nat Rev Mol Cell Biol, 2007. 8(5): p. 405-13.

53. Widlak, P. and W.T. Garrard, *Roles of the major apoptotic nuclease-DNA fragmentation factor-in biology and disease.* Cell Mol Life Sci, 2009. 66(2): p. 263-74.

54. Vandenabeele, P., T. Vanden Berghe, and N. Festjens, *Caspase inhibitors promote alternative cell death pathways.* Sci STKE, 2006. 2006(358): p. pe44.

55. Han, J., C.Q. Zhong, and D.W. Zhang, *Programmed necrosis: backup to and competitor with apoptosis in the immune system.* Nat Immunol, 2011. 12(12): p. 1143-9.

56. McComb, S., et al., *cIAP1 and cIAP2 limit macrophage necroptosis by inhibiting Rip1 and Rip3 activation.* Cell Death Differ, 2012.

57. Rajput, A., et al., *RIG-I RNA helicase activation of IRF3 transcription factor is negatively regulated by caspase-8-mediated cleavage of the RIP1 protein.* Immunity, 2011. 34(3): p. 340-51.

58. Christofferson, D.E., et al., *A novel role for RIP1 kinase in mediating TNFalpha production.* Cell Death Dis, 2012. 3: p. e320.

59. Liedtke, C., et al., *Loss of caspase-8 protects mice against inflammation-related hepatocarcinogenesis but induces non-apoptotic liver injury.* Gastroenterology, 2011. 141(6): p. 2176-87.

60. Welz, P.S., et al., *FADD prevents RIP3-mediated epithelial cell necrosis and chronic intestinal inflammation.* Nature, 2011. 477(7364): p. 330-4.

61. Trinchieri, G. and A. Sher, *Cooperation of Toll-like receptor signals in innate immune defence.* Nat Rev Immunol, 2007. 7(3): p. 179-90.

62. Barton, G.M. and J.C. Kagan, *A cell biological view of Toll-like receptor function: regulation through compartmentalization.* Nat Rev Immunol, 2009. 9(8): p. 535-42.

63. Kawai, T. and S. Akira, *Toll-like receptors and their crosstalk with other innate receptors in infection and immunity.* Immunity, 2011. 34(5): p. 637-50.

64. Dietrich, N., et al., *Murine toll-like receptor 2 activation induces type I interferon responses from endolysosomal compartments.* PLoS One, 2010. 5(4): p. e10250.

65. Shibata, T., et al., *Intracellular TLR4/MD-2 in macrophages senses Gram-negative bacteria and induces a unique set of LPS-dependent genes.* Int Immunol, 2011. 23(8): p. 503-10.

66. Qiu, Y., et al., *Divergent roles of amino acid residues inside and outside the BB loop affect human Toll-like receptor (TLR)2/2, TLR2/1 and TLR2/6 responsiveness.* PLoS One, 2013. 8(4): p. e61508.

67. Stewart, C.R., et al., *CD36 ligands promote sterile inflammation through assembly of a Toll-like receptor 4 and 6 heterodimer.* Nat Immunol, 2010. 11(2): p. 155-61.

68. McGettrick, A.F. and L.A. O'Neill, *Localisation and trafficking of Toll-like receptors: an important mode of regulation.* Curr Opin Immunol, 2010. 22(1): p. 20-7.

69. O'Neill, L.A., D. Golenbock, and A.G. Bowie, *The history of Toll-like receptors - redefining innate immunity.* Nat Rev Immunol, 2013. 13(6): p. 453-60.

70. Loegering, D.J. and M.R. Lennartz, *Protein kinase C and toll-like receptor signaling.* Enzyme Res, 2011. 2011: p. 537821.

71. Waltz, P., et al., *Lipopolysaccaride induces autophagic signaling in macrophages via a TLR4, heme oxygenase-1 dependent pathway.* Autophagy, 2011. 7(3): p. 315-20.

72. Prince, L.R., et al., *The role of TLRs in neutrophil activation.* Curr Opin Pharmacol, 2011. 11(4): p. 397-403.

73. Piccinini, A.M. and K.S. Midwood, *DAMPening inflammation by modulating TLR signalling.* Mediators Inflamm, 2010. 2010.

74. Wheeler, D.S., et al., *Extracellular Hsp72, an endogenous DAMP, is released by virally infected airway epithelial cells and activates neutrophils via Toll-like receptor (TLR)-4.* Respir Res, 2009. 10: p. 31.

75. Tang, D., et al., *High-mobility group box 1, oxidative stress, and disease.* Antioxid Redox Signal, 2011. 14(7): p. 1315-35.

76. Huang, H., et al., *Endogenous histones function as alarmins in sterile inflammatory liver injury through Toll-like receptor 9 in mice.* Hepatology, 2011. 54(3): p. 999-1008.

77. Marichal, T., et al., *DNA released from dying host cells mediates aluminum adjuvant activity.* Nat Med, 2011. 17(8): p. 996-1002.

78. Nace, G., et al., *Dendritic cells and damage-associated molecular patterns: endogenous danger signals linking innate and adaptive immunity.* J Innate Immun, 2012. 4(1): p. 6-15.

79. Kuipers, M.T., et al., *Bench-to-bedside review: Damage-associated molecular patterns in the onset of ventilator-induced lung injury.* Crit Care, 2011. 15(6): p. 235.

80. Goh, F.G. and K.S. Midwood, *Intrinsic danger: activation of Toll-like receptors in rheumatoid arthritis.* Rheumatology (Oxford), 2012. 51(1): p. 7-23.

81. Krysko, D.V., et al., *Emerging role of damage-associated molecular patterns derived from mitochondria in inflammation.* Trends Immunol, 2011. 32(4): p. 157-64.

82. Miller, Y.I., et al., *Oxidation-specific epitopes are danger-associated molecular patterns recognized by pattern recognition receptors of innate immunity.* Circ Res, 2011. 108(2): p. 235-48.

83. Mittal, D., et al., *TLR4-mediated skin carcinogenesis is dependent on immune and radioresistant cells.* EMBO J, 2010. 29(13): p. 2242-52.

84. Maroso, M., et al., *Toll-like receptor 4 and high-mobility group box-1 are involved in ictogenesis and can be targeted to reduce seizures.* Nat Med, 2010. 16(4): p. 413-9.

85. Yu, M., et al., *HMGB1 signals through toll-like receptor (TLR) 4 and TLR2.* Shock, 2006. 26(2): p. 174-9.

86. Celhar, T., R. Magalhaes, and A.M. Fairhurst, *TLR7 and TLR9 in SLE: when sensing self goes wrong.* Immunol Res, 2012.

87. Rubin, R.L., et al., *IgG subclasses of autoantibodies in systemic lupus erythematosus, Sjogren's syndrome, and drug-induced autoimmunity.* J Immunol, 1986. 137(8): p. 2528-34.

88. Ganguly, D., et al., *Self-RNA-antimicrobial peptide complexes activate human dendritic cells through TLR7 and TLR8.* J Exp Med, 2009. 206(9): p. 1983-94.

89. Lande, R., et al., *Plasmacytoid dendritic cells sense self-DNA coupled with antimicrobial peptide.* Nature, 2007. 449(7162): p. 564-9.

90. Bernard, J.J., et al., *Ultraviolet radiation damages self noncoding RNA and is detected by TLR3.* Nat Med, 2012.

91. Bourquin, C., et al., *Systemic cancer therapy with a small molecule agonist of toll-like receptor 7 can be improved by circumventing TLR tolerance.* Cancer Res, 2011. 71(15): p. 5123-33.

92. Alexandrescu, D.T., et al., *Immunotherapy for melanoma: current status and perspectives.* J Immunother, 2010. 33(6): p. 570-90.

93. Ubol, S. and S.B. Halstead, *How innate immune mechanisms contribute to antibody-enhanced viral infections.* Clin Vaccine Immunol, 2010. 17(12): p. 1829-35.

94. Sun, S., et al., *TLR7/9 antagonists as therapeutics for immune-mediated inflammatory disorders.* Inflamm Allergy Drug Targets, 2007. 6(4): p. 223-35.

95. Lee, K.H., et al., *A novel aminosaccharide compound blocks immune responses by Toll-like receptors and nucleotide-binding domain, leucine-rich repeat proteins.* J Biol Chem, 2011. 286(7): p. 5727-35.

96. Park, S.J. and H.S. Youn, *Suppression of homodimerization of toll-like receptor 4 by isoliquiritigenin.* Phytochemistry, 2010. 71(14-15): p. 1736-40.

97. Dizdaroglu, M., *Oxidatively induced DNA damage: Mechanisms, repair and disease.* Cancer Lett, 2012.

98. Rastogi, R.P., et al., *Molecular mechanisms of ultraviolet radiation-induced DNA damage and repair.* J Nucleic Acids, 2010. 2010: p. 592980.

99. Azzam, E.I., J.P. Jay-Gerin, and D. Pain, *Ionizing radiation-induced metabolic oxidative stress and prolonged cell injury.* Cancer Lett, 2011.

100. Aziz, K., et al., *Targeting DNA damage and repair: Embracing the pharmacological era for successful cancer therapy.* Pharmacol Ther, 2012. 133(3): p. 334-50.

101. Zheng, L., et al., *TLR9 engagement on CD4 T lymphocytes represses gamma-radiation-induced apoptosis through activation of checkpoint kinase response elements.* Blood, 2008. 111(5): p. 2704-13.

102. Fishelevich, R., et al., *Imiquimod-induced TLR7 signaling enhances repair of DNA damage induced by ultraviolet light in bone marrow-derived cells.* J Immunol, 2011. 187(4): p. 1664-73.

103. Scharer, O.D., *Nucleotide excision repair in eukaryotes.* Cold Spring Harb Perspect Biol, 2013. 5(10): p. a012609.

104. Vermeulen, W. and M. Fousteri, *Mammalian transcription-coupled excision repair.* Cold Spring Harb Perspect Biol, 2013. 5(8): p. a012625.

105. Iyama, T. and D.M. Wilson, 3rd, *DNA repair mechanisms in dividing and non-dividing cells.* DNA Repair (Amst), 2013. 12(8): p. 620-36.

106. Hoeijmakers, J.H., *Genome maintenance mechanisms for preventing cancer.* Nature, 2001. 411(6835): p. 366-74.

107. Reardon, J.T. and A. Sancar, *Nucleotide excision repair.* Prog Nucleic Acid Res Mol Biol, 2005. 79: p. 183-235.

108. Wang, Y., et al., *Evidence of ultraviolet type mutations in xeroderma pigmentosum melanomas.* Proc Natl Acad Sci U S A, 2009. 106(15): p. 6279-84.

109. Suarez, H.G., et al., *Activated oncogenes in human skin tumors from a repair-deficient syndrome, xeroderma pigmentosum.* Cancer Res, 1989. 49(5): p. 1223-8.

110. Giglia, G., et al., *p53 mutations in skin and internal tumors of xeroderma pigmentosum patients belonging to the complementation group C.* Cancer Res, 1998. 58(19): p. 4402-9.

111. Bodak, N., et al., *High levels of patched gene mutations in basal-cell carcinomas from patients with xeroderma pigmentosum.* Proc Natl Acad Sci U S A, 1999. 96(9): p. 5117-22.

112. Cleaver, J.E. and I. Revet, *Clinical implications of the basic defects in Cockayne syndrome and xeroderma pigmentosum and the DNA lesions responsible for cancer, neurodegeneration and aging.* Mech Ageing Dev, 2008. 129(7-8): p. 492-7.

113. Gorgels, T.G., et al., *Retinal degeneration and ionizing radiation hypersensitivity in a mouse model for Cockayne syndrome.* Mol Cell Biol, 2007. 27(4): p. 1433-41.

114. Niedernhofer, L.J., et al., *A new progeroid syndrome reveals that genotoxic stress suppresses the somatotroph axis.* Nature, 2006. 444(7122): p. 1038-43.

115. Groisman, R., et al., *The ubiquitin ligase activity in the DDB2 and CSA complexes is differentially regulated by the COP9 signalosome in response to DNA damage.* Cell, 2003. 113(3): p. 357-67.

116. Bregman, D.B., et al., *UV-induced ubiquitination of RNA polymerase II: a novel modification deficient in Cockayne syndrome cells.* Proc Natl Acad Sci U S A, 1996. 93(21): p. 11586-90.

117. Yang, L.Y., H. Jiang, and K.M. Rangel, *RNA polymerase II stalled on a DNA template during transcription elongation is ubiquitinated and the ubiquitination facilitates displacement of the elongation complex.* Int J Oncol, 2003. 22(3): p. 683-9.

118. Sugasawa, K., et al., *Xeroderma pigmentosum group C protein complex is the initiator of global genome nucleotide excision repair.* Mol Cell, 1998. 2(2): p. 223-32.

119. Wakasugi, M. and A. Sancar, *Assembly, subunit composition, and footprint of human DNA repair excision nuclease.* Proc Natl Acad Sci U S A, 1998. 95(12): p. 6669-74.

120. Sugasawa, K. and F. Hanaoka, *Sensing of DNA damage by XPC/Rad4: one protein for many lesions.* Nat Struct Mol Biol, 2007. 14(10): p. 887-8.

121. Oh, K.S., et al., *Influence of XPB helicase on recruitment and redistribution of nucleotide excision repair proteins at sites of UV-induced DNA damage.* DNA Repair (Amst), 2007. 6(9): p. 1359-70.

122. Evans, E., et al., *Mechanism of open complex and dual incision formation by human nucleotide excision repair factors.* EMBO J, 1997. 16(21): p. 6559-73.

123. Fan, L., et al., *XPD helicase structures and activities: insights into the cancer and aging phenotypes from XPD mutations.* Cell, 2008. 133(5): p. 789-800.

124. Liu, H., et al., *Structure of the DNA repair helicase XPD.* Cell, 2008. 133(5): p. 801-12.

125. Wolski, S.C., et al., *Crystal structure of the FeS cluster-containing nucleotide excision repair helicase XPD.* PLoS Biol, 2008. 6(6): p. e149.

126. Coin, F., V. Oksenych, and J.M. Egly, *Distinct roles for the XPB/p52 and XPD/p44 subcomplexes of TFIIH in damaged DNA opening during nucleotide excision repair.* Mol Cell, 2007. 26(2): p. 245-56.

127. Staresincic, L., et al., *Coordination of dual incision and repair synthesis in human nucleotide excision repair.* EMBO J, 2009. 28(8): p. 1111-20.

128. Ogi, T. and A.R. Lehmann, *The Y-family DNA polymerase kappa (pol kappa) functions in mammalian nucleotide-excision repair.* Nat Cell Biol, 2006. 8(6): p. 640-2.

129. Moser, J., et al., *Sealing of chromosomal DNA nicks during nucleotide excision repair requires XRCC1 and DNA ligase III alpha in a cell-cycle-specific manner.* Mol Cell, 2007. 27(2): p. 311-23.

130. Cleaver, J.E., E.T. Lam, and I. Revet, *Disorders of nucleotide excision repair: the genetic and molecular basis of heterogeneity.* Nat Rev Genet, 2009. 10(11): p. 756-68.

131. Hise, A.G., et al., *Innate immune responses to endosymbiotic Wolbachia bacteria in Brugia malayi and Onchocerca volvulus are dependent on TLR2, TLR6, MyD88, and Mal, but not TLR4, TRIF, or TRAM.* J Immunol, 2007. 178(2): p. 1068-76.

132. Balato, A., et al., *CD1d-dependent, iNKT-cell cytotoxicity against keratinocytes in allergic contact dermatitis.* Exp Dermatol, 2012. 21(12): p. 915-20.

133. Fishelevich, R., et al., *Ceramide-dependent regulation of human epidermal keratinocyte CD1d expression during terminal differentiation.* J Immunol, 2006. 176(4): p. 2590-9.

134. Gober, M.D., et al., *Human natural killer T cells infiltrate into the skin at elicitation sites of allergic contact dermatitis.* J Invest Dermatol, 2008. 128(6): p. 1460-9.

135. Burns, R., et al., *Keratinocyte-derived, CD80-mediated costimulation is associated with hapten-specific IgE production during contact hypersensitivity to TH1 haptens.* J Allergy Clin Immunol, 2005. 115(2): p. 383-90.

136. Lawley, W., et al., *Rapid lupus autoantigen relocalization and reactive oxygen species accumulation following ultraviolet irradiation of human keratinocytes.* Rheumatology (Oxford), 2000. 39(3): p. 253-61.

137. Griffiths, H.R., et al., *Molecular and cellular effects of ultraviolet light-induced genotoxicity.* Crit Rev Clin Lab Sci, 1998. 35(3): p. 189-237.

138. Guo, M., et al., *Baicalin inhibits Staphylococcus aureus-induced apoptosis by regulating TLR2 and TLR2-related apoptotic factors in the mouse mammary glands.* Eur J Pharmacol, 2013.

139. Kato, S., et al., *Involvement of Toll-like receptor 2 in apoptosis of Aggregatibacter actinomycetemcomitans-infected THP-1 cells.* J Microbiol Immunol Infect, 2013. 46(3): p. 164-70.

140. Chavez-Galan, L., et al., *Monocytes from tuberculosis patients that exhibit cleaved caspase 9 and denaturalized cytochrome c are more susceptible to death mediated by Toll-like receptor 2.* Immunology, 2012. 135(4): p. 299-311.

141. Fujita, Y., et al., *Toll-like receptors (TLR) 2 and 4 on human sperm recognize bacterial endotoxins and mediate apoptosis.* Hum Reprod, 2011. 26(10): p. 2799-806.

142. Lockshin, R.A. and Z. Zakeri, *Caspase-independent cell deaths.* Curr Opin Cell Biol, 2002. 14(6): p. 727-33.

143. Sen, S., *Programmed cell death: concept, mechanism and control.* Biol Rev Camb Philos Soc, 1992. 67(3): p. 287-319.

144. Christofferson, D.E., Y. Li, and J. Yuan, *Control of Life-or-Death Decisions by RIP1 Kinase.* Annu Rev Physiol, 2013.

145. Kaczmarek, A., P. Vandenabeele, and D.V. Krysko, *Necroptosis: the release of damage-associated molecular patterns and its physiological relevance.* Immunity, 2013. 38(2): p. 209-23.

146. Vande Walle, L., et al., *The mitochondrial serine protease HtrA2/Omi cleaves RIP1 during apoptosis of Ba/F3 cells induced by growth factor withdrawal.* Cell Res, 2010. 20(4): p. 421-33.

147. Rebe, C., et al., *Caspase-8 prevents sustained activation of NF-kappaB in monocytes undergoing macrophagic differentiation.* Blood, 2007. 109(4): p. 1442-50.

148. Duriez, P.J. and G.M. Shah, *Cleavage of poly(ADP-ribose) polymerase: a sensitive parameter to study cell death.* Biochem Cell Biol, 1997. 75(4): p. 337-49.

149. Norval, M. and G.M. Halliday, *The consequences of UV-induced immunosuppression for human health.* Photochem Photobiol, 2011. 87(5): p. 965-77.

150. Kubica, A.W. and J.D. Brewer, *Melanoma in immunosuppressed patients.* Mayo Clin Proc, 2012. 87(10): p. 991-1003.

151. Bellinghausen, I., et al., *Signals involved in the early TH1/TH2 polarization of an immune response depending on the type of antigen.* J Allergy Clin Immunol, 1999. 103(2 Pt 1): p. 298-306.

152. Spellman, C.W. and T.B. Tomasi, *Ultraviolet light-induced suppression of antigen presentation.* J Clin Immunol, 1983. 3(2): p. 105-10.

153. Ikehata, H. and T. Ono, *The mechanisms of UV mutagenesis.* J Radiat Res, 2011. 52(2): p. 115-25.

154. von Lukowicz, T., et al., *PARP1 is required for adhesion molecule expression in atherogenesis.* Cardiovasc Res, 2008. 78(1): p. 158-66.

155. Lankinen, M.H., L.M. Vilpo, and J.A. Vilpo, *UV- and gamma-irradiation-induced DNA single-strand breaks and their repair in human blood granulocytes and lymphocytes.* Mutat Res, 1996. 352(1-2): p. 31-8.

156. Lee, E.W., et al., *Ubiquitination and degradation of the FADD adaptor protein regulate death receptor-mediated apoptosis and necroptosis.* Nat Commun, 2012. 3: p. 978.

157. Murphy, G.M., *Ultraviolet radiation and immunosuppression.* Br J Dermatol, 2009. 161 Suppl 3: p. 90-5.

158. Noonan, F.P. and H.A. Hoffman, *Susceptibility to immunosuppression by ultraviolet B radiation in the mouse.* Immunogenetics, 1994. 39(1): p. 29-39.

159. Zhang, D.W., et al., *RIP3, an energy metabolism regulator that switches TNF-induced cell death from apoptosis to necrosis.* Science, 2009. 325(5938): p. 332-6.

160. Tewari, R., et al., *Involvement of TNFalpha-induced TLR4-NF-kappaB and TLR4-HIF-1alpha feed-forward loops in the regulation of inflammatory responses in glioma.* J Mol Med (Berl), 2012. 90(1): p. 67-80.

161. Wang, X., et al., *Increased MAPK and NF-kappaB expression of Langerhans cells is dependent on TLR2 and TLR4, and increased IRF-3 expression is partially dependent on TLR4 following UV exposure.* Mol Med Rep, 2011. 4(3): p. 541-6.

162. Pandey, A.K. and A. Sodhi, *Recombinant YopJ induces apoptotic cell death in macrophages through TLR2.* Mol Immunol, 2011. 48(4): p. 392-8.

163. Lin, S.C., Y.C. Lo, and H. Wu, *Helical assembly in the MyD88-IRAK4-IRAK2 complex in TLR/IL-1R signalling.* Nature, 2010. 465(7300): p. 885-90.

164. Sheikh, M.S., et al., *Ultraviolet-irradiation-induced apoptosis is mediated via ligand independent activation of tumor necrosis factor receptor 1.* Oncogene, 1998. 17(20): p. 2555-63.

165. Zhuang, L., et al., *TNF receptor p55 plays a pivotal role in murine keratinocyte apoptosis induced by ultraviolet B irradiation.* J Immunol, 1999. 162(3): p. 1440-7.

166. Imai, Y., et al., *Identification of oxidative stress and Toll-like receptor 4 signaling as a key pathway of acute lung injury.* Cell, 2008. 133(2): p. 235-49.

167. Bald, T., et al., *Ultraviolet-radiation-induced inflammation promotes angiotropism and metastasis in melanoma.* Nature, 2014. 507(7490): p. 109-13.

168. Yoshida, S., et al., *Urinary oxidative stress markers closely reflect the efficacy of candesartan treatment for diabetic nephropathy.* Nephron Exp Nephrol, 2009. 111(1): p. e20-30.

169. Tsunoda, M., et al., *Oxidative stress increases 6-nitronorepinephrine and 6-nitroepinephrine concentrations in rat brain.* Biomed Chromatogr, 2008. 22(6): p. 572-4.

170. Korff, S., et al., *Eritoran attenuates tissue damage and inflammation in hemorrhagic shock/trauma.* J Surg Res, 2013. 184(2): p. e17-25.

171. Shimamoto, A., et al., *Inhibition of Toll-like receptor 4 with eritoran attenuates myocardial ischemia-reperfusion injury.* Circulation, 2006. 114(1 Suppl): p. I270-4.

172. Lee, H.S., et al., *Expression of toll-like receptor 4 contributes to corneal inflammation in experimental dry eye disease.* Invest Ophthalmol Vis Sci, 2012. 53(9): p. 5632-40.